UNIVERSIDADE DE LISBOA

FACULDADE DE FARMÁCIA

IDENTIFICATION AND FUNCTIONAL CHARACTERISATION OF NOVEL TRANSCRIPTION FACTORS AND SIGNALLING MOLECULES REQUIRED IN HAEMATOPOIETIC STEM CELL SPECIFICATION

Ana Rita Tomé

MESTRADO EM CIÊNCIAS BIOFARMACÊUTICAS

Biologia do Desenvolvimento

2013

UNIVERSIDADE DE LISBOA

FACULDADE DE FARMÁCIA

IDENTIFICATION AND FUNCTIONAL CHARACTERISATION OF NOVEL TRANSCRIPTION FACTORS AND SIGNALLING MOLECULES REQUIRED IN HAEMATOPOIETIC STEM CELL SPECIFICATION

Ana Rita Tomé

Tese orientada por: Professor Roger Patient

Orientador Interno: Professor Susana Solá

MESTRADO EM CIÊNCIAS BIOFARMACÊUTICAS

Biologia do Desenvolvimento

2013

The studies presented in this thesis were carried out at the Molecular Haematology Unit (MHU) at the Weatherall Institute of Molecular Medicine, University of Oxford. The present study was supported by a fellowship from the MHU unit.

Publish Abstracts

The studies presented in this thesis have been published in abstract form:

Schneider, J., Pinheiro, P., Peterkin, T., Tome, A.R., Zuo, J., Monteiro, R., Patient, R. The role of Notch ligand *dll4* in blood stem cell development. *Annual Oxford Developmental Biology Meeting*. Oxford, United Kingdom (2012).

.

Abstract

Haematopoiesis is the developmental process that gives rise to mature blood cells. The production of adult blood initiates from the haematopoietic stem cells (HSCs). These cells have the ability to give rise to all blood lineages and to self-renew in order to maintain all blood lineages throughout the life span of an organism. HSCs emerge *de novo* from the haemogenic endothelium in the ventral wall of the dorsal aorta (VDA), from where they go on to seed adult sites of haematopoiesis. Development of HSCs is tightly regulated by several key signalling pathways. In particular, Notch signalling is considered an important factor in vascular, arterial and HSC development. However, little is known about the role of Notch ligands in haematopoiesis process. Morpholino knockdown of the *dll4* gene in zebrafish showed that this specific Notch ligand is essential for HSC programming. In fact, expression levels of definitive HSC markers and *runx1*, the master regulator of HSC emergence, had their expression levels decreased in *dll4* morphants. In order to identify novel transcription factors (TFs) and signalling molecules involved in this process and that were required in HSC specification, an mRNA-seq experiment and a subsequent Go-term analysis for TFs and signalling molecules was previously performed in the lab for both *dll4* and *runx1* morphants.

In the present study, the expression pattern of the common targets genes differentially regulated in both *dll4* and *runx1* morphants, was assessed by wholemount *in situ* hybridisation (WISH). The results showed that none of the analysed genes were expressed at the region of the dorsal aorta (DA), at the time when first HSCs are identified in the VDA. However, *follistatin a (fsta)*, which is not expressed in DA but it is an antagonist of a known haematopoietic regulator, was also differentially regulated in both morphant and hence it was considered the best candidate for further studies.

Notably, we have shown that Follistatin a is an important regulator of HSC specification in the zebrafish, which in turn is regulated, at least in part, by mechanisms dependent on *dll4* and *runx1*. In addition, functional analysis showed that knockdown of *fsta* gene leads to an increase of HSC derivatives and HSC numbers, thus revealing Fsta as a new potential regulator of HSC formation. Strikingly, we also demonstrate that *fsta* gene regulates venous programming, increasing venous sprouting in zebrafish. Taken together, these results add

significant new information on the molecular mechanisms surrounding haematopoiesis, revealing *fsta* gene as a downstream target of Dll4/Notch and Runx1 and a critical component of the haematopoietic microenvironment that regulates HSC number and venous programming. This might contribute to development of novel and safe regulators of haematopoiesis and potentially facilitating stem cells based-replacement therapy.

Keywords: *dll4*, *fsta,* haematopoiesis, *runx1*, stem cell.

Resumo

A hematopoiese é o processo do desenvolvimento que origina células sanguíneas maduras. A produção de todas as células sanguíneas é iniciada a partir de células estaminais hematopoéticas (CEHs). Estas células são multipotentes, possuindo a capacidade de auto-renovação e diferenciação de forma a manter todas as linhagens das células sanguíneas durante a vida de um organismo. As CEHs originam-se a partir do endotélio hemogénico na parede ventral da aorta. Posteriormente, estas células migram para órgãos específicos, onde ocorre a hematopoiese adulta. O desenvolvimento das CEHs é um processo regulado por diferentes vias de sinalização. Em particular, a via de sinalização Notch é considerada uma via crucial no desenvolvimento vascular, arterial e das CEHs. Porém, o papel dos ligandos desta via no processo de hematopoiese não é, ainda, completamente conhecido. Através da utilização de um morfolino para o *knockdown* do gene *dll4,* foi demonstrado em peixe-zebra, que este ligando do receptor Notch é essencial para a programação das CEHs. De facto, tanto o número de CEHs maduras, como os níveis de expressão de mARN do factor de transcrição *Runx1*, o principal indutor das CEHs, encontram-se reduzidos nos morfantes de *dll4.* Com o objectivo de identificar novos factores de transcrição e/ou moléculas de sinalização envolvidas no processo de especificação hematopoiética, foi realizada uma experiência de mARN-seq em ambos os morfantes *dll4* e *runx1.*

No presente estudo, analisaram-se os alvos significativamente alterados em ambos os morfantes (*dll4 e runx1*) na experiência de mARN-seq, através da técnica *wholemount hibridização in situ (*WISH*)*. A análise demonstrou que nenhum dos genes apresentava um padrão de expressão específico para a região da aorta; o local onde as CEHs são originalmente formadas e identificadas. No entanto, o gene *follistatin a* (*fsta*), expresso na região ventral dos somitos e antagonista de um conhecido regulador da hematopoiese, foi considerado o melhor candidato para estudos posteriores, uma vez que os seus níveis de expressão se encontraram significativamente aumentados em ambos os morfantes. Demostrámos que a molécula sinalizadora*,* Follistatin a, desempenha um papel importante na regulação da especificação CEHs no peixe-zebra. De facto, os nossos resultados demonstraram que o silenciamento do gene *fsta* origina um aumento das células derivadas das CEHs e, também, do número de CEHs, revelando assim que a Follistatin a é possivelmente um

novo e importante regulador da formação de CEHs. Curiosamente, demonstrámos também que o gene *fsta* regula a programação venosa em peixes-zebra, aumentando a angiogénese venosa. Em conclusão, os resultados sugerem que o gene *fsta*, controlado por *dll4* e *runx1*, é um modulador crítico do microambiente hematopoiético, regulando o número de CEHs, assim como da programação venosa. Estes resultados poderão contribuir, de forma significativa, para o desenvolvimento de reguladores do processo hematopoiético e para tornar a utilização das células estaminais mais eficaz e segura nas terapias de regeneração.

Palavras-chave: células estaminais, *dll4, fsta,* hematopoiese, *runx1*

Acknowledgements

First of all I would like to thank Professor Roger Patient for all the support, guidance and sharing of knowledge as my supervisor. I also would like to thank you, Roger, for the opportunity that you gave me of being in contact with such high standards of science by becoming part of your lab and by being hosted in the WIMM. In addition to that, I am very thankful for all the financial support since without that this wouldn't have been possible.

I would also like to thank Professor Susana Solá for being my internal supervisor and for all the availability and support; and to Professor Adriano O. Henriques, for all encouragement you gave me to join the Professor Roger's lab and the continuous availability and wise advice.

Thank you so much to all lab members for this amazing year that I spent with all of you.

Thanks to: Tess and Janina, for all the help and guidance during this project and corrections in this thesis. Phil (Daddy), for the best hugs in the world, and for making my days always better by maintaining the lab perfect and of course because of your lovely smile; Hannah, for kindly sharing your desk with me; Jana and Filipa, for sharing with us the cool stuff about heart regeneration; Stuart, for your friendship, for teaching me how to make sections, for the English lessons and for the very good atmosphere that you gave to the lab, together with the "coffee team" (Rui, Arif and Jana); Rui, um *Muito Obrigada* for all the patience, guidance and advice, which were so important for achieving what I achieved here; Arif, for your advice, English lessons and for helping me mock Stuart; Wenchau for all the help and advice and for your lovely smile (I love your apparent calm); Aldo and Rachel for sharing with us your knowledge about miRNAs; Jie, for sharing the Bioinformatics tips and by trying to make our lives easier; Linda for organizing and taking care of everything for us; and Andrew and all the aquarium people, for taking care of the fish and for all their availability and friendship.

I would like to give a very BIG THANK YOU to Linda and Kevin, for gently receiving me during this full year in your lovely house and for being always so kind and available, helping me with everything I needed. I really appreciated and enjoyed the time I spent with you and it was a pleasure to see the way you always have a smile and enjoy life. Also, I would like to thank to my housemates: Till, Supat, Kib and Mayis; to my Oxford friends in particular to Margarida and

João for the good times we spent together; and to all my friends back in Portugal, especially to Francisca, Canhão, Marina, Fátima and Joana, for always being there for me.

Last but not least, a HUGE thanks to my lovely friends in Cambridge, Tiago, Sara and Zé, for all the support, love and patience and for making this year such a special year. And of course to the X5 that allowed Oxford and Cambridge to become closer.

Finally, I would like to give a *Muito Obrigado* to those that without them all of this would be impossible: Mãe, Pai, Pedro, João and Filipa. Thank you for always being supportive and encourage me to continue. Thank you so much for all your Love.

.

Table of Contents

Abstract i

Resumo iii

Acknowledgements v

Table of Contents 7

List of Figures and Tables 11

Abbreviations 13

1. Introduction 15

1.1. An overview of haematopoiesis 16

1.2. Haemangioblast and primitive and pre-definitive haematopoiesis 18

1.3. Adult-definitive haematopoiesis 19

1.4. Programming blood - Signalling pathways that mediate haematopoietic stem cell specification 21

1.4.1. Notch signalling 22

1.5. Vascular development 23

1.5.1 Vasculogenesis 24

1.5.2. Angiogenesis 25

1.6. The zebrafish as a model system 25

1.7. Current and future clinical applications 27

1.8 Objectives 28

2. Materials and Methods 29

2.1. Maintenance and manipulation of zebrafish embryos 30

2.1.1. Maintenance of fish 30

2.1.2. Zebrafish lines 30

2.1.3. Staging of zebrafish embryos 30

2.1.4. Microinjection of embryos 31

2.1.5. Dechorionation and fixation of embryos 31

2.2. Solutions, morpholinos, primers 32

2.2.1. Solutions 32

2.2.2. Morpholinos 32

2.2.3. Primers 33

2.3. Preparation, manipulation and analysis of DNA 36

2.3.1. Bacterial culture 36

2.3.2. Transformation of chemically competent *E.coli* 36

2.3.3. Isolation and sequencing of plasmid DNA 36

2.3.4. Determination of nucleic acid concentration and purity 37

2.3.5. Agarose gel electrophoresis 37

2.3.6. Restriction enzyme digestion and DNA ligation 37

2.3.7. DNA purification and gel extraction 37

2.3.8. Polymerase chain reaction 38

2.4. RNA preparation, manipulation and analysis 38

2.4.1. Isolation of total RNA 38

2.4.2. Reverse transcription of RNA 39

2.4.3. Quantitative real-time RT-PCR 39

2.5. Isolation and analysis of Protein 40

2.5.1. Deyolking of zebrafish embryos, polyacrylamide gel electrophoresis and western blotting 40

2.6. Construction and *in vitro* synthesis of antisense probes 41

2.6.1. Novel antisense probe constructs 41

2.6.2. *in vitro* synthesis of antisense probes 41

2.7. Wholemount *in situ* hybridisation 45

2.8. Embedding and Sections of Zebrafish Embryos 46

2.9. Imaging zebrafish embryos 46

2.9.1. Still digital photography 46

2.9.2. Wide field fluorescence imaging 47

2.10. Bioinformatics tools: Blast and Sequence alignment 47

3. Identification of novel targets of both dll4 and runx1, involved in HSC specification 49

3.1. Introduction 50

3.1.1 mRNA-seq experiment 52

3.1.2. GO-Term analysis 54

3.2. Best candidate genes important for HSC specification 60

3.3. *follistatin a* is up – regulated and *sox9b* is down - regulated in both *dll4* and *runx1* morphants. 69

3.4. Discussion 72

4. Role of *follistatin a* in regulating HSC specification during zebrafish development. 75

4.1. Introduction 76

4.2. Expression of *fsta* in zebrafish embryos 79

4.3. *fsta* knockdown during zebrafish embryonic development 82

4.4. Loss of *fsta* gene increases HSC numbers 85

4.5. Increased thymus seeding of HSCs in *fsta* morphants 86

4.6. Myeloid and erythroid lineages are affected in *fsta* knockdown embryos 88

4.7. Follistatin a plays a role in the modulation of HSC and endothelial programming .. 90

4.8. Discussion 92

5. Conclusions and Future Perspectives 95

6. References 97

List of Figures and Tables

Figure 1.1 – Overview of heamatopoiesis. 17

Figure 1.2 – Fate Map of ALM and PLM at 14 hpf in zebrafish. 19

Figure 1.3. – Zebrafish haematopoiesis 20

Figure 2.1 – Stages of embryonic development of Zebrafish 31

Table 2.1 - List of solutions used in the present study. 32

Table 2.3. - Sequences of primers used in the present study. 33

Table 2.4. - List of antisense riboprobes used in the present study. 42

Figure 3.1- Knockdown of *dll4* leads to a decrease of HSC and HSCs derivatives 52

Figure 3.2 - Establishing *dll4* and *runx1* molecular targets in the zebrafish. 53

Figure 3.3 - Comparative analysis of the mRNA-seq experiment data. 54

Figure 3.4 - Analysis of common targets of *dll4* and *runx1* by GO-term analysis. 55

Table 3.1 – List of common target genes of both *dll4* and *runx1* morphants analysed in the present study. 57

Figure 3.5 – Schematic representation of the different steps involved to the analysis by WISH for each common target gene. 61

Figure 3.6 - Analysis of the expression patterns of mRNA-seq common target genes by WISH. 62

Figure 3.7 – Common target genes with expression pattern in neural tissues. 63

Figure 3.8 – Common target genes with expression patterns in neural tissues and the DA region 64

Figure 3.9 – Common target genes with broad expression pattern 65

Figure 3.10 – Common target genes with expression patterns in the somites 66

Figure 3.11 – Analysis of the expression pattern of the common target gene *prox2*. 66

Figure 3.12 – Schematic network of *sox9b* and *fsta*. 68

Figure 3.13 –. Analysis of the levels of *fsta* expression in both *dll4* and *runx1* morphants. 70

Figure 3.14 – Analysis of the levels of *sox9b* expression in both *dll4* and *runx1* morphants. 71

Figure 3.15 – Schematic hypothesis of the role of *fsta* in HSC emergence. 73

Figure 4.1 –.Bioinformatic analysis of Follistatin protein. 77

Figure 4.2 –. Time course of *runx1*,*dll4* and *fsta* expression pattern in wild type embryos. 80

Figure 4.3 – Analysis of *runx1,dll4* and *fsta* expression patterns in transverse sections of the trunk of 26 hpf wild type embryos..... 82

Figure 4.4 –. Schematic representation of the design of *fsta* morpholino. 83

Figure 4.5 – Phenotypes of embryos injected with different concentrations of *fsta* MO1. 83

Figure 4.6 – *fsta* gene expression is knowcked down by *fsta* MO1 injection. 84

Figure 4.7 – Follistatin a is an important modulator of HSC development. 86

Figure 4.8 – Loss of *fsta* increases thymic seeding of HSCs. 87

Figure 4.9 – Analysis of myeloid and erythroid markers in *fsta* knockdown embryos. 89

Figure 4.10 – *fsta* play a role in the modulation of the HSCs and endothelial programming. 91

Abbreviations

AGM	aorta–gonad–mesonephros
ALM	anterior lateral mesoderm
BMP	bone morphogenic protein
CHT	caudal haematopoietic tissue
DA	dorsal aorta
dpf	days post fertilisation
EDTA	ethylenediaminetetraacetic acid
(E)GFP	(enhanced) green fluorescent protein
fsta	Follistatin a
hpf	hours post fertilisation
HSC	haematopoietic stem cell
ICM	intermediate cell mass
LB	Luria Bertani
MO	Morpholino
PBS(T)	phosphate buffered saline (tween)
PCV	posterior cardinal vein
PFA	Paraformaldehyde
PLM	posterior lateral mesoderm
SSC	saline sodium citrate
TF(s)	Transcription factor(s)
TBS(T)	tris buffered saline (tween)
TGF-β	transforming growth factor beta
VDA	ventral wall of the dorsal aorta
Vegf	vascular endothelial growth factor
WISH	wholemount *in situ* hybridisation
Wt	Wild type

1. Introduction

1.1. An overview of haematopoiesis

Haematopoiesis is the developmental process that gives rise to mature blood cells. During the life span of an organism, every second millions of blood cells have to be replaced to maintain the blood system. All the blood lineages, including erythroid (erythrocyte), myeloid (macrophage, neutrophil, monocyte) and lymphoid (B cell and T cell) are differentiated from hematopoietic stem cells (HSCs), which also have the ability to self-renew in order to maintaining the HSC numbers throughout life (Loeffler et al., 2011). This is a highly conserved process throughout vertebrates (reviewed in (Chen and Zon, 2009).

In the developing vertebrate embryo, haematopoiesis occurs in discrete waves, termed either primitive or definitive. The primitive wave predominantly generate transitory haematopoietic cell populations of erythrocytes and some primitive macrophages during early embryonic development (Palis and Yoder, 2001); which facilitate tissue oxygenation as the embryo undergoes rapid growth (Orkin and Zon, 2008). The definitive wave originates later in development, where multipotent HSCs capable of self-renewing and differentiate in all blood lineages of the adult organism are produced (reviewed in (Chen and Zon, 2009) (**Figure 1.1**). The HSCs are generated from the endothelium of the ventral wall of the dorsal aorta (VDA) in an evolutionarily conserved process (Bertrand et al., 2010; Kissa and Herbomel, 2010). In the majority of organisms there is a transient wave of definitive haematopoiesis that produces progenitors called erythroid-myeloid progenitors (EMPs) (Bertrand et al., 2007; McGrath et al., 2011).

In zebrafish, the embryogenesis occurs during the first 3 days post fertilisation (dpf) and can be divided in seven periods: zygote, cleavage, blastula, gastrula, segmentation, pharyngula, and hatching periods (Kimmel et al., 1995). During the gastrula period, embryos develop three different germ layers - ectoderm, mesoderm and endoderm (Kimmel et al., 1995). The haematopoietic cells are differentiated from the mesoderm (Paik and Zon, 2010). The first circulating blood cells are just visible after 24 hours post fertilisation (hpf) in zebrafish, however during the gastrula period, by approximately 5 hpf, the processes required for HSC generation is already happening (Paik and Zon, 2010).

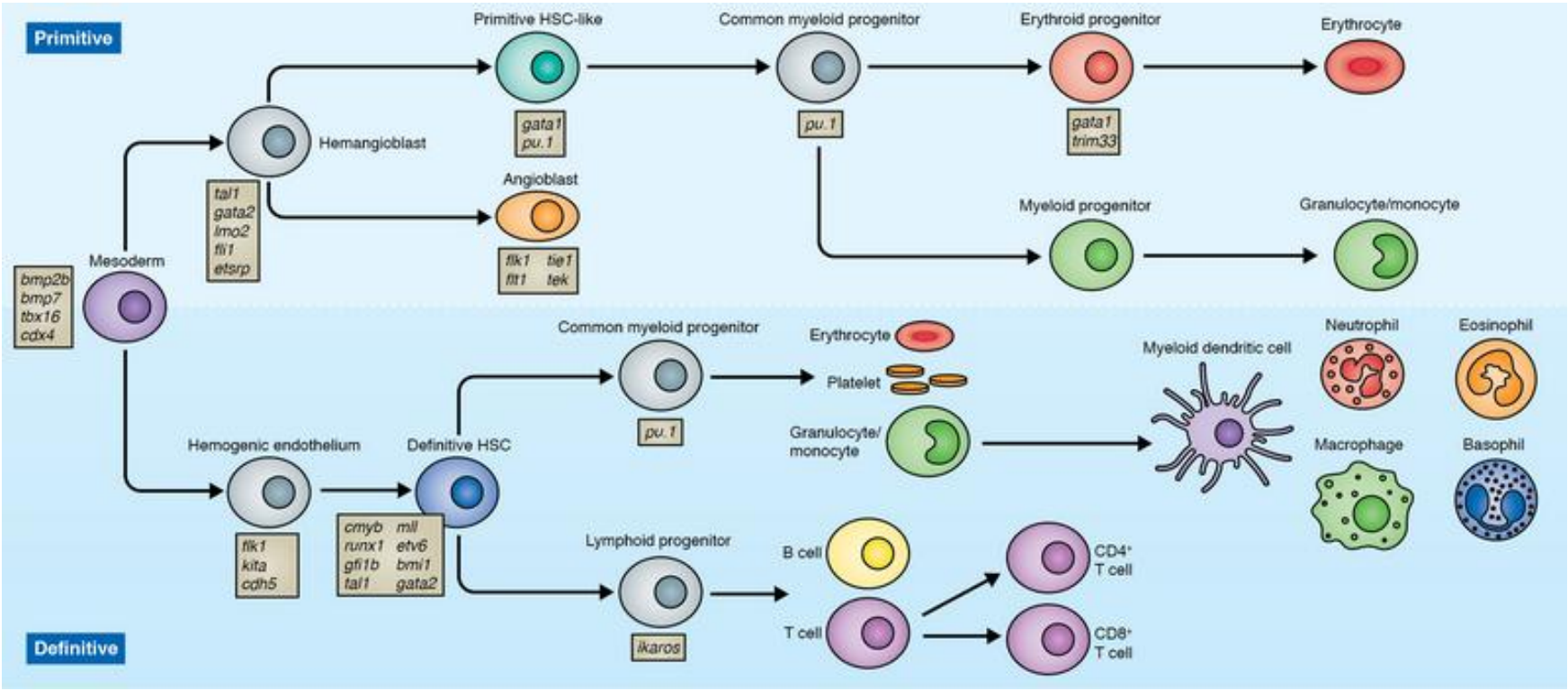

Figure 1.1 – Overview of heamatopoiesis. Schematic representation of the blood cells progeny and their specific markers in both primitive and definitive haematopoiesis. Figure adapted from (Jagannathan-Bogdan and Zon, 2013).

1.2. Haemangioblast and primitive and pre-definitive haematopoiesis

During embryogenesis blood cells arise from the ventral mesoderm via haemangioblast, a precursor that generates hematopoietic, endothelial and smooth muscle lineages (Kennedy et al., 1997; Motoike et al., 2003; Vogeli et al., 2006). Haemangioblast has the ability to differentiate into several tissues including haemogenic endothelium (HE). The HSCs are generated from HE through an evolutionarily conserved process called endothelial-haematopoietic transition (EHT), in which an adherent HE-like cell give rise to a non-adherent HSC-like cell (Bertrand et al., 2010; Kissa and Herbomel, 2010).

In zebrafish, the primitive wave occurs in two distinct embryonic locations: in the anterior lateral mesoderm (ALM); and in the posterior lateral mesoderm (PLM), which later becomes the intermediate cell mass (ICM) through the migration of the bilateral stripes of cells to the midline (Orkin and Zon, 2008). From 10 hpf, bilateral haemangioblast populations in both ALM and PLM co-express hematopoietic lineages markers, *scl, gata2,* and *lmo2* transcription factors (TFs), and the endothelial lineages markers, *kdrl* and *fli1a* TFs (Dooley et al., 2005; Gering et al., 1998). The haemangioblast in the ALM specify into either *pu.1*$^{+}$ myeloid progenitors or *kdrl*$^{+}$ endothelial cells (Bennett et al., 2001; Lieschke et al., 2002). At 16 hpf the *pu.1*$^{+}$ myeloid progenitors migrate to the midline where primitive myelopoisis occurs, hence producing macrophages and granulocytes (Herbomel et al., 1999). At the same time, and before the morphogenetic movement of haemangioblasts from the PLM to the ICM, occurs the specification of PLM-derived cells (Chen and Zon, 2009). Haemangioblasts in the PLM differentiate into *gata 1*$^{+}$ erythroid progenitors, *pu.1*$^{+}$ myeloid progenitors and endothelial cells in the trunk vasculature (Chen and Zon, 2009). Later between 24 - 26 hpf within the ICM, *gata 1*$^{+}$ erythroid progenitors enter the circulation and subsequently mature into primitive erythrocytes (Dooley et al., 2005; Gering et al., 1998). Between 24 - 30 hpf at the posterior blood island (PBI) (tissue derived from most posterior PLM), a transient wave of definitive haematopoiesis, pre-definitive haematopoiesis, generate a population of haematopoietic cells termed EMPs, which have the capacity to generate erythroid and myeloid cells (Bertrand et al., 2007) (**Figure 1.2**).

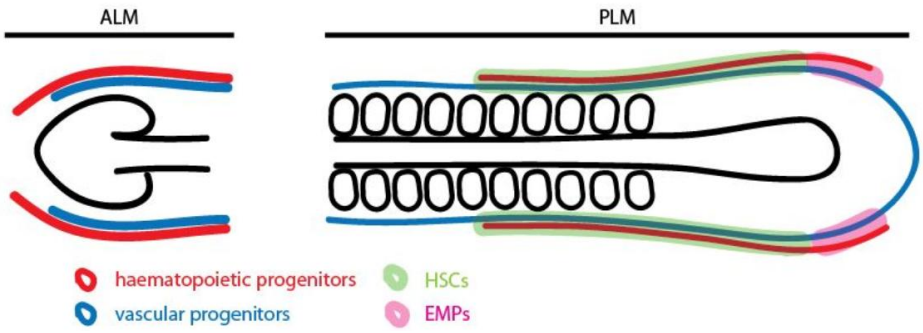

Figure 1.2 – Fate Map of ALM and PLM at 14 hpf in zebrafish. Figure adapted from (Monteiro et al., 2011).

1.3. Adult-definitive haematopoiesis

The definitive wave produces HSCs that are capable of generating all the mature blood lineages throughout adult life. This wave initiates with the specification of HSCs in a thin mesenchyme between the dorsal aorta (DA) and the posterior cardinal vein (PCV) at 24 hfp in zebrafish (Murayama et al., 2006); this is a region anatomical and functional homologue of the aorta–gonad–mesonephros (AGM) in mammals. These cells express *runx1*, a TF which is a key regulator of definitive haematopoiesis (Kalev-Zylinska et al., 2002; Murayama et al., 2006). Then, at 30 hpf, the earliest HSCs emerge from the VDA expressing *runx1* through EHT process (Kissa and Herbomel, 2010). During this process, these HSCs are release into the AGM and sequentially enter into the vein and then migrate to the caudal haematopoietic tissue (CHT) in the posterior region of the tail through blood circulation (Bertrand et al., 2010; Dzierzak and Speck, 2008; Kissa and Herbomel, 2010). These cells, around 36 hpf, express markers, such as *runx1*,*c-myb, CD41* and *ikaros* in the AGM (reviewed in (Chen and Zon, 2009)*)*. Later, at 48 hpf, *c-myb*$^{+}$ cells are found in the CHT (Jin and Wen, 2007). By 3 dpf, the expanded HSCs (*Ikaros*$^{+}$ *cells* and *c-myb*$^{+}$ *cells)* continue their migration to the thymus, where the lymphopoiesis occurs: immature lymphoblast originate T-cells in the thymus. These cells express T cell specific markers, such as *gata3*, *ikaros, lck, rag-1* and *rag-2* at 4 dpf (Chen and Zon, 2009; Murayama et al., 2006). One day later the HSCs (*runx1*$^{+}$ *cells, scl*$^{+}$ *cells, Ikaros*$^{+}$ *cells and c-myb*$^{+}$ *cells)* migrate from the AGM and CHT to seed the kidney marrow, which is analogous to the bone marrow in mammals, to maintain haematopoiesis throughout life (reviewed in (Jagannathan-Bogdan and Zon, 2013; Murayama et al., 2006; Zhang et al., 2013). The definitive wave of

erythropoiesis begins in the CHT, as indicated by the *hbbe1.1* and *gata1* expression in this region (Zhang and Rodaway, 2007). The definitive erythrocytes gradually replaced the primitive erythrocytes and the erythropoiesis switches from the CHT to the kidney (Jin et al., 2009). The definitive wave of myelopoiesis is also observed around 3 dpf in the CHT by *l-plastin* expression and then transits from the CHT to the kidney (Jin et al., 2009). As with erythropoiesis and myelopoiesis, the site of trombopoiesis begins in the CHT, by approximately 2 dpf, and transits to the kidney; by 5 dpf the thrombocytes express *CD41* (Lin et al., 2005).

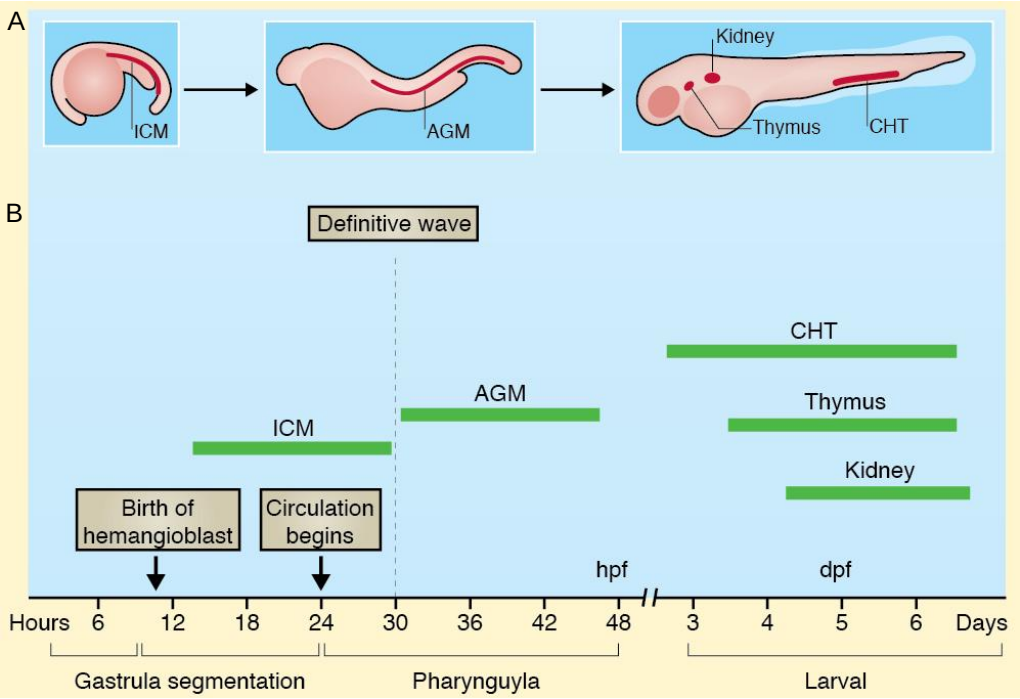

Figure 1.3. – Zebrafish haematopoiesis (A) Haemotopoiesis at various sites in zebrafish. The ICM is a place of primitive haematopiesis, while definitive haematopoiesis occours in the AGM, CHT and thymus and kidney; (B) Timing of haematopiesis in zebrafish; hpf – hours post fertilisation, dpf- days post fertilisation. Figure adapted from (Jagannathan-Bogdan and Zon, 2013).

Runx1 is a TF expressed in hematopoietic and neuronal cells during early embryogenesis. It has been described as a important player in haematopoiesis, vasculogenesis and neuropoiesis (Kalev-Zylinska et al., 2002). In haematopoiesis, Runx1 was defined as key regulator of definitive haematopoiesis in all vertebrates (Burns et al., 2002; Kalev-Zylinska et al., 2002). During development, *runx1* gene is expressed in the VDA and modulate both the efficiency of HSC emergence from the HE and the survival of these HSCs (Kissa and Herbomel,

2010; Lam et al., 2010). Knockdown of *runx1* in zebrafish affects definitive haematopoiesis but seems to marginally affect primitive erythropoiesis (Burns et al., 2005; Gering and Patient, 2005; Kalev-Zylinska et al., 2002). When *runx1* is lost, the HSC emergence in the DA and its activity is lost (Gering and Patient, 2005; North et al., 1999). Curiously, *RUNX1* gene has been associated with acute leukemia, being the most frequent target for chromosome translocations in this disease (Speck and Gilliland, 2002). In fact, 30% of all human leukemias are caused by loss-function mutations of RUNX1 (Ito and Miyazono, 2003).

Although, HSCs are the most well described stem cell systems in the body, their ontogeny is not yet completely understood (Medvinsky et al., 2011). In fact, despite the several decades of research, a detailed knowledge of the signalling pathways and their interactions with TFs that are important for HSC programming is still missing (reviewed in (Marcks-Bluth and Pimanda, 2012).

1.4. Programming blood - Signalling pathways that mediate haematopoietic stem cell specification

The production of HSCs during development is a process in which multiple regulatory pathways work in concert. Several signalling pathways, such as Wnt, Hedgehog, Vegf, Notch, and bone morphogenic protein (BMP), have been identified (Burns et al., 2005; Clements et al., 2011; Gering and Patient, 2005; Wilkinson et al., 2009). These different pathways are essential at different developmental stages of blood programming, from specification and proliferation to migration and maintenance (reviewed in (Jagannathan-Bogdan and Zon, 2013; Zhang et al., 2013)). Despite the decades of research and the knowledge of these molecular pathways involved in blood programming, their precise molecular mechanisms and exact temporal-spatial activity and integration remain unclear (Loeffler et al., 2011). These signalling pathways involved in blood programming, also controlling other developmental and adult cell fate decisions. In addition to that, a wide range of ligands and receptors with unclear interactions, as well as the potential extracellular and intracellular modifiers involved in these signalling pathways make the study of blood programming very complex and difficult (Loeffler et al., 2011; Zhang et al., 2013).

1.4.1. Notch signalling

The Notch signalling pathway has been shown to be pivotal in the control of embryonic cell fate decisions, including haematopoiesis. This pathway is an important player in stem cell regulation and differentiation, and has been described as an important regulator of hematopoietic differentiation (Bigas and Espinosa, 2012).

The Notch signalling network is formed by Notch receptors, ligands, positive and negative regulators, and TFs (reviewed in (Pajcini et al., 2011)). The Notch signalling pathway through the interaction of their ligands and receptors is able to influences lineage determination by two mechanisms of delivery paracrine signals: lateral inhibition - the Notch signalling in one cell inhibits Notch signalling of a neighbour cell; and boundary induction - the Notch signalling in one layer of cells induces Notch signalling of a neighbour layer of cells (reviewed in (Pajcini et al., 2011)).

In mammals, there are three transmembrane Notch ligands of the Delta (*Dll1*, *Dll3* and *Dll4*) and two of Jagged (*Jag1* and *Jag2*) families (reviewed in (Pajcini et al., 2011)). In zebrafish, there are five ligands of the Delta (*dla, dlb, dlc, dld* and *dll4*) and three Jagged ligands (*jagged 1a, jagged 1b* and *jagged 2*) families (reviewed in (Clements and Traver, 2013). During normal Notch signalling, a transmembrane ligand on a particular cell interacts with one of the Notch receptors present in other cell, including Notch 1 to Notch 4 in mammals or Notch 1a, Notch 1b, Notch 2 and Notch 3 in zebrafish. This in turn, activates Notch receptor by ligand-induced proteolysis (reviewed in (Clements and Traver, 2013)). In fact, Notch activation occurs in two successive proteolytic events which mature the receptor and release an intracellular receptor fragment, the Notch intracellular domain (NICD), which then binds DNA-binding CBF1/suppressor of hairless/Lag-2 (CSL), and mediates transcriptional activation in coordination with the Mastermind (Mam) co-activator (reviewed in (Clements and Traver, 2013; Gering and Patient, 2009). The first proteolytic event is mediated by extracellular proteases, known as A desintegrin and metalloprotease (ADAM) which cleaves the extracellular domain of the Notch receptor (reviewed in (Clements and Traver, 2013; Gering and Patient, 2009). Then, the second proteolytic cleavage is mediated by the γ-secretase complex which releases NICD allowing it to translocate into the nucleus, where it associates with the DNA binding protein CSL (reviewed in (Caolo et al., 2012; Clements and Traver, 2013; Gering and Patient, 2009).

Nuclear translocation of NICD leads to the formation of a transcriptionally active complex comprising NICD, CSL and a member of the Mastermind-like (MamL) family, which then recruit co-activators and regulates the transcription of downstream genes (**Figure 1.4 (A);** reviewed in (Caolo et al., 2012; Clements and Traver, 2013; Gering and Patient, 2009)

During embryogenesis, the Notch/Runx1 pathway is a signalling pathway involved in regulation of both HSC and arterial and venous specification (Burns et al., 2005; Chen and Zon, 2009; Jakobsson et al., 2009; Roca and Adams, 2007). In mice, it has been demonstrated that Notch1 receptor activates *Gata2* (Robert-Moreno et al., 2005), which in turn is one of the critical factors for *Runx1* activation (Nottingham et al., 2007) and HSC specification (**Figure 1.4 B**).

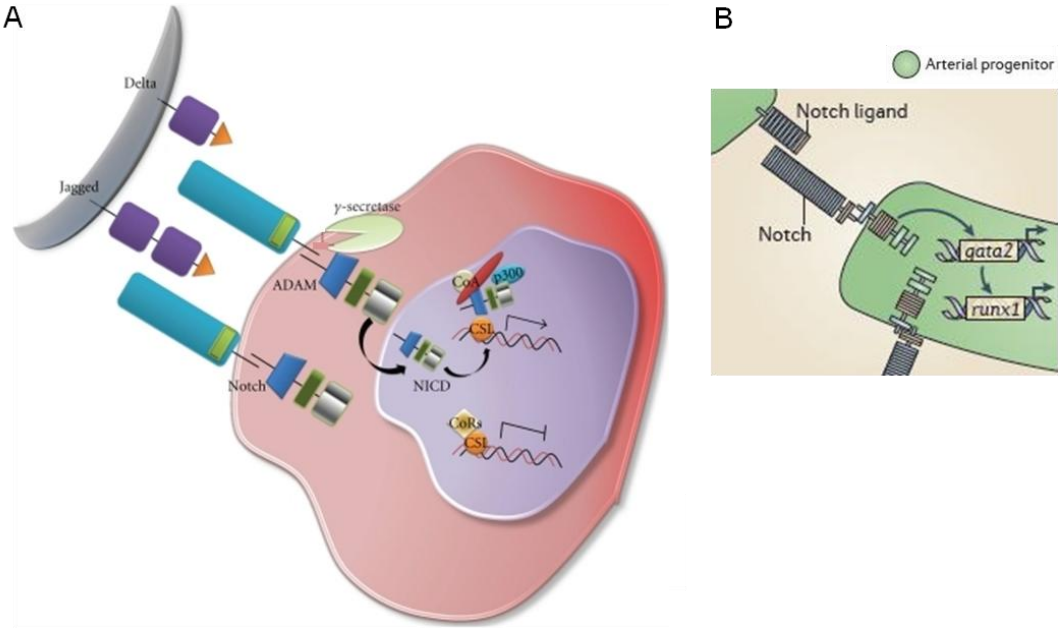

Figure 1.4 - Overview of Notch Pathway activation. (A) General mechanism of Notch activation by ligand-induced proteolysis. Figure adapted from (Morrison et al., 2011); (B) Notch ligands expressed by neighbouring cells activate Notch receptors to specify HSCs by activating gata2 expression, which in turn activates runx1 expression. Figure adapted from (Clements and Traver, 2013).

1.5. Vascular development

The development of the embryonic blood occurs in association with the developing of blood vessels. Indeed, differentiation of blood and endothelial cells occurs from the common progenitor, haemangioblast (Vogeli et al., 2006). The blood vessels of the vertebrate circulatory system have several crucial functions throughout embryonic and adult life. The circulatory

system is formed through the processes of vasculogenesis and angiogenesis, supplying the tissues with oxygen and nutrients, removing tissue metabolic wastes, and transporting liquids and cells (reviewed in (Lawson and Weinstein, 2002)). The proper formation and maintenance of circulatory system is critical during development and after birth (reviewed in (Beets et al., 2013). The circulatory system can be divided into two types of blood vessels: arteries and veins, which are structurally different. In the past, the functional definition of arteries and veins was based by the direction of blood flow that they carry out (reviewed in (Lawson and Weinstein, 2002). Nevertheless, recent findings indicate that the endothelial cells in arteries and veins are both functionally and molecularly distinct (Swift and Weinstein, 2009). The arterial-venous identity and the establishment of distinct networks of arterial and venous vessels are determined in the developing embryo, before circulation begins and are critical for a functional circulatory system (reviewed in (Aniket et al., 2012; Lawson and Weinstein, 2002; Swift and Weinstein, 2009)).

1.5.1 Vasculogenesis

Vasculogenesis consist of the *de novo* formation of blood vessels through the coalescence of endothelial cells. This process often involves extensive migration of endothelial cells from their point of origin to the site of vessel formation (reviewed in (Lawson and Weinstein, 2002). During zebrafish vasculogenesis, angioblasts derived from the posterior lateral mesoderm migrates to the midline region to form the DA and PCV in the trunk (Jin et al., 2005; Lawson and Weinstein, 2002, 2002). Endothelial cells expressing *Efnb2* gene contribute to artery but not to venous specification. Whereas *Ephb4*, a gene that encodes the putative receptor for *Efnb2* is expressed in both veins and arteries, but is found in much higher levels in veins than arteries (Gerety et al., 1999; Wang et al., 1998). The determination of arterial - venous identity has been demonstrated to be related among other with the Vegf-Notch pathway (Lawson et al., 2001).

1.5.2. Angiogenesis

Angiogenesis is the formation process of new blood vessels from pre-existing ones. After vasculogenesis, angiogenic processes remodel the primary vessel network in order to generate a complex vascular network (Isogai et al., 2003). In zebrafish embryonic trunk, developmental angiogenesis is a highly coordinated process which takes place in two spatial - temporal distinct steps: in the first sprouting angiogenic event, around 20-24 hpf, the primary intersegmental vessels (ISVs) originate from the roof of the DA (Blum et al., 2008; Leslie et al., 2007). Subsequently, these sprouts grow dorsally and reach the top of the neural tube at approximately 30 hpf (Leslie et al., 2007), where they bifurcate and extend along the body axis. Finally, these longitudinal sprouts connects to form the dorsal longitudinal anastomotic vessel (DLAV) (Isogai et al., 2003); the second sprouting angiogenic event is initiated approximately at 32 hpf from the PCV, during this event intersegmental veins and lymphatic vascular precursors are generated, which extend ventrally and interconnect to form the caudal vein plexus (CVP) (Isogai et al., 2003; Wiley et al., 2011; Yaniv et al., 2006). These processes are regulated by Vegf and their receptors (Wiley et al., 2011). However, it has recently been demonstrated that BMP is the main stimulus for sprouting angiogenesis from the PCV, and it is independent of Vegf-A. Vegf-A, in turn, is the main stimulus for sprouting from DA (Wiley et al., 2011).

1.6. The zebrafish as a model system

Several model organisms have been used to study haematopoiesis process, including mice, frog, chick and zebrafish, each of which with its own advantages. Although, during the last two decades, the zebrafish (*Danio rerio)* has been extensively used as model organism for studying haematopoiesis, since it combines many attributes of other developmental models (Chen and Zon, 2009; Zhang et al., 2013). Indeed, the haematopoiesis associated genes, cell types and signalling pathways in zebrafish are highly conserved with those found in higher vertebrates, ensuring that lessons from this model might be easily applied to higher vertebrates.

The zebrafish can be handled in large numbers (~200 eggs per week) and develop externally and rapidly (Chen and Zon, 2009; Wolpert et al., 2001). The optical transparency and

large size of the embryos allow an easy life imaging and make it easier to identify developmental abnormalities. Additionally, their external development allows loss-of-function experiments using antisense oligonucleotides (through microinjections of RNA and synthetic DNA (morpholinos, MO)) or chemical inhibitors dissolved in the water (facilitated by the small size of the zebrafish and their ability to absorb chemicals from surrounding water); and gain-of-function experiments through the overexpression with exogenous RNA or DNA. The zebrafish has been proved particularly powerful in the study of haematopoietic and also in the vascular development (Chen and Zon, 2009), facilitated by numerous mutants generated from forward genetic screens which exhibit haematopoietic and vascular defects and also for the several transgenic lines available (Ransom et al., 1996; Stainier et al., 1995; Weinstein et al., 1996).

Antisense morpholino oligonucleotides are used to specifically knockdown gene function (Heasman, 2002). Morpholinos are chemically modified antisense oligonucleotides that can specifically inhibit proper gene translation of a target mRNA. The morpholinos are analogues to nucleic acids; the ribose ring is replaced with a morpholine ring, and the phosphate linkage groups are replaced with non-ionic phosphorodiamidate to provide resistance to nucleases (Eisen and Smith, 2008). The morpholinos, can be designed to bind the 5' untranslated region (UTR) of a mRNA, or up to 25 nucleotides downstream of the translation start site to prevent the translation of the mRNA; or to target splice acceptor or donor sites, altering the splicing pattern of the mRNA, which in turn can result in truncated or altered proteins degraded, or not, by the cell (Eisen and Smith, 2008; Heasman, 2002). The morpholinos persist in the embryos approximately until 5 days after injection and so it is important monitor their activity (Chen and Zon, 2009). Thereby they can only be used to evaluate gene function during the first few days of development.

1.7. Current and future clinical applications

The basic HSC research is very important to help us to understand the genetic network and molecular aspects controlling the development and functions of stem cells and may contribute to treatment of human haematopoietic diseases. These cells are the component of the bone marrow which it is used in transplants to treat patients with leukaemia and congenital blood disorders (Clements and Traver, 2013). Due to the ability of HSCs to repopulate the entire blood system, these cells have successfully been used for cell replacement therapy for several years (Loeffler et al., 2011). Despite that, their application has faced several restrictions related with immune compatible donors and with the low number of clinically available HCSs. Both restrictions could be overcome with the generation of HSCs from patient-specific induced pluripotent stem cell (iPSC) or embryonic stem cells (ESCs) (Loeffler et al., 2011). However despite decades of research, HSC generation from iPSCs or ESCs has not been accomplished, suggesting that key specification requirements are unknown, and so a better understanding of how HSCs normally arise during embryonic development is needed (reviewed in (Clements and Traver, 2013)).

A clear understanding of the molecular mechanisms that leads to the developmental specification of HSCs *in vivo* might provide novel critical insights that will contribute to the improving of protocols for efficient generation of HSCs *in vitro* with regenerative and therapeutic purposes (reviewed in (Loeffler et al., 2011; Medvinsky et al., 2011)).

1.8 Objectives

Many important regulators of haematopoiesis and HSC function remain to be described. The understanding of the molecular mechanisms required for blood programming in the developing embryo will be crucial in designing novel regenerative medicine protocols. The generation of HSCs would provide a source of therapeutic cells for blood diseases. Blood programming is highly controlled and several signalling pathways, TFs and transcriptional complexes have been described as crucial to this process. However, the same TFs and signalling molecules are able to interact with different partners in different cell types and display different binding patterns, making their study so complex. The HSC research in zebrafish will help us to understand the interplay between these TFs/signalling molecules during blood programming and therefore will provide new biological insights and likely contribute for novel and efficient therapies.

Previous work in Patient lab has shown that *dll4* is required for *runx1* expression and subsequent for HSC emergence. In addition, a pool of target genes of *dll4* and *runx1* morphant zebrafish, have been established using a mRNA-seq experiment. The work presented here took advantage of those observations and more specifically from the list of common target genes of *dll4* and *runx1* previously established, to identify candidate genes with an important role for haematopoiesis and hence characterise their potential role in haematopoiesis in the zebrafish.

Briefly, through a screen by WISH of selected common target genes of *dll4* and *runx1* morphants obtained in the mRNA-seq experiment, the general goal of this study was to identify novel TFs and/or signalling molecules that possibly regulate the blood programme; Specifically, we will investigate the molecular mechanisms and relationships of these novel TFs and/or signalling molecules in blood programming by loss-of-function experiments and extend the understanding the cellular function of these molecules throughout developmental haematopoiesis.

2. Materials and Methods

2.1. Maintenance and manipulation of zebrafish embryos

2.1.1. Maintenance of fish

The zebrafish (*Danio rerio*) used in the present study were maintained in flowing system water on a 14 hours light/ 10 hours dark cycle at 28.5 °C, with a conductance between 450-550 µS, and pH 7.1-7.2. Fish were fed with a mix of flake food, high protein pellets and shrimp (BMS Staff, University of Oxford). The experiments involving the use of model organism *Danio rerio* were approved by the University of Oxford research ethics committee.

2.1.2. Zebrafish lines

The zebrafish lines used in the present study were Tg (*lck*:Enhanced green fluorescent protein (EGFP)) (Langenau et al., 2004); Tg (*CD41*:EGFP) (Lin et al., 2005); Tg (*kdrl1:*GFP/*gata1*:DsRed) (Jin et al., 2005; Traver et al., 2003).

2.1.3. Staging of zebrafish embryos

In order to obtain the zebrafish embryos marbles boxes were placed in the tanks for approximately 15 hours before the lights came on. After, the eggs were collected and washed in system water and placed in Petri dishes with system water or E3 medium supplemented with methylene blue (to inhibit fungal growth). The embryos were then grown between 22 °C - 32 °C and staged under a dissecting microscope according to (Kimmel et al., 1995).

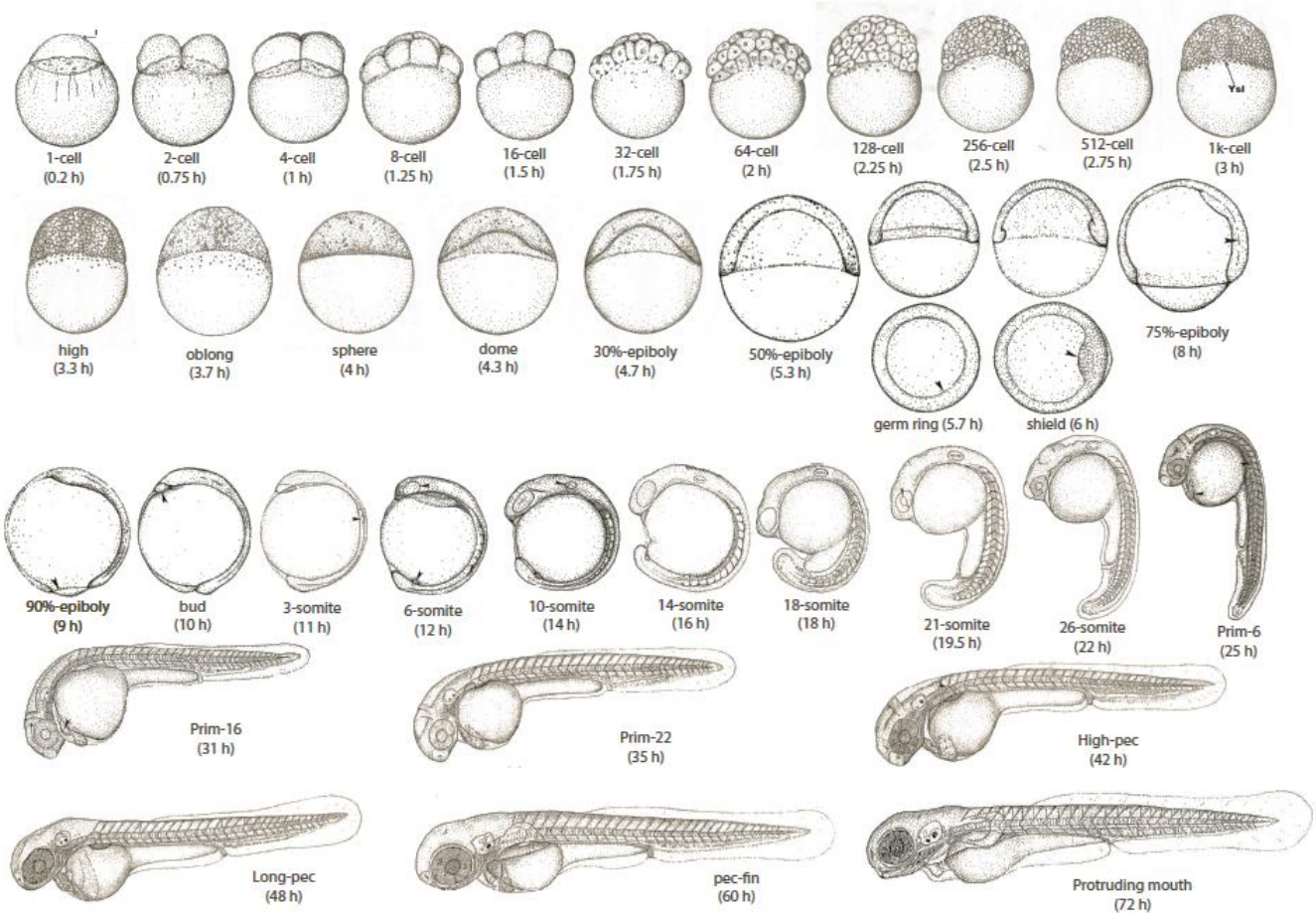

Figure 2.1 – Stages of embryonic development of Zebrafish. Figure adapted from (http://www.cores.utah.edu/wp-content/uploads/2013/07/stage2.jpg).

2.1.4. Microinjection of embryos

Injections of 0.5 nl of morpholino was performed into the yolk of 1- to 4- cell embryos that were positioned against a glass slide.

2.1.5. Dechorionation and fixation of embryos

The embryos were manually dechorionated with forceps or placed in 1 mg/mL pronase solution (diluted in phosphate-buffered saline with tween (PBST)) for the time required for removal of the chorions in accordance with the stage of development of the embryo. The embryos were fixed in 4% paraformaldehyde (PFA) in PBST for at least 2 hours at room temperature or overnight at 4 ºC. Subsequently, embryos were dehydrated into ethanol through PBS/ethanol series (25%, 50%, 75% and 100% ethanol) and stored at -20 °C. For embryos

younger than 18-somite stage the fixation was performed first and only after that the embryos were fixed and stored.

2.2. Solutions, morpholinos, primers

2.2.1. Solutions

The solutions used in the present study were prepared with MilliQ and autoclaved when necessary. All solutions were stored at room temperature, 4 °C (*) or -20 °C (†) (**Table 2.1.)**.

Table 2.1 - List of solutions used in the present study.

Name	Composition
AP Buffer	100 mM Tris-HCl pH 9.5, 100 mM NaCl, 50 mM $MgCl_2$, 0.1% Tween (freshly made)
Bleaching	10% hydrogen peroxide, 5% formamide, 0.5% SSC (prepared fresh)
Deyolking buffer	55 mM NaCl, 1.8 mM KCl, 1.25 mM $NaHCO_3$
E3 (*) 60 x	1.75% NaCl, 0.08% KCl, 0.3% $CaCl_2 \cdot 2H_2O$, 0.5% $MgCl_2 \cdot 6H_2O$, pH 7.2
Hybe -/- (*)	50% Formamide, 5x SSC, 9.2 mM Citric Acid, 0.1% Tween
Hybe +/+ (*)	50% Formamide, 5x SSC, 9.2 mM Citric Acid, 0.1% Tween, 0.05% tRNA, 0.005%
LB (Agar(*))	1% Bactotryptone, 0.5% Bactoyeast, 1% NaCl, pH 7.0 (1.5% Bactoagar)
Lysis buffer	2x SDS buffer; 10 mM fresh DTT; 1x proteinase inhibitor (Roche)
MAB Block (†)	0.1 M maleic Acid, 0.15 M NaCl, pH 7.5, 2% Boehringers Blocking Reagent
MABT (*)	0.1 M maleic Acid, 0.15 M NaCl, 0.1% Tween, pH 7.5
MS222 (*)	0.4% Ethyl-3-amino benzoate methanesulfonate salt, pH 7.0
PBS(T)	0.8% NaCl, 0.02% KCl, 0.15 % Na_2HPO_4, 0.025% KH_2PO_4, pH 7.2 (0.1% tween)
SSC (*) 20 x	3 M NaCl, 0.3 M Sodium Citrate
SDS 2x	100 mM Tris-HCl pH 6.8, 4%(w/v) SDS, 0,2% (v/v) glycerol
TAE 50 x	2 M Tris-acetate, 50 mM EDTA
TBS(T)	0.9% NaCl, 0.02% KCl, 0.3% Tris base, pH 7.4 (0.1% tween)
TE buffer	10 mM Tris, 0.1 mM EDTA, pH 7.6

2.2.2. Morpholinos

The morpholinos used in the present study were previously designed to targeting a splice junction to alter the splicing pattern and were obtained from Gene Tools, Oregon, USA (**Table 2.2**). The stock solution of morpholino was prepared in MiliQ for a final concentration of

50 μM and stored at -80 ºC. The working concentration of morpholinos (**Table 2.2**) was prepared in MiliQ and 10% of phenol red and stored at -20 °C. All the morpholinos before used were heated to 65 °C during 10 minutes.

Table 2.2. - List of morpholinos used in the present study.

Target gene	MO	MO Target	MO Sequence (5' – 3')	Concetration	Reference
fsta	*fsta* MO1	Exon 2 / Intron 2	CAATACTGACGGGATCGTACCTTTA	[5-10 ng/nL]	Tsukada et al., 2010
dll4	*dll4* MO4	Exon 4/ Intron 4	TGATCTCTGATTGCTTACGTTCTTC	6 ng/nL	Hogan et al., 2009
runx1	*re1* MO	Exon 2 / Intron 2	AGCGCTCTTACCGTATTTGGCGTCC	4 ng/nL	Gering & Patient, 2005
	re6 MO	Intron 5/ Exon 6	GTGTGAATGTGTAAACTCACAGTGT	5 ng/nL	Tessa Peterkin & Philip Pinheiro, Patient Lab

Legend: MO-Morpholino

2.2.3. Primers

The primers used in the present study were obtained from Sigma and resuspended to a stock concentration 100 μM and stored at -20 °C (**Table 2.3.**).

Table 2.3. - Sequences of primers used in the present study.

Primer name	fwd/rev	Sequence (5' - 3')	Reference
ef1α f	fwd	CACCCTGGGAGTGAAACAG	(Patterson et al., 2005)
ef1α r	rev	ACTTGCAGGCGATGTGAGC	(Patterson et al., 2005)
T7	fwd	TAATACGACTCACTATAGGG	Promega
Sp6	rev	ATTTAGGTGACACTATAGAA	Promega
g6pd_Q1f	fwd	GTCCCGAAAGGCTCCACTC	reviewed in (McCurley and Callard, 2008)
g6pd_Q1r	rev	CCTCCGCTTTCCTCTC	reviewed in (McCurley and Callard, 2008)
rpl13a_Q1f	fwd	TCTGGAGGACTGTAAGAGGTATGC	reviewed in (Tang et al., 2007)
rpl13a_Q1r	rev	AGACGCACAATCTTGAGAGCAG	reviewed in (Tang et al., 2007)
fsta Mo_Fw_3	fwd	CTGGTAACTGCTGGCTTCAAC	This study
fsta Mo_Rev_3	rev	CATTTGCCTTGATACTGGACCT	This study
fsta qPCR_Fw_3	fwd	CAACGATGGGATTGTTTACGC	This study
fsta qPCR_Rev_3	rev	GGCCTTGATGCATTTTCCTT	This study
sox9b qPCR_Fw_2	fwd	GACTACAAATACCAGCCCAGACG	This study
sox9b qPCR_Rev_2	rev	AACAGCGCATTGGTGGAGAT	This study
sox21a_1f	fwd	GCCCATGGATCATGTTAAGC	This study
sox21a_1r	rev	TGCAGCATATGCCAGGTAAG	This study

neurod4_1f	fwd	ACGGAAAACCAGGAGATGTG	This study
neurod4_1r	rev	GGCTCGAAAGCCATGTCTAA	This study
twist3_1f	fwd	CCCATTGAAGAAGAGCAGGA	This study
twist3_1r	rev	TAGTGAGTGGCGGACATGG	This study
med18_1f	fwd	CGTCACGGGTGGAACTATAAA	This study
med18_1r	rev	GGTGAACGAGAGGTTTGAGC	This study
olig4_1f	fwd	TCCTCGCCAGATCTCACAGT	This study
olig4_1r	rev	GAGAGGCTGGCACAAAGAAC	This study
taf5_1f	fwd	GCTGAAGGAACCAGAGATCG	This study
taf5_1r	rev	TGTCCAATATCCCACAGCAA	This study
ilf2_1f	fwd	GGAACCAAGACCTCAGTCCA	This study
ilf2_1r	rev	CTGGGTCTCCATGCTTTCAT	This study
GTF2A1L_2f	fwd	CAGTGGCCACCTTCTCTCTG	This study
GTF2A1L_2r	rev	GTCTGCGTCTCTCTCCTTCG	This study
MAPK12 (1 of 2)_1f	fwd	CAGGATTTTATCGCCAGGAG	This study
MAPK12 (1 of 2)_1r	rev	CTGTGTTGTCCATGGAGTGG	This study
CR354435.1_1f	fwd	CCACCGGCTAAAGCTCCTA	This study
CR354435.1_1r	rev	TCTTGGGCTTTGCAACTTTC	This study
CABZ01086354.1_1f	fwd	AAGAAGGGCTCCAAGAAAGC	This study
CABZ01086354.1_1r	rev	GTACTTGGTGACGGCCTTTG	This study
wu:fe11b02_1f	fwd	AAGACCGCACCCAAGAAAG	This study
wu:fe11b02_1r	rev	TGGAGCTGGTGTACTTGGTG	This study
FP236812.2_1f	fwd	AGGTAAAACCGGAGGCAAAG	This study
FP236812.2_1r	rev	CAGCCTTCTCGGTCTTCTTG	This study
mcm3_1f	fwd	GGGAGGCTCAGAGGGATTAC	This study
mcm3_1r	rev	CAGCACCTTCTCCACTCCTC	This study
zgc:171759.F_1f	fwd	ATGCCTGAACCCGCTAAAG	This study
zgc:171759.F_1r	rev	GAGCTGGTGTATTTGGTGACG	This study
rfc3_1f	fwd	GTGTGGCGATTTTCCTCATT	This study
rfc3_1r	rev	AAGGCCTCCAGGTGGTAGAT	This study
zgc:110216_1f	fwd	CCGCCAGCTAAAGCTCCTAA	This study
zgc:110216_1r	rev	TCTTGGGAGCGGCCTTCTTA	This study
mcm5_1f	fwd	TGTGGACACTGAAGGAGCAG	This study
mcm5_1r	rev	TAGCAAGTGACTCCGCAATG	This study
mcm4_1f	fwd	GTTTCAGCGTTTCCTTCAGC	This study
mcm4_1r	rev	GTAGATGCTGGGAGCCAGAG	This study
mcm7_1f	fwd	ATGGCCCCGAAGGATTATAC	This study
mcm7_1r	rev	AGCTCTTCATCGCTCAGCTC	This study
mcm2_1f	fwd	TAAACCCGGAGATGAGATCG	This study
mcm2_1r	rev	CCTGGTCCATCTGGTTGAGT	This study
rag2_1f	fwd	ACAACGAGCTGTCCTCCAGT	This study
rag2_1r	rev	CAGATATTGGGGTCCACCTG	This study
polr2b_1f	fwd	ATGAAATCACCCCTGACCTG	This study

polr2b_1r	rev	CGTTCTGCTCCTGAATCACA	This study
paics_1f	fwd	GTTCGGAAGGATCAGATGGA	This study
paics_1r	rev	ATGCGAAGAGACGACCAGAT	This study
drap1_1f	fwd	CGCCGGCTAGAATAAAGAAG	This study
drap1_1r	rev	TCATCATCGTCCTCCTCCTC	This study
thap11_1f	fwd	TGCGATTCTACACCTTTCCA	This study
thap11_1r	rev	TCCTCTTGATGATGGTGTTGG	This study
rfc4_1f	fwd	CAGGCGTTTCTGAAAGGTTC	This study
rfc4_1r	rev	GTGCGTGACTCCTTCTCCAT	This study
pcna_1f	fwd	CACGTCTGGTTCAGGGATCT	This study
pcna_1r	rev	TTTGACGTGTCCCATGTCTG	This study
mybl2_1f	fwd	CCCGTGTGCAGTCAGAAAG	This study
mybl2_1r	rev	TGTTGCCAGCACTGGTTTAG	This study
dnmt1_1f	fwd	ATTCCTCTGGCTCCTGGTTC	This study
dnmt1_1r	rev	TCTCCTGCTTCACAGGCTCT	This study
smarce1_1f	fwd	GCTATGGGAGATTGGCAAGA	This study
smarce1_1r	rev	CCTCAGGGGTGTTGTCTGAT	This study
tcf7l1a_1f	fwd	GCCTCTTCTTGACGTTCCTG	This study
tcf7l1a_1r	rev	ACGAGGTAGGGCTGTCACAC	This study
pold1_1f	fwd	ACTGAGGGAGGGGAGGACTA	This study
pold1_1r	rev	TCCTGCATACTCCTGTGCTG	This study
taf9_1f	fwd	GGAGTACGAACCCAGAGTGG	This study
taf9_1r	rev	CATCCTCATCTTCATGCTTCC	This study
klf2b_2f	fwd	CCAGAAGGAGAAGCTCTGGG	This study
klf2b_2r	rev	GCATGTATGTGTCGCCATGC	This study
FBXL19_1f	fwd	AGCCAGAGGAGGAGGAAGAG	This study
FBXL19_1r	rev	TCAGGTGGGAGTCTTTGAGG	This study
terfa_2f	fwd	ACAACCGGAGATTCACAGGG	This study
terfa_2r	rev	TCCCAGTGTCCCACACCATA	This study
smarcc1a_2f	fwd	CTGGCACAGCTCCTGAAGAA	This study
smarcc1a_2r	rev	GGAGGAGGACCTGGGTACAT	This study
arid2_2f	fwd	GGTTGATTTCCGAACAACGCA	This study
arid2_2r	rev	GGAGCACTAGGAGCGTTAGC	This study
sox9b_2f	fwd	GGACGAGCAGGAGAAGTTCC	This study
sox9b_2r	rev	GCTGCTCGCTGTACTCTGTA	This study
tcea3_1f	fwd	AGCCTGGATGGACGAAGAG	This study
tcea3_1r	rev	CCCCTGCCAAGACATTTTT	This study
rfx1a_1f	fwd	CAACTCCAGCATACGTGAGG	This study
rfx1a_1r	rev	ACGGACTGTAGGCTGGTGAC	This study
prox2_1f	fwd	CAAAGACGAAGAGTGCCACA	This study
prox2_1r	rev	CCTGACGAGCAAACTTCTCC	This study
dll4_1f	fwd	TGCAGGACTTTCTTCCGAGT	This study
dll4_1r	rev	CTTGTGAAAGCATGGGGAAT	This study

MRAS (1 of 2)_1f	fwd	GGCAAGAGCGCACTCACTAT	This study
MRAS (1 of 2)_1r	rev	ATTTGCCTTTCCGCTTTTTC	This study
fsta_1f	fwd	CCACCCGGGAATGATTTTAT	This study
fsta_1r	rev	CGCGACTCATCTTTGCATC	This study
dnmt5_1f	fwd	TGCATTCACTTGCAATCCAG	This study
dnmt5_1r	rev	AGATCTGCTGGGAAAGATGG	This study

2.3. Preparation, manipulation and analysis of DNA

2.3.1. Bacterial culture

Bacteria were grown at 37 °C for 9–18 hours in liquid culture of Luria-Bertani (LB) medium with shaking or solid culture (LB agar) and when necessary cultures were supplemented with 100 µg/ml of ampicillin.

2.3.2. Transformation of chemically competent *E.coli*

DH5α competent cells (NEB) were incubated with DNA at 4 °C for 30 minutes. Cells were heat shocked for 45 seconds at 37 °C and placed immediately at 4 °C for 2 minutes. Then, 600 µl LB was added and bacteria were grown for 60 minutes at 37 °C before plating on LB agar.

2.3.3. Isolation and sequencing of plasmid DNA

In order to isolate plasmid DNA, was used the Quicklyse mini-kit (Qiagen) following manufacturer's instructions. DNA was eluted in MiliQ and stored at -20 °C. The sequencing of the plasmids was done by semi-automated Sanger sequencing (*WIMM sequencing service*) with the appropriate primers and the respective sequences were blasted using National Centre for Biotechnology Information (NCBI) website and aligned with multiple alignment server ClustalW2.

2.3.4. Determination of nucleic acid concentration and purity

ND-1000 spectrophotometer was used to determine nucleic acid concentration (A_{260}) and purity ($A_{230:260:280}$). Purity was also determined when needed by the profile of the sample on an agarose gel.

2.3.5. Agarose gel electrophoresis

Nucleic acids were analysed in a 1% or 1.5% agarose/0.5 X TAE gel supplemented with 0.01% GelRed (Cambridge Bioscience). The gel was run at 100 V in 0.5 X TAE and the nucleic acid was visualised/photographed/analysed using ChemiDoc MP System and Image Lab software (BioRad). 100 bp and/or 1KB DNA ladders (NEB) were used.

2.3.6. Restriction enzyme digestion and DNA ligation

DNA was digested for 2-16 hours with the specific restriction enzyme and buffer (NEB) following manufacturer's instructions. To confirm the digestion, part of the sample was analysed by electhrophoresis. The ligations were performed in general, using a 1:1 molar ratio of the DNA fragment to the vector (pGEM-T Easy) and using T4 DNA ligase and ligase buffer (Promega) following manufacturer's instructions. The ligation reactions were incubated overnight at 4 ºC and then used to transform bacteria.

2.3.7. DNA purification and gel extraction

DNA was clean by QIAGEN QIAquick PCR Purification Kit (Qiagen) following manufacturer's instructions. For the gel extraction of DNA, after electrophoresis the gel was placed on a UV box and the specific band which we wanted purify was cut and purified using QIAquick Gel Extraction Kit following manufacturer's instructions.

2.3.8. Polymerase chain reaction

PCR reactions were prepared using 10 pmol of forward and reverse primer and JumpStart taq (Sigma) following manufacturer's instructions. In general the PCR conditions used were: 95 ºC for 3 minutes and 30 cycles of: 95 ºC for 15 seconds; 56 ºC for 45 seconds and 72 ºC for 1 minute and 30 seconds; and a final step of extension of 72 ºC for 7 minutes. The reactions were analysed on agarose gels.

To perform colony PCR initially individual colonies were picked and resuspended in 20 µl of MiliQ. Then, the colony PCR reactions were prepared using 5 µl of the colony suspension, 10 pmol of forward and reverse primer and JumpStart taq (Sigma) following manufacturer's instructions. The PCR reactions were placed in the thermocycler (DNA engine) and the conditions used were: 95 ºC for 5 minutes and 30 cycles of: 95 ºC for 30 seconds; 55 ºC for 45 seconds and 72 ºC for 1 minute and 10 seconds; and a final step of extension of 72 ºC for 7 minutes. And by last the reactions were analysed on agarose gels for determine the positive clones and then, the remaining 15 µl of colony suspension from the positive colonies was used to inoculate liquid culture.

2.4. RNA preparation, manipulation and analysis

2.4.1. Isolation of total RNA

For total RNA isolation, the zebrafish embryos were homogenised in 500 µl TRIzol (Sigma) by a homogenizer. After, further 500 µl TRIzol the cell debris was removed by centrifugation. For the isolation of the nucleic acids was added 200 µl chloroform, the sample was mixed and centrifuged and the aqueous phase which contained the nucleic acids was removed for a new tube. Then, RNA was precipitated with 500 µl isopropanol; the supernatant was removed and the RNA pellet washed with ethanol 70% and centrifuged; Then RNA pellet was air dry and resuspended in MiliQ; For quantitative real-time PCR (qRT-PCR), the RNA isolation was performed using RNeasy Mini Kit (Qiagen) following manufacturer's instructions. Isolated RNA was stored at -80 °C.

2.4.2. Reverse transcription of RNA

In order to produce cDNA, the reverse transcription of RNA was performed using: 1 µg of RNA, 1 mM dNTPs (Invitrogen) and 25 ng/µL random primers (Invitrogen) for a total volume of 20 µl. RNA was made up to 10.5 µl and heated to 65 °C for 5 minutes, then placed at 4 °C for 3 minutes. After addition of 1X FS Buffer (Invitrogen), 0.1 M DTT (Invitrogen) and 0.5 µl Rnasin (Invitrogen) the tube was incubated at room temperature for 2 minutes and then 0.5 µl of reverse transcriptase RT - SuperScript III enzyme (Invitrogen) was added. Then the reaction was placed thermocycler (DNA engine) and the conditions used were: 21 °C for 10 minutes, 50 °C for 50 minutes and 85 °C for 5 minutes. For RT-PCR, was added to the cDNA 30 µl of MiliQ and 1 µl used per reaction. For qRT-PCR, was added to the cDNA 180 µl of MiliQ and 3 µl used per reaction. The cDNA was stored at -20 °C.

2.4.3. Quantitative real-time RT-PCR

qRT-PCR assays were performed using the Applied Biosystem 7500 real-time cycler and FAST SYBR green following manufacturer's instructions. We used FAST SYBR green master mix (Applied Biosystems) in a final volume of 20 µL containing 3 µL of cDNA diluted 1:10 in MiliQ, 1 µL of each primer and 18 µL of FAST SYBR green (Applied Biosystems). Each reaction was carried out in triplicate and the specificity of the primers was tested by the analysis of the melting curve. The data analysis was performed using the ΔΔCt method (Dussault and Pouliot, 2006). The Ct values were normalized to the *glucose-6-phosphate dehydrogenase* (*g6pd)* endogenous housekeeping gene. The result presented in the present study corresponds to one biological sample (with three technical replicates) but was reproduced in another biological sample. Error bars were representative of the standard deviation about the mean, and significance assessed by a two-tailed Student's t-test ($P < 0.05$ was considered to be significant).

2.5. Isolation and analysis of Protein

2.5.1. Deyolking of zebrafish embryos, polyacrylamide gel electrophoresis and western blotting

To perform western blot analysis approximated 40 zebrafish embryos per condition were deyolked in 500 μl of deyolking buffer (**Table 2.1**) followed by homogenization by pipetting through a 200 μl tip and shaken at 1100 rpm for 5 minutes at 4 ºC (Thermomixer, Eppendorf). Next, the supernatant was removed after centrifugation at 300 g for 30 seconds and the pellet was stored at -80 °C until necessary or was immediately lysed at 4 ºC with the lysis buffer (1 μl /embryo) (**Table 2.1**). In order to destroy genomic DNA, the samples were sonicated. Then, the samples were heated to 90 °C for 5 minutes and placed immediately at 4 °C. Supernatant proteins and Rainbow marker (Amersham) were run on 10% Bis-Tris polyacrylamide precast gel placed in MES SDS running buffer (Invitrogen) for 30 minutes at 100 V and afterwards at 200 V. Then the proteins were transferred to a Trans-Blot Turbo Mini nitrocellulose membrane (BioRad) by Trans-Blot Turbo transfer starter system (BioRad). The membrane was washed in tris-buffered saline with tween (TBST) and blocked for 1 hour in 5% non-fat milk (Sigma) in TBST. The blots were incubated in 1:500 rabbit anti-Follistatin a (Sigma SAB2701665) in blocking solution overnight at 4 °C. Then, the blots were washed 3 x 10 minutes in TBST and incubated in 1:10 000 anti-rabbit IgG – peroxidise antibody produced in goat (Sigma A0545) for 1 hour at room temperature and washed again 3 x 10 minutes. All antibody incubations and washes were performed with gentle rotation and rocking. The blots were laid on a flat surface and covered with enhanced chemiluminescence developing reagent (Santa Cruz Biotechnology, Inc) at room temperature for 5 minutes and placed into a plastic cover and exposed to photographic film (Kodak) in the dark for the appropriate time. The film was developed in *WIMM developing facility* following manufacturer's instructions and the image digitised at 300 dpi. After, the membrane was stripped with Restore Stripping buffer (Thermo Scientific) for 20 minutes at room temperature and re-blocking as mention above and incubated with monoclonal anti-β-Actin-peroxidase conjugated (Sigma A3854) at 1:35 000 as a loading control. Next was performed the washing and developing steps as mentioned above.

2.6. Construction and *in vitro* synthesis of antisense probes

2.6.1. Novel antisense probe constructs

The construction of novel antisense probes in the present study was performed through the amplification by PCR of approximately 500 – 1000 bp of the genes of interest using as template Wild type (Wt) cDNA of 26 hpf zebrafish embryos and specific primers designed based on ENSEMBL sequences (www.ensemble.org) (**Table 2.3**). The PCR product was analysed in agarose gel and cloned into the pGEM-T Easy vector system (Promega) following manufacturer's instructions. Then, was performed colony PCR for some of the resultant colonies, and the positive clones were grown and plasmid DNA was extracted and sequenced with T7 and Sp6 primers to confirm which restriction enzyme and RNA polymerase should be used to linearize the plasmid and synthesised the probe respectively.

2.6.2. *in vitro* synthesis of antisense probes

For the synthesis of the antisense probes was prepared a reaction of 20 µl containing: 1 µg of linearised DNA plasmid; 1 µl of appropriate RNA polymerase (Sp6, T3 or T7) (**Table 2.4**), 0.5 µl RNaseOUT (Invitrogen), 2 µl DIG-dUTP NTP mix (Roche) and the appropriated buffer. The reaction was incubated at 37ºC during at least 2 - 6 hours depending of the RNA polymerase. Then, was added 1 µl of DnaseI (NEB) and the reaction was incubated for 15 minutes at 37 ºC. To stop this reaction 80 µl of MiliQ and ethylenediaminetetraacetic acid (EDTA) at a final concentration of 10 mM was added. After, the probe was precipitated with 1/3 volume 10 M ammonium acetate (NH_4Oac) and 2.5 volumes ethanol. The probe was then centrifuged at 4 ºC and the pellet was washed with 70% ethanol and centrifuged again; the pellet was air dried and resuspended with MiliQ. The purity of the probe was analysed on an agarose gel and the probe was stored at -20 ºC.

Table 2.4. - List of antisense riboprobes used in the present study.

Gene name	Restriction Enzyme	RNA Polimerase	Primer Forward (5'-3')	Primer Reverse (5'-3')	Reference
arid2	NdeI	T7	GGTTGATTTCCGAACAACGCA	GGAGCACTAGGAGCGTTAGC	This study
CABZ01086354.1	NsiI	T7	AAGACCGCACCCAAGAAAG	GTACTTGGTGACGGCCTTTG	This study
c-myb	EcoRI	T7			(Thompson et al., 1998)
CR354435.1	SacI	T7	CCACCGGCTAAAGCTCCTA	TCTTGGGCTTTGCAACTTTC	This study
dll4	SpeI	T7	TGCAGGACTTTCTTCCGAGT	CTTGTGAAAGCATGGGGAAT	This study
dll4	SpeI	T7			Martin Gering, unpublished
dnmt1	NcoI	Sp6	ATTCCTCTGGCTCCTGGTTC	TCTCCTGCTTCACAGGCTCT	This study
dnmt5	SphI	Sp6	TGCATTCACTTGCAATCCAG	AGATCTGCTGGGAAAGATGG	This study
drap1	NcoI	Sp6	CGCCGGCTAGAATAAAGAAG	TCATCATCGTCCTCCTCCTC	This study
FBXL19	ApaI	Sp6	AGCCAGAGGAGGAGGAAGAG	TCAGGTGGGAGTCTTTGAGG	This study
flk1	EcoRI	T7			(Fouquet et al., 1997)
foxn1	SalI	T7			(Wilkinson et al., 2009)
FP236812.2	SphI	Sp6	GGGAGGCTCAGAGGGATTAC	CAGCCTTCTCGGTCTTCTTG	This study
fsta	NcoI	Sp6	CCACCCGGGAATGATTTTAT	CGCGACTCATCTTTGCATC	This study
GTF2A1L	NcoI	Sp6	CAGTGGCCACCTTCTCTCTG	GTCTGCGTCTCTCTCCTTCG	This study
ikaros	SalI	T3			(Willett et al., 2001)
ilf2	SphI	Sp6	GGAACCAAGACCTCAGTCCA	ATGAAAGCATGGAGACCCAG	This study
klf2b	NcoI	Sp6	CCAGAAGGAGAAGCTCTGGG	GCATGTATGTGTCGCCATGC	This study
MAPK12 (1 of 2)	SphI	Sp6	CAGGATTTTATCGCCAGGAG	CTGTGTTGTCCATGGAGTGG	This study
mcm2	NcoI	Sp6	TAAACCCGGAGATGAGATCG	CCTGGTCCATCTGGTTGAGT	This study
mcm3	AatII	Sp6	ATGCCTGAACCCGCTAAAG	CAGCACCTTCTCCACTCCTC	This study
mcm4	SpeI	T7	GTTTCAGCGTTTCCTTCAGC	GTAGATGCTGGGAGCCAGAG	This study
mcm5	ApaI	Sp6	TGTGGACACTGAAGGAGCAG	TAGCAAGTGACTCCGCAATG	This study

mcm7	SpeI	T7	ATGGCCCCGAAGGATTATAC	AGCTCTTCATCGCTCAGCTC	This study
med18	NsiI	T7	CGTCACGGGTGGAACTATAAA	GGTGAACGAGAGGTTTGAGC	This study
mpx	EcoRI	T7			(Bennett et al., 2001)
MRAS (1 of 2)	NdeI	T7	GGCAAGAGCGCACTCACTAT	ATTTGCCTTTCCGCTTTTTC	This study
mybl2	SpeI	T7	CCCGTGTGCAGTCAGAAAG	TGTTGCCAGCACTGGTTTAG	This study
neurod4	SpeI	T7	ACGGAAAACCAGGAGATGTG	GGCTCGAAAGCCATGTCTAA	This study
olig4	NdeI	T7	TCCTCGCCAGATCTCACAGT	GAGAGGCTGGCACAAAGAAC	This study
paics	NcoI	Sp6	GTTCGGAAGGATCAGATGGA	ATGCGAAGAGACGACCAGAT	This study
pcna	SphI	Sp6	CACGTCTGGTTCAGGGATCT	TTTGACGTGTCCCATGTCTG	This study
pold1	NcoI	Sp6	ACTGAGGGAGGGGAGGACTA	TCCTGCATACTCCTGTGCTG	This study
polr2b	NcoI	Sp6	ATGAAATCACCCCTGACCTG	CGTTCTGCTCCTGAATCACA	This study
prox2	SpeI	T7	CAAAGACGAAGAGTGCCACA	CCTGACGAGCAAACTTCTCC	This study
rag1	HindIII	T7			(Willett et al., 1997)
rag2	NdeI	T3			(Willett et al., 1997)
rfc3	SpeI	T7	GTGTGGCGATTTTCCTCATT	AAGGCCTCCAGGTGGTAGAT	This study
rfc4	SphI	Sp6	CAGGCGTTTCTGAAAGGTTC	GTGCGTGACTCCTTCTCCAT	This study
rfx1a	NcoI	Sp6	CAACTCCAGCATACGTGAGG	ACGGACTGTAGGCTGGTGAC	This study
runx1	HindIII	T7			(Kalev-Zylinska et al., 2002)
smarcc1a	ApaI	Sp6	CTGGCACAGCTCCTGAAGAA	GGAGGAGGACCTGGGTACAT	This study
smarce1	NcoI	Sp6	GCTATGGGAGATTGGCAAGA	CCTCAGGGGTGTTGTCTGAT	This study
sox21a	SpeI	T7	GCCCATGGATCATGTTAAGC	TGCAGCATATGCCAGGTAAG	This study
sox9b	SphI	Sp6	GGACGAGCAGGAGAAGTTCC	GCTGCTCGCTGTACTCTGTA	This study
taf5	SphI	Sp6	GCTGAAGGAACCAGAGATCG	TGTCCAATATCCCACAGCAA	This study
taf9	NcoI	Sp6	GGAGTACGAACCCAGAGTGG	CATCCTCATCTTCATGCTTCC	This study
tcea3	SpeI	T7	AGCCTGGATGGACGAAGAG	CCCCTGCCAAGACATTTTT	This study
tcf7l1a	SpeI	T7	GCCTCTTCTTGACGTTCCTG	ACGAGGTAGGGCTGTCACAC	This study

terfa	NcoI	Sp6	ACAACCGGAGATTCACAGGG	TCCCAGTGTCCCACACCATA	This study
thap11	SphI	Sp6	TGCGATTCTACACCTTTCCA	TCCTCTTGATGATGGTGTTGG	This study
twist3	NdeI	T7	CCCATTGAAGAAGAGCAGGA	TAGTGAGTGGCGGACATGG	This study
wu:fe11b02	SpeI	T7	AGGTAAAACCGGAGGCAAAG	TGGAGCTGGTGTACTTGGTG	This study
zgc:110216	NdeI	T7	CCGCCAGCTAAAGCTCCTAA	TCTTGGGAGCGGCCTTCTTA	This study
zgc:171759.f	SphI	Sp6	CGCCCAAGAAGGGATCTAA	GAGCTGGTGTATTTGGTGACG	This study
hbbe1.1	XhoI	T3			(Quinkertz and Campos-Ortega, 1999)

The probes were produced using linearised plasmids digested with the indicated restriction enzyme and with the indicated RNA polymerase.

2.7. Wholemount *in situ* hybridisation

Wholemount *in situ* hybridisation (WISH) was performed in fixed embryos in 100% ethanol. Initially the embryos were rehydrated to PBST using a graded ethanol/PBST series (75%, 50% and 25% ethanol) and washed 4 x PBST; each wash was perform for 5 minutes at room temperature with gentle rocking. Then, the embryos were subjected or not to treatment with proteinase K, with a specific concentration in accord to their development stage. The treatment of proteinase K was stopped by washing the embryos 2 x 5 minutes with 2 mg/ml glycine in PBST at room temperature with gentle rocking. The embryos treated with proteinase K were washed 2 x 5 minutes with PBST at room temperature with gentle rocking and finally fixed with 4% PFA for 20 min. All the embryos (subjected or not to treatment proteinase K) were extensively washed 5 x 5 minutes in PBST at room temperature with gentle rocking. After this, the embryos were transferred to 50% hybe+/+ in PBST for 5 min, then 100% hybe+/+ for at least 1 hour at 65 °C. Finally, the embryos were incubated overnight at 65 ºC with probe diluted at 1:200 in hybe+/+.

The second and third day of the WISH protocol was performed using Biolane HT-1 *in situ* machine (Intavis) with gentle rocking. After removal of the probes the embryos were transferred to a plate of 24 or 48 wells and placed on *in situ* machine (Intavis). Embryos were washed at 65 °C through hybe -/- / 2 x saline sodium citrate (SSC) series, (100%, 75%, 25% hybe-/- in 2 x SSC, and a 100% 2 x SSC), each wash was done for 10 minutes; then the embryos were washed 4 x 15 minutes in 0.2 x SSC. At room temperature, embryos were washed through 0.2 x SSC / MABT series (75%, 50%, 25% 0.2 x SSC in MABT and 100% MABT) and each wash was done for 5 minutes. Then was done the blocking, incubating the embryos with MAB block for 1 hour at room temperature. The embryos were incubated with anti-DIG antibody (Roche) at 1:5000 in MAB block at 4 °C for 10 hours. After, the embryos were washed 8 x 15 minutes in MABT and 3 x 5 minutes in AP buffer at room temperature. After this the embryos were transferred for a disposable plate of 24 or 48 wells and was added the developing solution (BM Purple (Roche) mixed 1:1 with AP buffer) to the embryos. The plate was placed on the rocker at room temperature or 4 ºC and the staining was controlled by analysis under the light microscope; the staining was stopped by fixation in 4% PFA for at least 20 minutes at room temperature followed by 3 x 5 minutes washes in PBST at room

temperature with gentle rocking. For embryos older than 26 hpf a additional step of bleaching was performed in order to remove the pigments and so improve the analysis of the WISH signal The embryos were bleached with bleaching solution (**Table 2.1**) on a light box during the necessary time for their development stage; then were washed 3 x 5 minutes in PBST at room temperature with gentle rocking. After the PBST washes all the embryos were stored in 80% glycerol and placed at 4 ºC until their analysis under the microscope.

2.8. Embedding and Sections of Zebrafish Embryos

For histological analysis, embryos after WISH were fixed overnight in 4% PFA at 4 ºC. Fixed embryos were washed 2 x 30 minutes in PBST, and dehydrated in 50%, 70%,85%, and 95% of ethanol washes for 30 minutes each, and 3x 30 minutes in 100% ethanol, and then were stored overnight at 4ºC. Dehydrated embryos were washed 2 x 30 minutes in 100% xylene at room temperature and next in 1:1 xylene/wax for 45 minutes at 70 ºC. After the embryos were washed 4x 30 minutes in 100% wax at 70 ºC and incubated overnight in 100% wax at 70 ºC. Finally the embryos were mounted in the correct orientation in a plastic embedding container with 100% wax. Wax sections were prepared using a Leica rotary microtome and the resulting 10–15 µm sections were mounted onto glass slides. At last, the wax was removed from the sections through 3 x 5 minutes washes with xylene and the contrast staining was performed using neutral red (Vector Laboratories). The glass slides of the sections were place into the solution of neutral red for 3 minutes, rinse with water, and finally dehydrated with ethanol and clear with xylene.

2.9. Imaging zebrafish embryos

2.9.1. Still digital photography

In order to acquire pictures of the zebrafish embryos, the embryos were placed under a light dissecting microscope which had attached a Q-Imaging Micropublisher 5.0RTV camera with Q-Capture Pro 7 software. The embryos were mounted in 100% glycerol or for live

embryos were imaged in 1:30 E3 medium/MS222 or mounted in 3% methylcellulose. For the picture manipulation was used Adobe Photoshop CS5.

2.9.2. Wide field fluorescence imaging

For the analysis of transgenic lines the embryos were imaged on a SteREO Lumar.V12 microscope (Zeiss). The acquisition and analysis of the pictures were performed with the Zeiss AxioVision software. For the picture manipulation was used Adobe Photoshop CS5.

2.10. Bioinformatics tools: Blast and Sequence alignment

Sequences were blasted using NCBI website (www.blast.ncbi.nlm.nih.gov/) and aligned with multiple alignment server ClustalW2 (www.ebi.ac.uk/Tools/msa/clustalw2/) or MultiAlin (http://multalin.toulouse.inra.fr/multalin/).The schematic representation of genomic sequences of *fsta* was design using the program Exon-Intron Graphic Maker (http://wormweb.org/exonintron).

3. Identification of novel targets of both dll4 and runx1, involved in HSC specification

3.1. Introduction

Among the several signalling pathways important for the programming of arterial endothelium and/or HSC (Gering and Patient, 2005; Lawson et al., 2002; Wilkinson et al., 2009), the Notch pathway has been extensively studied and has been well established that this pathway is involved in arterial development (Lawson et al., 2001) and HSC emergence (Burns et al., 2009; Gering and Patient, 2005).

It was shown through the study of zebrafish embryos homozygous for a mutation in the ubiquitin ligase gene – *mind bomb* (*mib)* (which is required for Notch signalling), that Notch signalling is required for the generation of HSCs; these mutants lose *runx1* and *c-myb* expression in the VDA at 1 dpf and *rag1* in the thymus at 4 dpf (Burns et al., 2005; Gering and Patient, 2005, 2009). In addition to that, the requirement of Notch signalling in the generation of HSCs was also demonstrated through the analysis of zebrafish embryos treated with γ-secretase inhibitor (DAPT), which has also shown a lack of *runx1* expression (Gering and Patient, 2005, 2009). On the other hand, the analysis of *mib* mutant embryos and γ-secretase inhibitor treated embryos demonstrated that the requirement of Notch signalling in the primitive wave of haematopoiesis seems to be dispensable, since the primitive wave in these embryos was not affected (Burns et al., 2005; Gering and Patient, 2005). In general, the role of Notch signalling in inducing definitive haematopoiesis is well accepted. However, its role in HSC maintenance remains highly controversial (Bigas and Espinosa, 2012; Gering and Patient, 2009; Loeffler et al., 2011).

Although the requirement of Notch in haematopoiesis is well established and has been thoroughly described (Burns et al., 2009; Gering and Patient, 2005), there is still missing a detailed description about the ligands required. In zebrafish, two Notch ligands*, dllc* and *dl4*, are expressed in the DA (Lawson et al., 2001; Siekmann and Lawson, 2007). Recently, *dllc* together with *dld* (which is not expressed in the DA) has been described as a distinct non-cell-autonomous combination required for HSC specification in zebrafish (Clements et al., 2011). On the other hand, knockdown of *dll4* in zebrafish has previously only been described to cause an angiogenic (Hogan et al., 2009b; Leslie et al., 2007; Siekmann and Lawson, 2007) and lymphatic phenotype (Geudens et al., 2010). Both angiogenic and lymphatic phenotypes occur

later in development and the angiogenic phenotype which is observed earlier than the lymphatic phenotype, is not observed prior to 28-32 hpf (Geudens et al., 2010; Hogan et al., 2009b; Leslie et al., 2007). This indicates that when HSCs are first observed in the DA (24-27 hpf) the arterial programme is normal in *dll4* morphants. The expression of *Dll4* in mice has also been reported in the DA (Kumano et al., 2003; Robert-Moreno et al., 2005). However, mice carrying homozygous or heterozygous deletions of *Dll4* die early in development due to a severe arterial phenotype (Gale et al., 2004; Krebs et al., 2004) thus not allowing the use of mice as a model to study the role of *Dll4* in HSC emergence.

Taking into account the late angiogenic phenotype of the *dll4* zebrafish morphant (Leslie et al., 2007) and the impossibility of using mice to study the role of *Dll4* in HSC emergence (Gale et al., 2004; Krebs et al., 2004), the zebrafish is thus considered a good model to investigate the role of the dll4/Notch pathway in HSC specification.

Recent work performed in the lab, using a previously characterised splicing-morpholino spanning the splice donor sequence of exon 4 (Hogan et al., 2009b), has shown that knockdown of *dll4* in the zebrafish leads to the loss of *runx1* expression at 26 hpf in the VDA; which in turn results in HSC loss (Monteiro & Schneider, unpublished data). The loss in HSCs appears to not be transitory, since HSC specific markers at 36 hpf and progenitor markers of definitive lineages at 4 dpf were reduced (**Figure 3.1;** (Schneider, unpublished data)). These observations indicated that the lack of *runx1* at 26 hpf results in dysfunctional HSCs, in the absence of *dll4* (Schneider, unpublished data).

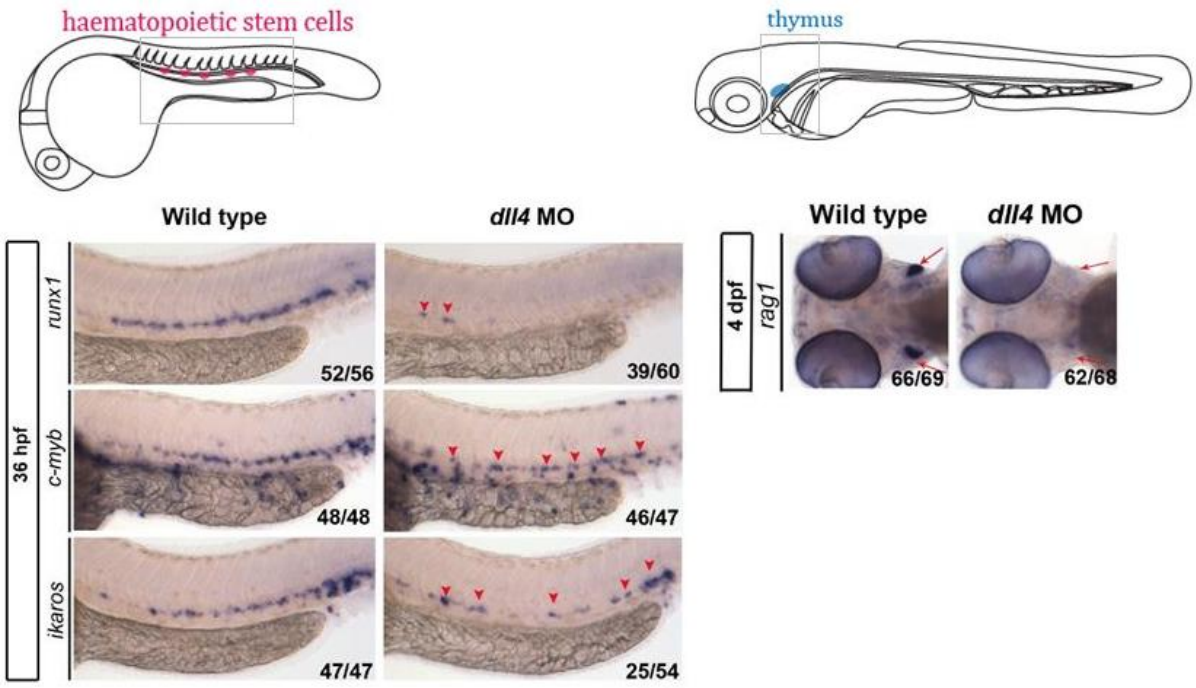

Figure 3.1- Knockdown of *dll4* leads to a decrease of HSC and HSCs derivatives. Analysis by WISH of the expression of *runx1*, *c-myb* and *ikaros* in 36 hpf *dll4* morphants and of *rag1* in 4 dpf *dll4* morphants; red arrows highlight the decreased expression of the markers analysed; (x/y), x - correspond to the number of embryos with the phenotype represented in the picture and y – total of embryos analysed. Figure adapted from (Schneider, unpublished data).

To better understand the molecular mechanism by which Dll4 induces HSC specification, we aimed to identify novel targets of Dll4 that are important to establish HSC specification. For that, was performed an mRNA-seq experiment of *dll4* morphants. Since, Dll4 plays an important role in other biological process and additionally could be acting in HSC specification through various effectors; an mRNA-seq experiment of *runx1* morphants was also performed to increase the possibility of identifies true targets of Dll4 in HSC specification. (Peterkin, Pinheiro & Schneider, unpublished data).

3.1.1 mRNA-seq experiment

In order to identify novel players involved in HSC specification, an mRNA-seq experiment of *dll4* and *runx1* zebrafish morphants at 26 hpf was performed previously in the lab (**Figure 3.2.;** (Peterkin, Pinheiro & Schneider, unpublished data)). 26 hpf was considered the ideal time in development for the identification of Dll4/Runx1 targets involved in HSC

specification since at this time the role of Dll4 is distinct from the later angiogenic role and because the circulation has started already (Peterkin, Pinheiro & Schneider, unpublished data). To minimise the dilution effect of the strong expression of *runx1* and *dll4* in the head, the embryos were dissected, the heads discarded and the trunks and tails used. These regions contain the DA, where HSCs emergence occurs and therefore the genes of interest should be enriched in this population. The mRNA-seq experiment and differential expression analysis was carried out by the High – Throughput Genomics Group at the Wellcome Trust Centre for Human Genetics, Churchill Hospital, University of Oxford.

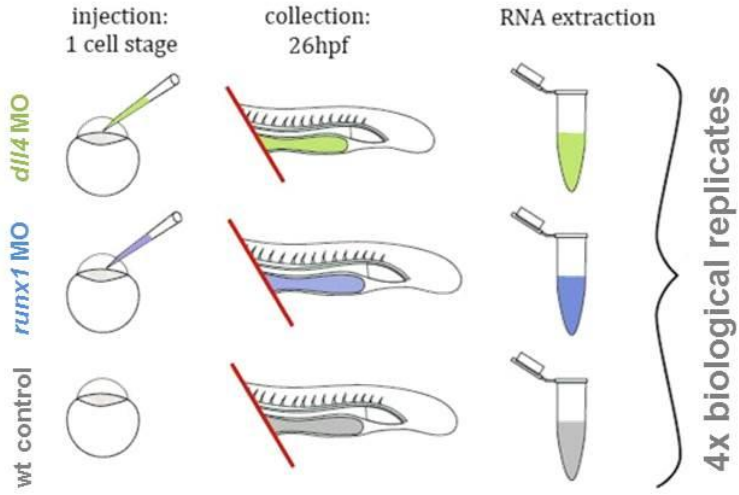

Figure 3.2 - Establishing *dll4* and *runx1* molecular targets in the zebrafish. mRNA-seq experimental setup: *dll4* morpholino (*dll4* MO4; **Table 2.1**) or *runx1* morpholino (*re6* MO; **Table 2.1**) were injected at the single cell stage. Trunk/tail regions were dissected for 200 embryos for each injection and 400 for the uninjected control at 26 hpf. Trunk/tails were collected for RNA extraction for each condition per experiment, in 4 replicates; MO – morphant. Figure from (Schneider, unpublished data).

The mRNA-seq experiment generated a list of raw data of approximately 30 000 genes. The analysis of this list was performed by excluding genes with less than 10 average reads per sample and genes which were not significantly differentially expressed across all biological replicates (High – Throughput Genomics Group at Wellcome Trust Centre for Human Genetics, Churchill Hospital, University of Oxford). The mRNA-seq experiment gave rise to a list of 1031 differentially expressed genes (397 genes up - regulated and 634 down - regulated) for *dll4* morphant fish and a list of 2347 differentially expressed genes (1135 genes up - regulated and

1212 genes down - regulated) for *runx1* morphant fish (**Figure 3.3**) (High – Throughput Genomics Group at Wellcome Trust Centre for Human Genetics, Churchill Hospital, University of Oxford). Surprisingly, since *runx1* is supposed to be down-stream of *dll4*, the number of genes differentially expressed in the *runx1* morphant list was more than the double the number of the *dll4* morphant list.

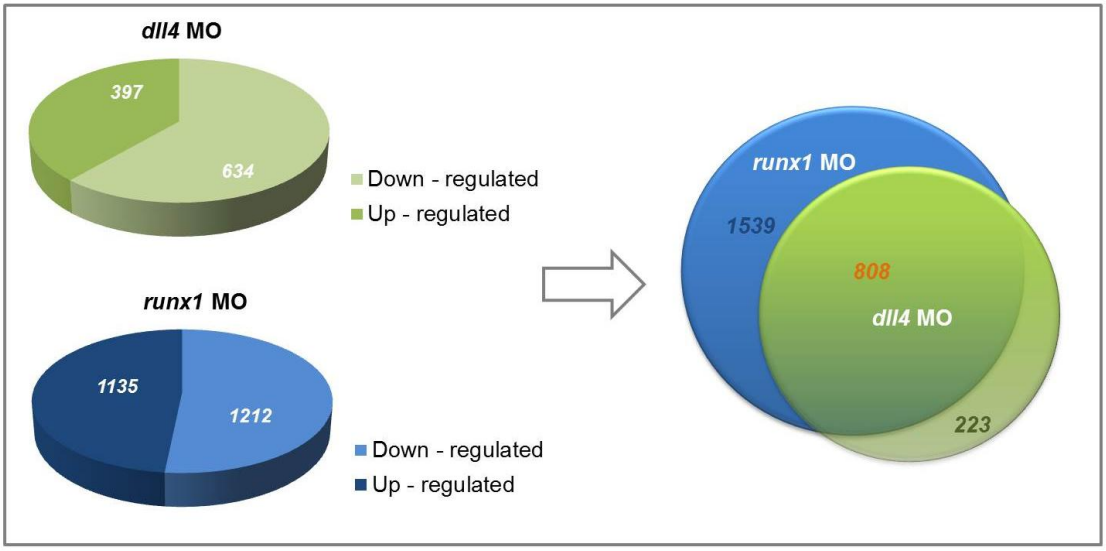

Figure 3.3 - Comparative analysis of the mRNA-seq experiment data. Analysis of the number of differentially expressed genes in both dll4 and runx1 morphants. Figure adapted from (Peterkin, Pinheiro & Schneider, unpublished data).

By comparing the *dll4* target genes to the *runx1* target genes, common target genes were established (Schneider, unpublished data). As both *runx1* and *dll4* are co-expressed in the DA at this time point, the overlapping mRNA-seq target list is likely to be enriched for genes involved in HSC formation. This has resulted in a list of 808 common genes (**Figure 3.3**). These target genes then were subjected to Go-term analysis. The Go-term analysis was carried out by Dr Jie Zuo from Prof. Patient's lab (WIMM, University of Oxford).

3.1.2. GO-Term analysis

HSC specification is tightly controlled at the transcription level (Wilkinson and Göttgens, 2013). The study of these transcriptional regulators such as TFs, epigenetic modifiers and

signalling pathway effectors is very important and will give us a better understanding of HSC specification, emergence, expansion, homeostasis and differentiation (Wilkinson and Göttgens, 2013).

The TFs are one of the early “decision makers” in the cell; they have the ability to regulate gene expression and ultimately to implement cell fate. Their identification is very important in order to gain new leads on the molecular and cell biological processes concerning HSC specification (Tanaka et al., 2012). In this project, TF activity and signalling pathway effectors were chosen over other GO-terms. The genes were annotated with “transcription activator”, “transcription repressor”, “transcription regulator”, “DNA binding” and “signalling” (Zuo, unpublished data).

Through Go-term analysis a list of 106 common target genes (20 genes up - regulated and 86 down - regulated) was obtained (Schneider & Zuo, unpublished data). The Go-term analysis data therefore appeared to provide a powerful filter by reducing candidate targets from over 800 to just 106 (**Figure 3.4.**).This analysis demonstrated strong enrichment for genes corresponding to “DNA binding” (approximately 58% of the common genes) and also a minor enrichment for genes corresponding to “transcription repressor” (approximately 2% of the common genes) (**Figure 3.4.**; (Zuo, unpublished data)).

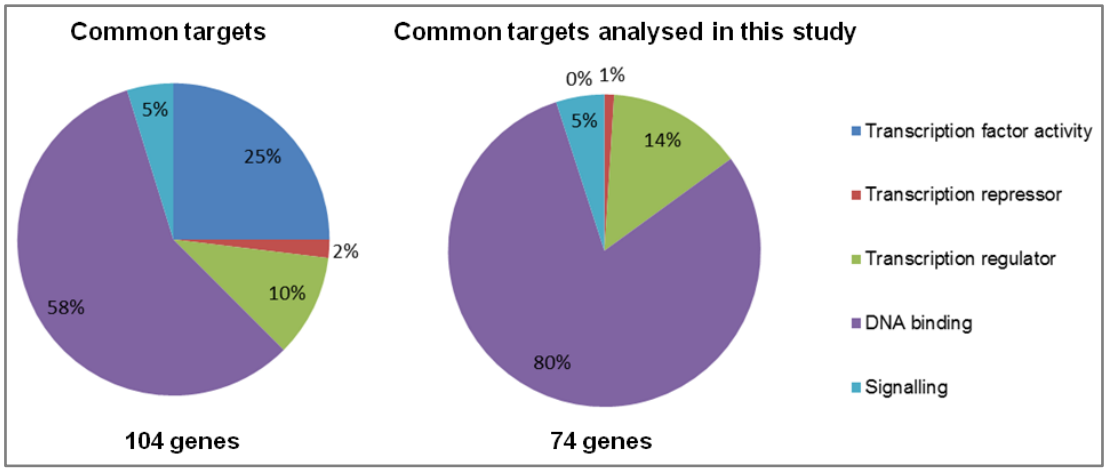

Figure 3.4 - Analysis of common targets of *dll4* and *runx1* by GO-term analysis. Through Go-term analysis the genes were annotated according to their transcription regulator activity with “transcription activator”, “transcription repressor”, “transcription regulator”, “DNA binding” or “ signalling”, identified as signalling pathway effectors. Figure adapted from (Peterkin, Pinheiro, Schneider & Zuo, unpublished data).

Interestingly, the common genes presented similar expression patterns in both morphants; in other words, a gene up or down - regulated in the *dll4* morphant was also up or down - regulated in the *runx1* morphant respectively (**Table 3.1.;** (Schneider, unpublished data)).

From the analysed list of the common target genes (**Table 3.1.**) the genes coding for epigenetic modifiers and duplicated genes, were not subjected to further analysis (**Table 3.1.** – red arrows). Epigenetic modifiers, have an important role in the control of cellular transcription. However, the TFs are the master controllers that establish a crosstalk with epigenetic modifiers in order to regulate the transcription levels in the cell. Taking this into account we decided to not analyse them throughout this study. The genes that appeared duplicated in the genome of zebrafish were further analysed by bioinformatics tools. Only genes which could be designed primers to specific amplify the gene were evaluated in subsequent analysis.

From the 74 genes present in the common list, 46 were analysed in the present study, once 28 of the genes present in the list had been determined as epigenetic modifiers or multiple copies of the same gene (**Table 3.1.** – red arrows).

Table 3.1 – List of common target genes of both *dll4* and *runx1* morphants analysed in the present study. From (Peterkin, Pinheiro & Schneider, unpublished data).

Associated Gene Name	Ensembl id	log2 Fold change *runx1* list	log2 Fold change *dll4* list	Transcription factor activity	Transcription repressor activity	Transcription activator activity	Transcription regulator activity	DNA binding	Signalling
		DOWN-REGULATED total = 68							
sox21a	ENSDARG00000031664	-1,31	-1,13		✓		✓	✓	
neurod4	ENSDARG00000003469	-1,54	-0,95				✓		
twist3	ENSDARG00000019646	-1,5	-1,48				✓		
med18	ENSDARG00000041237	-1,21	-0,94				✓		
olig4	ENSDARG00000052610	-1,05	-0,93				✓		
taf5	ENSDARG00000018325	-1	-0,92				✓		
ilf2	ENSDARG00000014591	-0,97	-1,05				✓	✓	
GTF2A1L	ENSDARG00000063670	-0,8	-0,91				✓		
MAPK12 (1 of 2)	ENSDARG00000006409	-1,42	-0,85						BMP + *vegf*
CR354435.1	ENSDARG00000051718	-1,77	-1,63					✓	
➢ **zgc:173552**	ENSDARG00000070287	-1,75	-1,42					✓	
➢ **zgc:173552**	ENSDARG00000051737	-1,75	-1,57					✓	
CABZ01086354.1	ENSDARG00000076129	-1,75	-1,59					✓	
➢ **CR762436.3**	ENSDARG00000074937	-1,7	-1,78					✓	
➢ **zgc:171759**	ENSDARG00000075216	-1,67	-1,7					✓	
➢ **zgc:171759**	ENSDARG00000034203	-1,64	-1,63					✓	
wu:fe11b02	ENSDARG00000078724	-1,63	-1,65					✓	
➢ **zgc:171759**	ENSDARG00000079909	-1,63	-1,78					✓	
➢ **CR354435.6**	ENSDARG00000070297	-1,64	-1,8					✓	
➢ **zgc:171759**	ENSDARG00000051778	-1,6	-1,5					✓	
FP236812.2	ENSDARG00000075220	-1,59	-1,78					✓	
➢ **H2BFM**	ENSDARG00000074491	-1,56	-1,63					✓	
➢ **zgc:110434**	ENSDARG00000051775	-1,5	-1,58					✓	

➢	**zgc:173552**	ENSDARG00000078294	-1,46	-1,67	✓
➢	**zgc:173552**	ENSDARG00000070282	-1,47	-1,51	✓
➢	**zgc:171759**	ENSDARG00000070289	-1,48	-1,61	✓
	mcm3	ENSDARG00000024204	-1,49	-1,08	✓
➢	**zgc:110434**	ENSDARG00000051770	-1,43	-1,65	✓
	zgc:171759	ENSDARG00000075482	-1,42	-1,62	✓
➢	**zgc:171759**	ENSDARG00000039547	-1,45	-1,47	✓
➢	**hist2h3ca1**	ENSDARG00000077587	-1,44	-1,61	✓
➢	**zgc:171759**	ENSDARG00000051726	-1,36	-1,64	✓
➢	**CU302436.2**	ENSDARG00000068928	-1,36	-1,54	✓
	rfc3	ENSDARG00000055969	-1,35	-1,19	✓
	zgc:110216	ENSDARG00000077456	-1,32	-1,49	✓
➢	**CR354435.5**	ENSDARG00000070286	-1,33	-1,38	✓
	mcm5	ENSDARG00000019507	-1,33	-0,97	✓
	mcm4	ENSDARG00000040041	-1,31	-1,03	✓
	mcm7	ENSDARG00000035761	-1,33	-1,25	✓
➢	**zgc:110434**	ENSDARG00000070265	-1,3	-1,49	✓
	mcm2	ENSDARG00000015911	-1,29	-1,04	✓
➢	**HIST2H4B (1 of 7)**	ENSDARG00000070285	-1,25	-1,18	✓
➢	**zgc:114037**	ENSDARG00000051736	-1,25	-1,48	✓
➢	**CR762436.4**	ENSDARG00000075379	-1,25	-1,23	✓
	rag2	ENSDARG00000052121	-1,26	-0,96	✓
➢	**FP236812.1**	ENSDARG00000074260	-1,26	-1,64	✓
	polr2b	ENSDARG00000012592	-1,26	-1,18	✓
	Paics	ENSDARG00000033539	-1,21	-0,94	✓
	drap1	ENSDARG00000041203	-1,21	-1,19	✓
	thap11	ENSDARG00000036055	-1,2	-1,07	✓
	rfc4	ENSDARG00000042458	-1,18	-1,03	✓

➢ **h2afx**	ENSDARG00000029406	-1,2	-1,16					✓	
➢ **CU682604.1**	ENSDARG00000068434	-1,17	-0,94					✓	
Pcna	ENSDARG00000054155	-1,11	-1,02					✓	
mybl2	ENSDARG00000032264	-1,08	-0,89					✓	
dnmt1	ENSDARG00000030756	-1,1	-0,83					✓	
smarce1	ENSDARG00000016871	-1,08	-1,08					✓	
tcf7l1a	ENSDARG00000038159	-1,04	-1,19					✓	
pold1	ENSDARG00000027689	-1,05	-0,92					✓	
taf9	ENSDARG00000077870	-1,04	-0,93					✓	
klf2b	ENSDARG00000040432	-0,96	-0,86					✓	
FBXL19	ENSDARG00000076929	-0,96	-1,06					✓	
Terfa	ENSDARG00000039302	-0,95	-0,95					✓	
➢ **HIST2H3A**	ENSDARG00000068941	-0,92	-1,16					✓	
➢ **msh6**	ENSDARG00000011666	-0,92	-1,02					✓	
smarcc1a	ENSDARG00000017397	-0,92	-1,04					✓	
arid2	ENSDARG00000007413	-0,81	-0,95					✓	
sox9b	ENSDARG00000043923	-0,7	-0,81					✓	
Associated Gene Name	**Ensembl id**	**log2 Fold change *runx1* list**	**log2 Fold change *dll4* list**	**Transcription factor activity**	**Transcription repressor activity**	**Transcription activator activity**	**Transcription regulator activity**	**DNA binding**	**Signalling**
		UP-REGULATED total = 6							
tcea3	ENSDARG00000004724	0,9	1,04				✓	✓	
rfx1a	ENSDARG00000005883	1,08	1,08				✓	✓	
prox2	ENSDARG00000041952	2,29	1,29				✓	✓	
MRAS (1 of 2)	ENSDARG00000062865	1,78	1,66						BMP
Fsta	ENSDARG00000052846	2,32	1,6						BMP
dnmt5	ENSDARG00000057863	1,17	1,11					✓	

3.2. Best candidate genes important for HSC specification

In order to investigate the common target genes with a most likely role in HSC determination, the 46 genes were initially assessed by expression pattern analysis. Through the analysis of the expression patterns, we aimed to establish whether the target genes were expressed in tissues related to HSC emergence, such as the DA or tissues surrounding the DA. The expression pattern analysis was carried out by WISH on 26 hpf embryos; the same developmental time as the mRNA-seq experiment was conducted. In fact, this time point coincides with when the HSCs can first be detected by in situ hybridisation in the DA (between 26 and 28 hpf) (**Figure 1.3**) (Bertrand et al., 2008; Bertrand et al., 2007; Kissa et al., 2008).

For expression pattern analysis, gene specific probes were designed and constructed. The construction of each probe involved the design of a specific pair of primers, to amplify a product of approximately 1000 bp. In order to amplify by PCR the region of each interesting gene, total mRNA was extracted from whole Wt embryos at the same developmental stage as the mRNA-seq experiment (26 hpf). cDNA was synthesised and the PCR was performed using the designed primers (**Table 2.3**). Subsequently, the PCR product was cloned into an expression plasmid and sequenced in order to confirm the correct gene sequence and determine which restriction enzyme and RNA polymerase should be used to linearize the plasmid and synthesise the probe respectively (**Figure 3.5**).

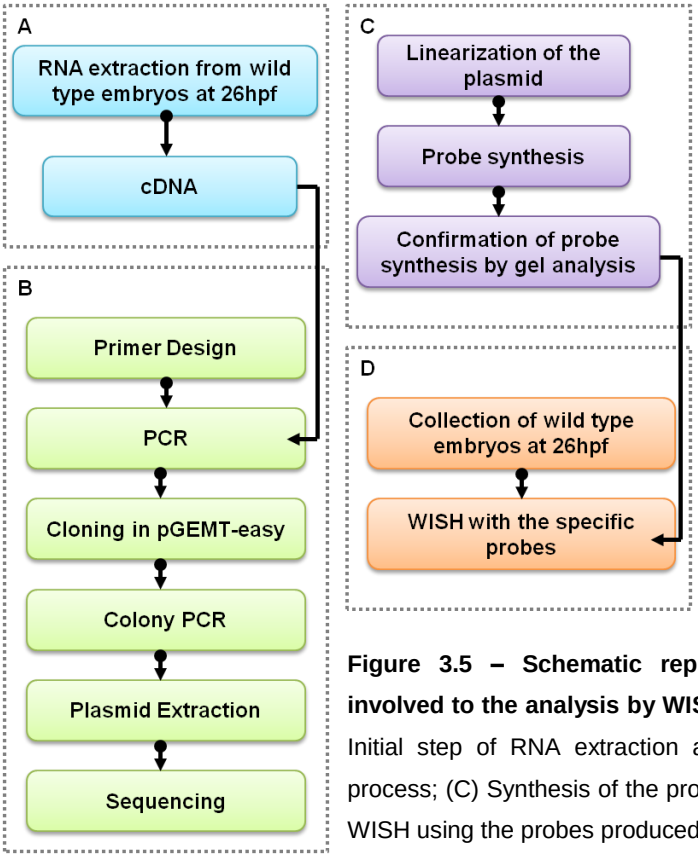

Figure 3.5 – Schematic representation of the different steps involved to the analysis by WISH for each common target gene. (A) Initial step of RNA extraction and production of cDNA; (B) Cloning process; (C) Synthesis of the probe; (D) Analysis of gene expression by WISH using the probes produced in (C).

It was not possible to produce successful probes for 9 genes; in which the cloning process was not successful.

The general WISH analysis, allowed us to group the different analysed genes into five classes, based on the expression pattern: (1) neural tissues, (2) neural tissue and DA region, (3) broad, (4) somites and (5) eye (**Figure 3.6 (B)**). This analysis showed that approximately 50% and 30% of the genes have either broad expression or are expressed in the neural tube and DA region, respectively, while several of them were exclusively expressed in neural tissues (**Figure 3.6 (B)**).

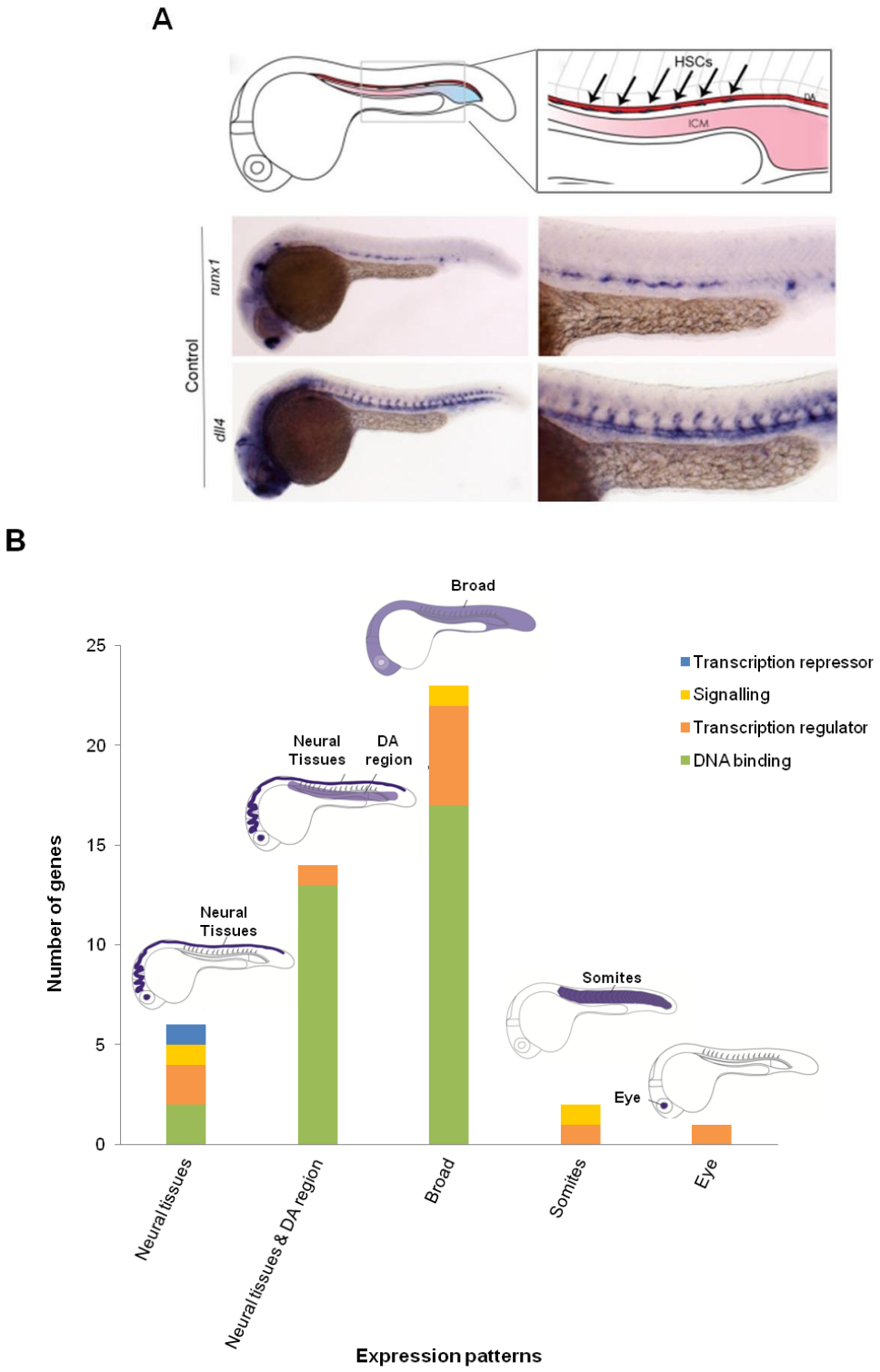

Figure 3.6 - Analysis of the expression patterns of mRNA-seq common target genes by WISH. (A) Analysis of expression pattern of *runx1* and *dll4* in 26hpf Wt embryos. Scheme adapted from (Monteiro, unpublished); (B) Graphic representation of the expression patterns obtained by the WISH screen of the common target genes of *runx1* and *dll4* morphants.

(1) Neural tissues – approximately 13% of the analysed genes had a specific expression in neural tissues, some specifically in the neural tube, such as *sox21a, neurod4, MAPK12, dnmt1*. All the genes were down-regulated in both morphants. However, the clear/clean expression pattern in the neural tissues, led us to exclude them from the most promising candidate genes having a possible role in HSC specification. Although, their possible involvement in HSCs cannot be completely discarded. Recently a functional interplay between the haematopoietic system and the sympathetic nervous system was described, showing that neuronal-mediated signalling from the developing sympathetic nervous system to the DA regulates haematopoietic stem cell emergence during embryogenesis (Fitch et al., 2012). This finding highlights the fact that HSC development needs to be viewed in the context of the development of other tissues (Fitch et al., 2012). On the other hand, it may reflect the importance of *runx1* and *dll4* during neural specification (Benedito and Duarte, 2005; Kobayashi et al., 2012; Theriault et al., 2005; Zagami and Stifani, 2010) (**Figure 3.7**).

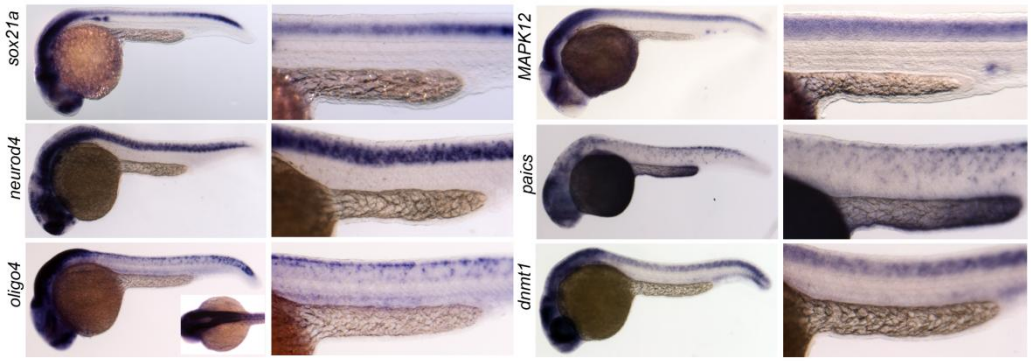

Figure 3.7 – Common target genes with expression pattern in neural tissues.

(2) Neural tissues and DA region – these embryos show an expression pattern in neural tissues, such as neural tube and/or individual neurons together with the expression on the region of the DA, although not specific to the DA. As already mentioned approximately 30% of the analysed genes had an expression pattern in neural tissue and the DA region. This expression pattern might possibly be the most interesting, due to their expression in the DA region. In this class, we observed the presence of several genes coding for conserved mini-chromosome maintenance proteins (MCM) which form

heterohexamers and play important roles in initiation and elongation during DNA replication (reviewed in (Ryu et al., 2005). In addition, other genes such as *pcna* and *replication factor C*, which are required for the elongation of primed DNA templates by DNA polymerase, had this expression pattern. These results indicated that both *runx1* and *dl4* morphants possibly affect the cell-cycle. (**Figure 3.8.**).

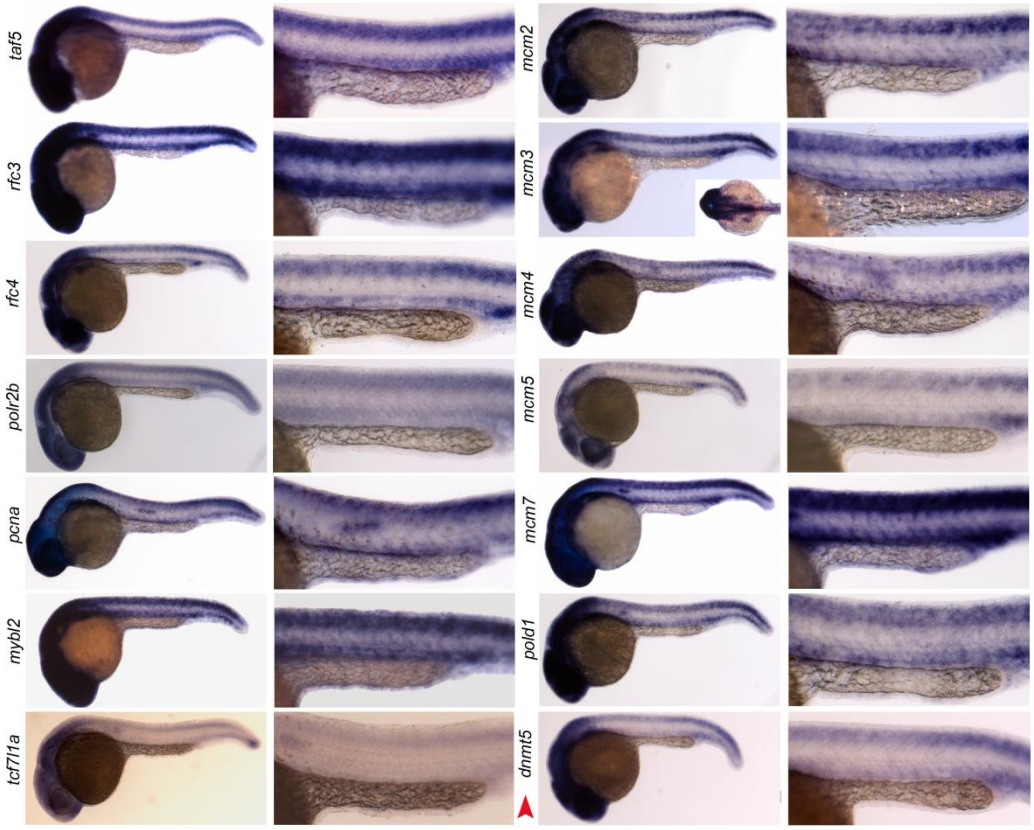

Figure 3.8 – Common target genes with expression patterns in neural tissues and the DA region (Red arrow indicates up-regulated gene in the morphants).

(3) Broad – the majority (50%) of the common genes had broad expression, reflecting possibly the general and pivotal role of these genes in the cell. Due to their broad expression, we cannot rule out expression in the DA; further analysis of gene expression on sections would be required.

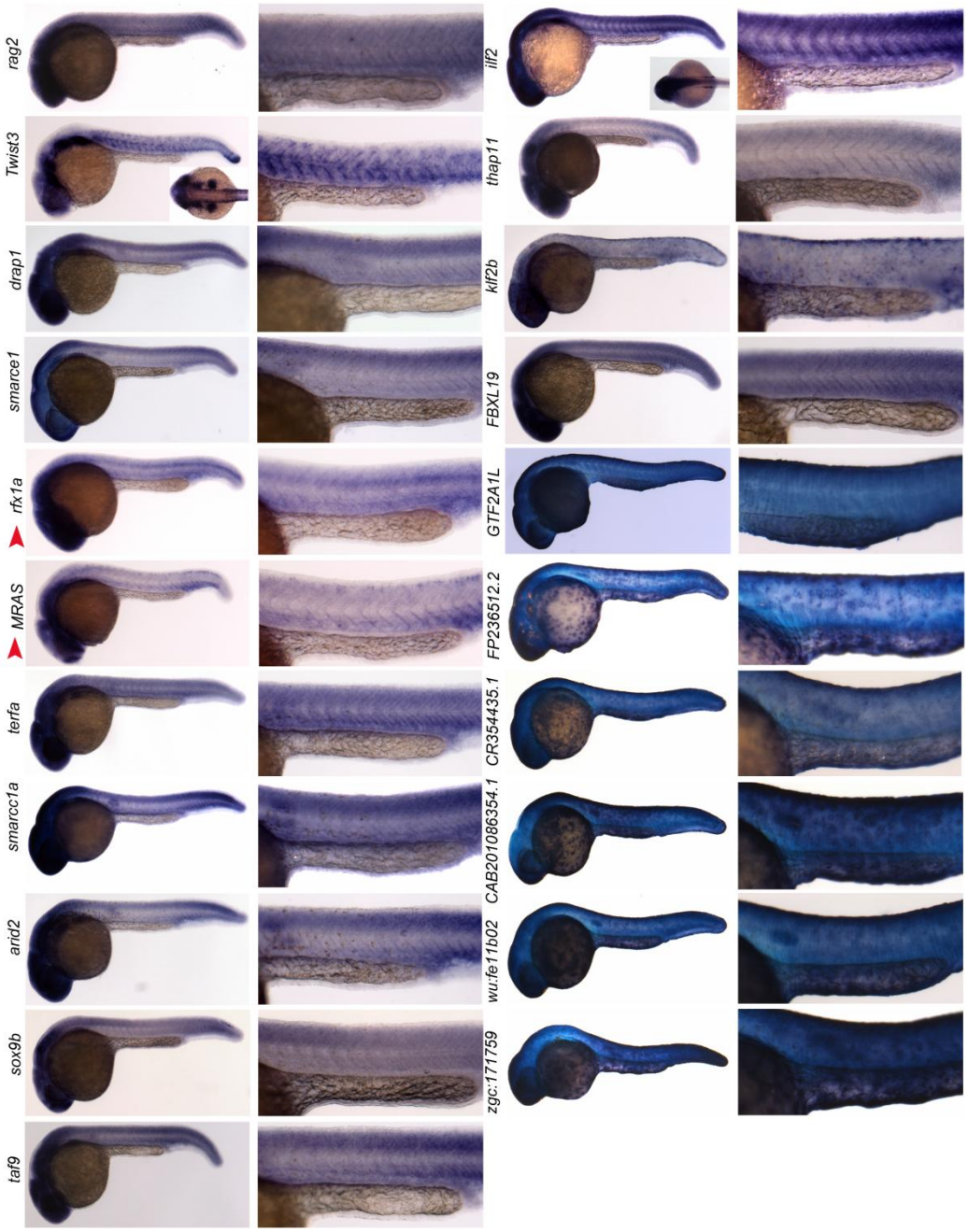

Figure 3.9 – Common target genes with broad expression pattern (Red arrows indicate up-regulated genes in the morphants).

(4) Somites – *tcea3* and *follistatin a (fsta)* are expressed in the somites. *fsta* is expressed in the ventral region of the somites, which is adjacent to the DA region and is known to play a role in setting up signals required for HSC emergence (**Figure 3.10** ; (Clements et al., 2011)).

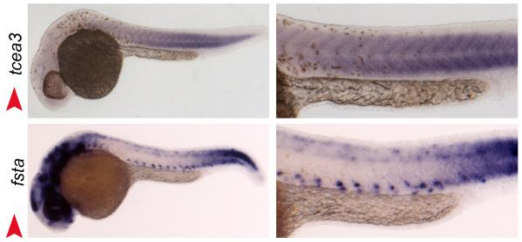

Figure 3.10 – Common target genes with expression patterns in the somites (Red arrows indicate up-regulated genes in the morphants).

(5) Eye – *prox2* is specifically expressed in the eye (**Figure 3.11 (A)**). As already described, the mRNA–seq experiment was performed using only the tail and trunk region of the fish. Thus, a further analysis of this gene would be required in order to understand whether ectopic expression is observed in the tail/trunk of the morphants. However, the analysis of the expression pattern of *prox2* in the morphants revealed a broad expression in the ventral posterior region of the tail, decreasing the likely importance of this gene in HSC emergence (**Figure 3.11 (B)**).

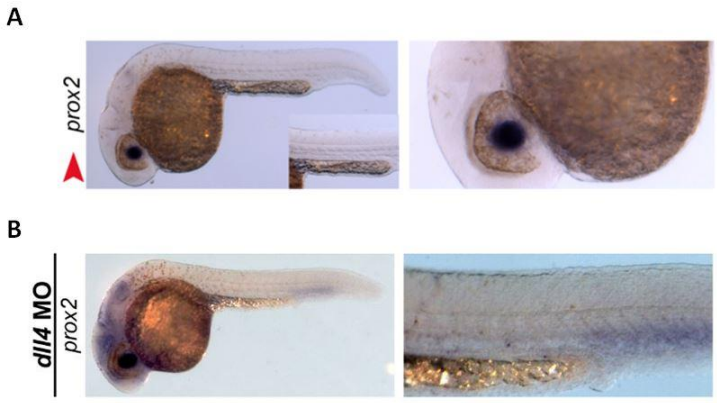

Figure 3.11 – Analysis of the expression pattern of the common target gene *prox2*. (A) Expression pattern in Wt zebrafish at 26 hpf (Red arrow indicates up-regulated genes in the morphants); (B) Expression pattern in *dll4* morphants at 26 hpf.

Through the analysis of the expression patterns by WISH, we did not find any gene specifically expressed in the DA region. And so we were not able to identify which Dll4 and Runx1 target genes are most likely to play a role in HSC development. However, the expression patterns classified as neural tube and DA region and broad are likely to be the most promising

ones. Taking into account these results, and in order to take advantage of the screen information, we looked carefully into each gene analysing its possible roles through the annotated result and literature review. We were looking for a relationship between the analysed genes and known players in HSC programming

During the literature search, several genes came to our attention, including: *twist3*, *rag2* and *zgc:110216.* The recent work of Cannon *et al*. has shown that the transcripts of *twist3, rag2* and *zgc:110216* (genes present in our list) are enriched threefold or more in the blood and/or vascular endothelial cells compared with the rest of the embryo at 26 – 28 hpf (the same time period of the mRNA-seq experiment) (Cannon et al., 2013). In addition to these genes, *MRAS* has also been annotated as an important player in the BMP signalling. The importance of BMP signalling in HSC specification is well established (Wilkinson et al., 2009). Finally, *sox9b* and *fsta* have also come to our attention. Dalcq and colleagues have suggested that *sox9b* together with *runx3*, EGR1 and *fsta* form a regulatory cascade required to modulate BMP-signalling during cranial development in zebrafish (**Figure 3.12.**; (Dalcq et al., 2012)). Indeed, *fsta* was annotated as a signalling molecule important in BMP pathway (Go-term analysis; Zuo, unpublished data).

In the possible network model described by Dalcq and colleagues, in Wt embryos, pharyngeal endoderm expresses a regulatory cascade composed of three TFs, *runx3, erg1* and *sox9b*, which down-regulates *fsta* expression; this down-regulation of *fsta* allows the binding of BMP ligands to their receptor and consequently induces *runx2b* expression in cranial neural crest cells (**Figure 3.12 (A -1.)**; (Dalcq et al., 2012)). However embryos lacking any of the *runx3-erg1-sox9b* cascade have an overexpression of *fsta* and consequently the BMP ligands are unable to bind their receptor and so there is no BMP signalling in cranial neural crest cells and no *runx2* expression (**Figure 3.12 (A -2.);** (Dalcq et al., 2012)).

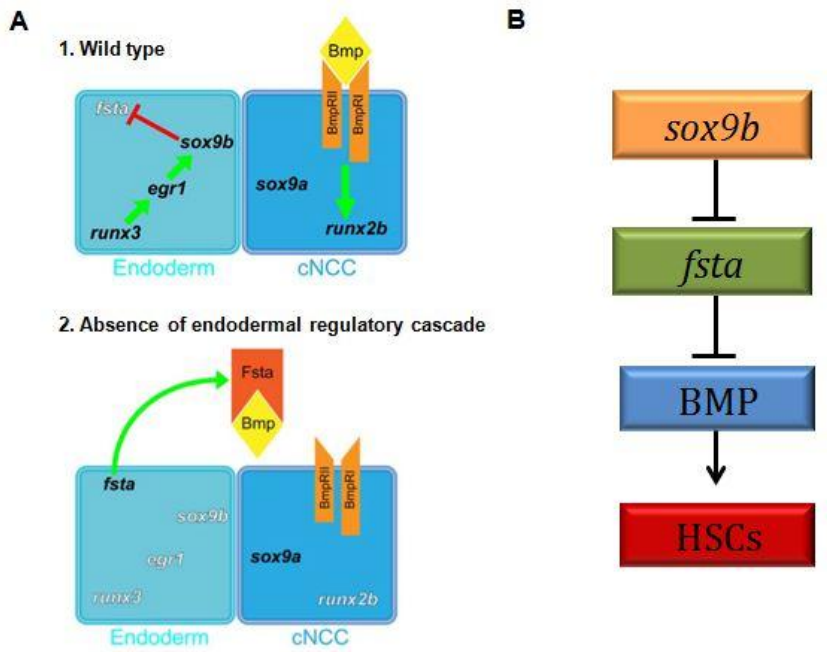

Figure 3.12 – Schematic network of *sox9b* and *fsta*. (A) Regulatory cascade required to modulate BMP-signalling during cranial cartilage development in zebrafish – Signalling model in Wt embryos (1.) and in embryos lacking the endodermal regulatory cascade (2.) Adapted from (Dalcq et al., 2012); (B) Scheme of a possible network to induce HSCs.

The mRNA-seq analysis showed that inhibition of *dll4* or *runx1* signalling leads to a decrease of *sox9b* expression and an increase of *fsta* expression (**Table 3.1;** Peterkin, Pinheiro, & Schneider, unpublished data). This is in accordance with the signal model described by Dalcq *et al.* In addition, it is well established that Follistatin a is a signalling molecule important for BMP signalling, it is known as an antagonist of BMP (Bauer et al., 1998). Moreover it has been described that inputs from BMP signalling are required to correctly programme the first HSCs (Wilkinson et al., 2009).

Altogether, this makes *sox9b* and *fsta* good candidates to play an important role in HSC emergence (**Figure 3.12**).

3.3. *follistatin a* is up – regulated and *sox9b* is down - regulated in both *dll4* and *runx1* morphants.

To validate the results of the mRNA-seq for *fsta* and *sox9b*, qRT-PCR was performed by using mRNA from tails and trunks of zebrafish embryos at 26 hpf of both *dll4* and *runx1* morphants (experimental procedure was carried out by Janina Schneider from Prof. Patient's lab (WIMM, University of Oxford)). The qRT-PCR was performed using specific primers for *fsta* and *sox9b* (**Table 2.3**) and *g6ph* was used as a housekeeping gene for normalisation. This analysis was performed using two different morphants of *runx1*, *re6* MO (the morpholino used in the mRNA-seq experiment) and *re1* MO (used as a known null-inducing positive control) and one morphant of *dll4* (*dll4* MO4).

Our results showed an up-regulation of *fsta* expression levels in both *dll4* and *runx1* morphants (**Figure 3.13 (A)**). *runx1 m*orphant: *re1* MO – 4.4 fold change ± 0.048 ($P < 0.001$); *re6* MO – 5.5 fold change ± 0.419 ($P < 0.001$); *dll4 m*orphant: *dll4* MO4 – 2.7 fold change ± 0.232 ($P < 0.001$). The results obtained reproduce one biological sample (with three technical replicates) but was reproduced in a second biological sample. Error bars are representative of standard deviations from three technical replicates. Moreover, WISH analysis also demonstrated an up-regulation of *fsta* expression in both *runx1* and *dll4* morphants. In the *dll4* morphants, 58 out of 101 embryos had *fsta* gene expression increased when compared with Wt. For *runx1* morphants, 16 out of 19 embryos had *fsta* expression increased when compared with Wt (**Figure 3.13 (B)**).

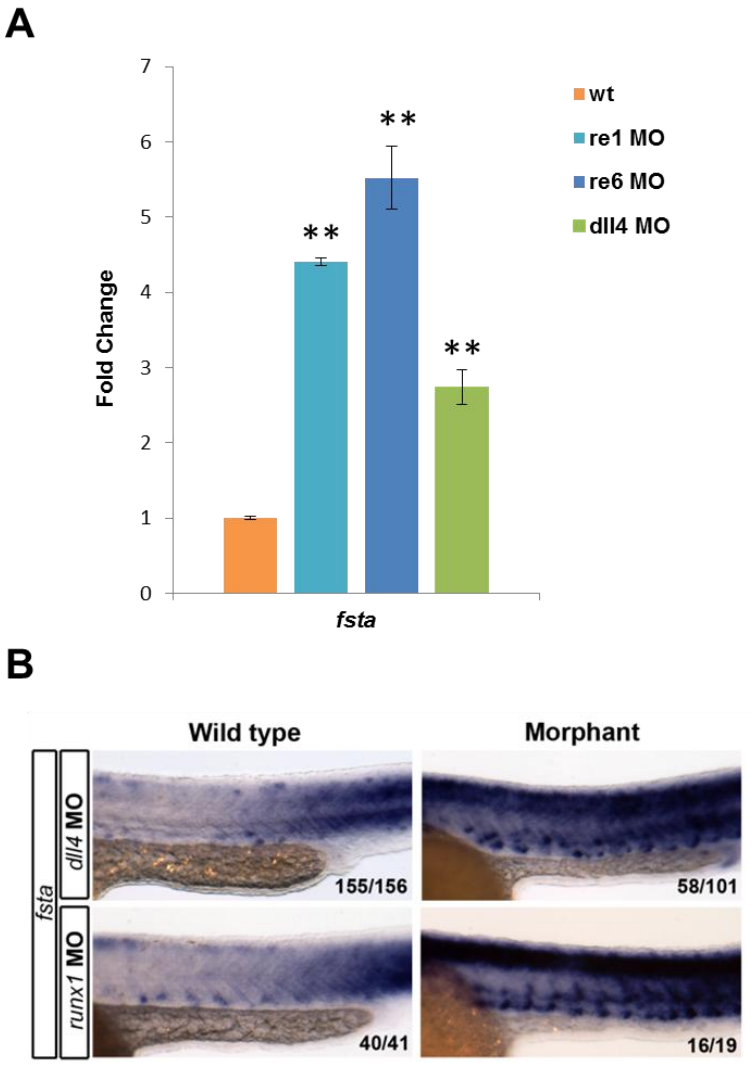

Figure 3.13 –. Analysis of the levels of *fsta* expression in both *dll4* and *runx1* morphants. (A) Quantitative RT-PCR analysis of *fsta* expression in both *dll4 (dll4* MO4) and *runx1* (*re1* MO and *re6* MO) morphants. Error bars are representative of the standard error from three technical replicates; ** $P < 0.001$. (B) WISH analysis of *fsta* expression in both *dll4 (dll4* MO4) and runx1 (*re6* MO) morphants.

Interestingly, and in according with the mRNA-seq experiment, the analysis of *sox9b* expression by qRT-PCR in both morphants has revealed down-regulation of *sox9b* expression levels. Nevertheless, the fold change observed for both morphants was not significantly different (*runx1 m*orphant: *re1* MO – 0.9 fold change ± 0.046 ($P < 0.01$); *re6* MO – 0.7 fold change ± 0.011 ($P < 0.001$); *dll4 m*orphant: *dll4* MO4 – 0.8 fold change ± 0.034 ($P < 0.001$)) (**Figure 3.14 (A)**). Analysis by WISH for *sox9b* in *dll4* morphants was performed however its broad expression made the analysis very difficult. We conclude that WISH is not sensitive enough to determine changes in the expression levels of *sox9b* (**Figure 3.14 (B)**).

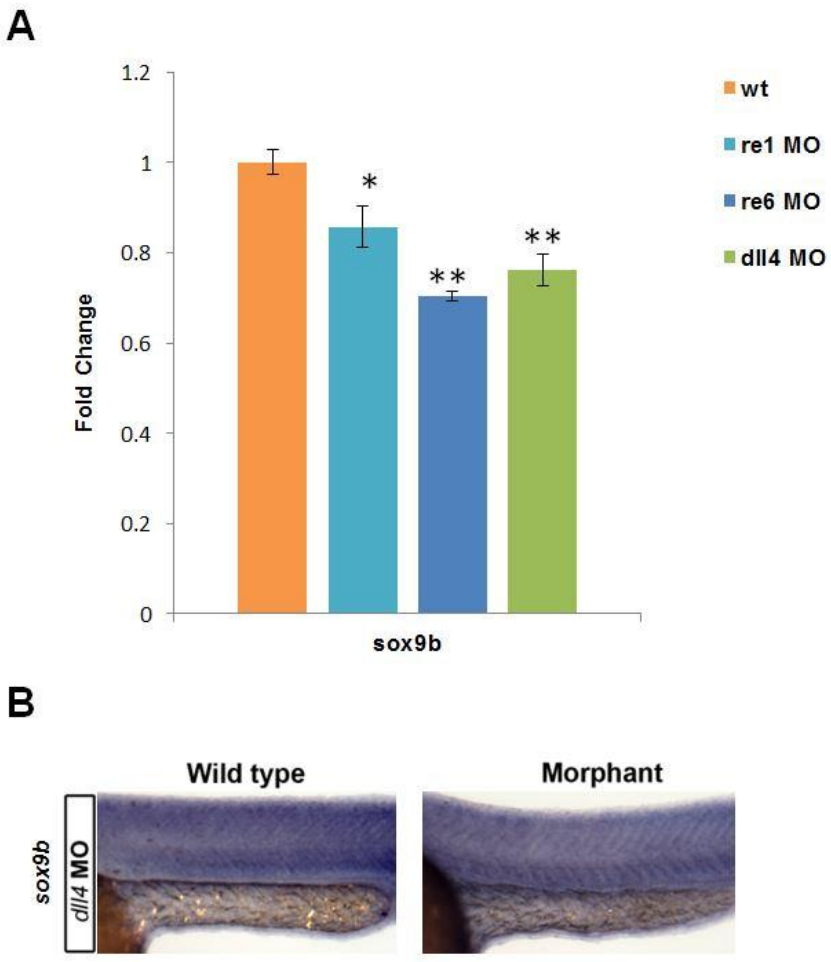

Figure 3.14 – Analysis of the levels of *sox9b* expression in both *dll4* and *runx1* morphants. (A) Quantitative RT-PCR analysis of *fsta* expression in both *dll4 (dll4* MO4) and *runx1* (re1 MO and re6 MO) morphants. Error bars are representative of the standard error from three technical replicates; * $P < 0.01$ ** $P < 0.001$. (B) WISH analysis of *fsta* expression in *dll4* morphants *(dll4* MO4).

Together these results provided additional support for the validity of the mRNA-seq experiment data and identified *fsta* as a more promising candidate target gene compared to *sox9b*. To further explore the potential role of *fsta* in HSC specification, we next performed a knockdown experiment (section **4.** of this thesis).

3.4. Discussion

Here, through the analysis of expression patterns of the previously identified common target genes in both *dll4* and *runx1* morphant lists by WISH, and a careful literature review of each gene, we identified some possible candidate genes including: *twist 3, rag2, zgc:110216, MRAS, sox9b* and *fsta*. However we decided to further explore the potential role of *fsta* in HSC specification given its role in antagonizing the BMP pathway, which in turn is required for HSC specification (Bauer et al., 1998; Wilkinson et al., 2009). Curiously, we detected more significant differential expression levels of *fsta* in both morphants when compared with *sox9b* expression pattern, which in turn was specific and stronger in the ventral region of the somites, adjacent do the DA region.

Furthermore, we concluded that using WISH as a methodology to address the question whether target genes obtained from the mRNA-seq experiment have a possible role in the haematopoietic process, is possibly not the most informative methodology. As an alternative approach, we could have done a morpholino screen instead of WISH but this would have been prohibitively expensive.

Nevertheless, through this screen, we were able to conclude that neural signalling is being affected in both morphants, since several of the target genes had an expression pattern in neural tissues. However, as we already mentioned such pathways might be related to HSC development; both morphants possibly are affecting the cell-cycle, since several cell-cycle related TFs were affected in both morphants. It will be important to gain insight into these topics and their possible relation to HSCs.

The up-regulation of the mRNA expression levels of *fsta* in both *dll4* and *runx1* morphants (**Figure 3.15 (A)**) and the expression pattern of *fsta* in the ventral region of the somites together with the Follistatin a role as an antagonist of BMP (**Figure 3.15 (B. i.)**; (Bauer et al., 1998)) and the requirement of BMP in HSC specification, previously described (**Figure 3.15 (B. ii.)**; (Wilkinson et al., 2009)), make *fsta* an interesting candidate gene for further exploration of its potential role in HSC development.

A. mRNA-seq Results

Gene	log2fold change *runx1*	log2fold change *dll4*
fsta ↑	2.32	1.6

B. Literature Review

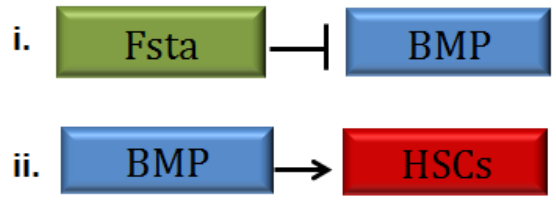

C. Hypothesis

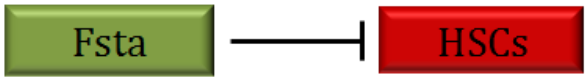

Figure 3.15 – Schematic hypothesis of the role of *fsta* in HSC emergence. (A) Expression levels of *fsta* in both *dll4* and *runx1* morphants obtained by mRNA-seq (Peterkin, Pinheiro & Schneider, unpublished data). (B) Literature review observations: i. Follistatin a is an antagonist of BMP (Bauer et al., 1998); ii. BMP is required for HSC specification (Wilkinson et al., 2009). (C) Hypothesis of the role of fsta in HSC emergence; Fsta – Follistatin a.

Thereby to further explore the potential role in HSC specification of Follistatin a we decided to perform a functional analysis by knockdown of *fsta* using a morpholino (section **4.** of this thesis).

4. Role of *follistatin a* in regulating HSC specification during zebrafish development.

4.1. Introduction

Follistatin, a secreted glycoprotein, was originally described as an inhibitor of activins by Nakamura and colleagues (Nakamura et al., 1990). This protein binds directly to activins with high affinity, and functions as an activin antagonist, preventing the binding of activins to their transmembrane receptors (de Winter et al., 1996). In addition, it has been reported that Follistatin also binds with lower affinity to several other members of the TGF-β superfamily, modulating their actions. These include myostatin, growth differentiation factor-9 (GDF-9), $TGF\beta_3$ and BMPs, including BMPs 2, 4, 6, 7, 11 and 15 (Amthor et al., 2002; de Kretser et al., 2012; Gamer et al., 1999; Glister et al., 2004; Iemura et al., 1998; Li et al., 2011; Otsuka et al., 2001; Thompson et al., 2005; Zong et al., 2013). Although Follistatin interacts directly with BMP, it does not prevent the ligand binding to its own receptor (Iemura et al., 1998). However, it has been suggested that conformational changes of BMP caused by Follistatin binding prevent receptor activation. The interaction between Follistatin and BMP seems to be subtype specific; where distinct affinities have been observed for the different BMPs (Iemura et al., 1998).

Mammals and birds have single copies of *Follistatin* gene while zebrafish, presumably as a result of an ancient duplication of the genome, has two orthologues of the mammalian *Follistatin* gene: *follistatin a* (*fsta*) (Gene ID: ENSDARG00000052846) and *follistatin b (fstb)* (Gene ID: ENSDARG00000057992). Nevertheless *fsta* is more closely related to its mammalian orthologues than *fstb* (Dal-Pra et al., 2006; Macqueen and Johnston, 2008). Indeed, alignment of vertebrate orthologues of Follistatin revealed a high degree of conservation at the protein level (**Figure 4.1.**). At the protein level, Follistatin a shares around 70%-75% identity with human and mouse Follistatin, whereas Follistatin b shares around 66-68% identity with its human and mouse orthologues (**Figure 4.1.**).

A

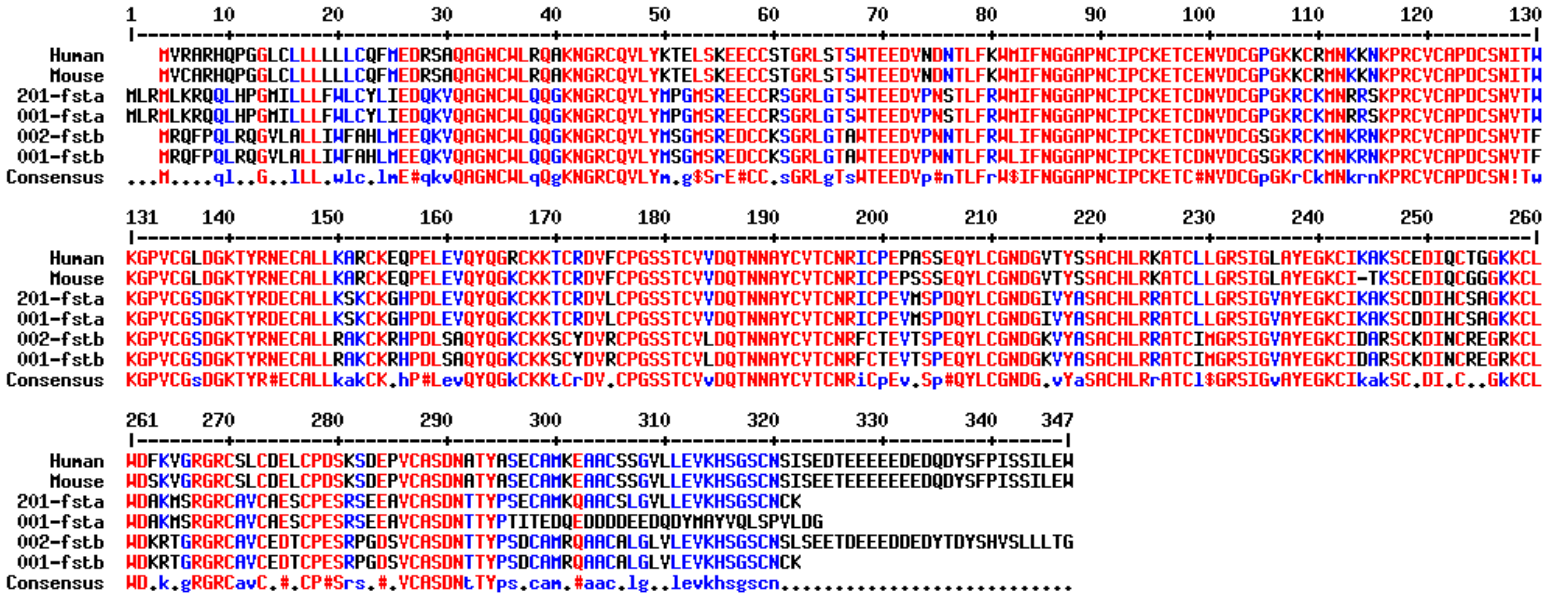

B

SeqA	Name	Length	SeqB	Name	Length	Score
1	Human	344	2	Mouse	343	97.67
1	Human	344	3	201-fsta	322	74.84
1	Human	344	4	001-fsta	324	70.06
1	Human	344	5	002-fstb	344	65.99
1	Human	344	6	001-fstb	319	68.03
2	Mouse	343	3	201-fsta	322	74.53
2	Mouse	343	4	001-fsta	324	69.75
2	Mouse	343	5	002-fstb	344	66.18
2	Mouse	343	6	001-fstb	319	68.03
3	201-fsta	322	4	001-fsta	324	91.61
3	201-fsta	322	5	002-fstb	344	78.26
3	201-fsta	322	6	001-fstb	319	79.62
4	001-fsta	324	5	002-fstb	344	74.69
4	001-fsta	324	6	001-fstb	319	72.73
5	002-fstb	344	6	001-fstb	319	99.37

Figure 4.1 –.Bioinformatic analysis of Follistatin protein. (A) Follistatin protein sequence alignment of human (GenBank: AAH04107.1), mouse (GenBank: CAA82648.1) and zebrafish (*fsta*-002 ENSDART00000146237; *fsta* -201 ENSDART00000051065; fstb-001 ENSDART00000080772; fstb-ENSDART00000110443) using MultiAlin (http://multalin.toulouse.inra.fr/multalin/). Red-High consensus; Blue-Low consensus; Black-Neutral; (B) Scores of identity between human, mouse and zebrafish follistatin protein using clustalW2 (www.ebi.ac.uk/Tools/msa/clustalw2/.

Similarly with what happens in higher vertebrates, two different variants of *fsta* transcripts have been identified in zebrafish: a longer variant, *fsta*-201, with 324 amino acids (Trancript ID: ENSDART00000146237) and a truncated variant, *fsta*-001, with 322 amino acids (Trancript ID: ENSDART00000051065), which differ in the last 11 amino acids at the carboxyl terminus (Bauer et al., 1998) (**Figure 4.1.**). The N-terminal region of zebrafish Follistatin contains a putative signal peptide consisting of 2 basic amino acids (KR) (which indicates that Follistatin is a secreted protein), a central hydrophobic region (ILLLFWLCYLI), and a more polar region (EDQKVQ) anterior to the putative cleaving site (A/ G) which are responsible for the binding of the protein to their targets (von Heijne, 1986; Keutmann et al., 2004).

Taking into account the ability of Follistatin to bind several members of the TGF-β superfamily, many studies have been performed to investigate the role of Follistatin in different biological processes. In this regard, it has been reported that Follistatin exerts a pleiotropic effect, directly or indirectly influencing a wide range of biological effects (Amthor et al., 2002; Phillips and de Kretser, 1998; Zong et al., 2013).

It has been previously shown that Follistatin knockout mice survive to birth, but exhibit defects in size, skeletal muscle development; dying shortly after delivery (Matzuk et al., 1995). Therefore, zebrafish has been used as a model to study several processes of the development in which *fsta* plays a role (Bauer et al., 1998; Dalcq et al., 2012; Li et al., 2011). However, studies revealing the importance of *fsta* in the development of HSCs were never described.

Initially, Follistatin was reported to play a key role in the regulation of gonadal development and oocyte maturation, since it is a specific inhibitor of the biosynthesis and secretion of pituitary follicle stimulating hormone (fsh) (reviewed in (Phillips and de Kretser, 1998)). Later, several other functions of *fsta* in zebrafish have been described. The activation of *fsta* gene was shown to induce neural specification (Hemmati-Brivanlou et al., 1994; Ragland and Raible, 2004) and to inhibit BMP signalling (Bauer et al., 1998; Dal-Pra et al., 2006). However, it is not involved in organizer function or early phases of dorso/ventral patterning normally regulated by BMP, since its expression occurs too late during embryonic development to play a major role in dorsal/ventral axis formation in zebrafish (Bauer et al., 1998; Dal-Pra et al., 2006). Furthermore, Follistatin was shown to be important during ectopic otic tissue

formation (Kwon and Riley, 2009), regulation of myogenesis (Li et al., 2011) and development of cranial cartilage in zebrafish (Dalcq et al., 2012).

In the present study the role of *fsta* in haematopoiesis during the development of zebrafish was explored.

4.2. Expression of *fsta* in zebrafish embryos

In contrast to their homologues in *Xenopus* embryos, *fsta* transcripts were not detected prior to the onset of gastrulation during zebrafish early embryogenesis (Bauer et al., 1998). In fact, both WISH and RT-PCR analyses have shown that *fsta* expression is initially detected at 50% epiboly and observed throughout later stages, with a maximum value at 8 and 15 somites stages (Bauer et al., 1998; Thisse et al., 2001; Zong et al., 2013).

In the present study, we investigated the spatial and temporal patterns of *fsta* expression in comparison to *runx1* and *dll4* by WISH at five different time points, corresponding to: 50% and 80% epiboly stage, 13 somites, 20 somites and 26 hpf (**Figure 4.2** and **Figure 4.3**).

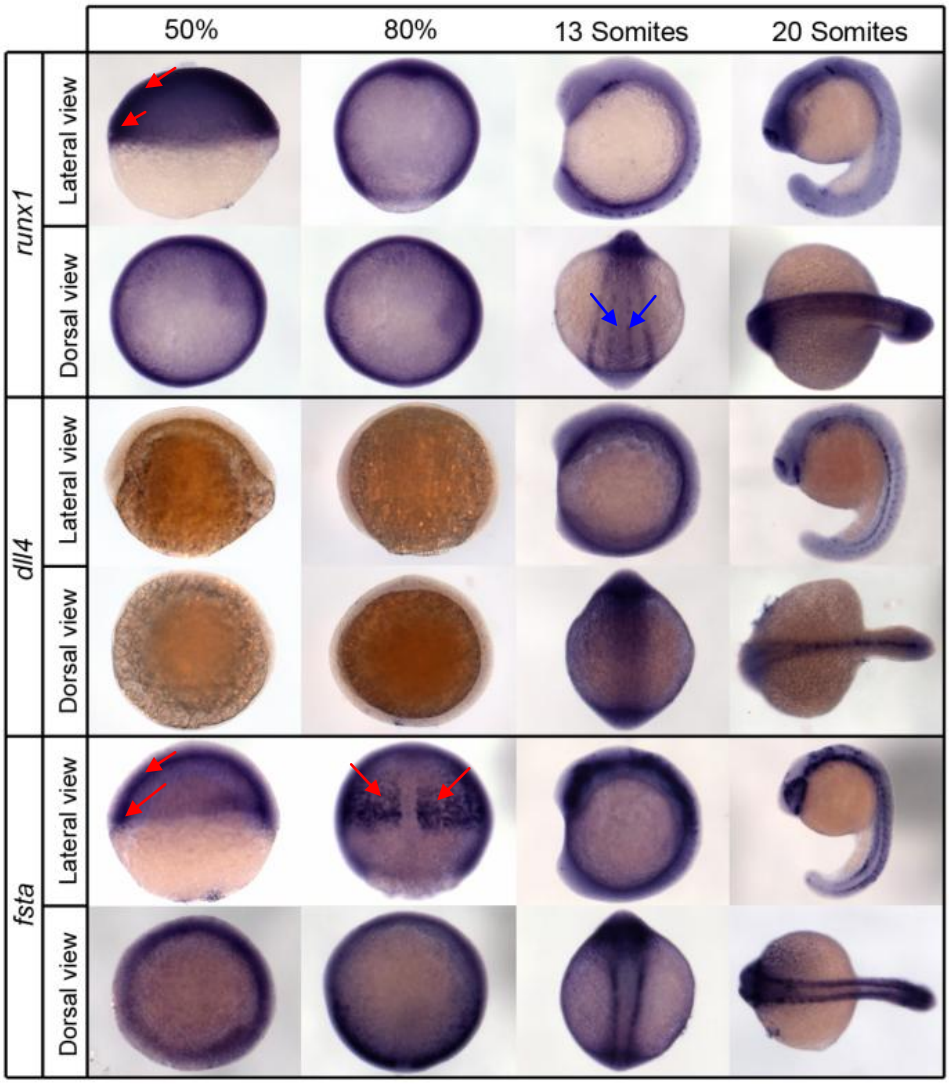

Figure 4.2 –. Time course of *runx1*,*dll4* and *fsta* expression pattern in wild type embryos. Expression pattern of *runx1,dll4* and *fsta* in zebrafish embryos at indicated stages (50% epiboly – 5.3 hpf; 80% epiboly - 8.5 hpf; 13 somites – 15 hpf, 20 somites – 19 hpf) detected by WISH.

WISH revealed an initial expression of *fsta* and *runx1* transcripts at 50% epiboly, while *dll4* transcripts expression was first observed at 13 somites (**Figure 4.2)**. The fact that *dll4* expression does not start until around 13 somites supports the idea that the up-regulation of expression of *fsta* in both *dll4* and *runx1* morphants was not a consequence of an early phenotype of the morphants.

At the onset of gastrulation, *runx1* and *fsta* RNA are expressed in mesoderm (red arrows). During gastrulation, at 80% epiboly stage, it was possible to observe that *fsta* expression was in presumptive cephalic mesendoderm (red arrows), but it was excluded from

the medial region (from notochord precursors) as previously described (**Figure 4.2**) (Dal-Pra et al., 2006). At later stages, such as 13 somites, 20 somites and 26 hpf, *fsta* expression was visualized in the head, eyes and somites regions (**Figure 4.2** and **4.3**). At 13 somites stage, *runx1* was expressed in the lateral plate mesoderm and in Rohon-Beard cells (blue arrows) in developing haematopoietic and neuronal cells respectively. Later at 26 hpf, *runx1* has a strong expression in the DA, as previously described (Kalev-Zylinska et al., 2002). *dll4* was initially expressed at 13 somites in a diffuse way, while later becomes specific to the DA, the intersomitic vessels and to some neurons (Leslie et al., 2007).

In order to more accurately determine the locations of *runx1*, *dll4 a*nd *fsta* expression at the time point when HSCs become detected by WISH (same time point used in mRNA-seq experiment), transverse sections through the trunk/tail of 26 hpf embryos were carried out (**Figure 4.3**). These sections were executed using WISH-analysed embryos for *runx1*, *dll4* and *fsta*. In the transverse sections of the embryos expressing *runx1*, positive cells for *runx1* were localized at the the VDA region; exactly where occurs emergence of HSCs (Burns et al., 2002; Kalev-Zylinska et al., 2002; North et al., 1999). As previously described (Leslie et al., 2007), analysis of *dll4* expression in sectioned embryos, revealed a strong expression pattern in the DA and also in intersomitic vessels. The expression of *fsta*, in turn, was observed in a diffuse way along the somites, but most strongly at the ventral region of the somites and in neural tissue. It is important to remember that Follistatin *a* is a soluble factor which is secreted (Phillips and de Kretser, 1998). Therefore, its presence at the ventral region of the somites, which is physically close to the DA, suggests that protein could be a player of the HSC emergence. Thus, both the biological activity and the time and place of expression in the embryo coincide with the HSC emergence activity previously defined (Burns et al., 2002; Gering and Patient, 2005). Altogether, these observations strongly suggest a possible role for *fsta* in HSC emergence. In order to study this hypothesis we performed a knockdown of *fsta* in zebrafish using antisense morpholino oligonucleotides.

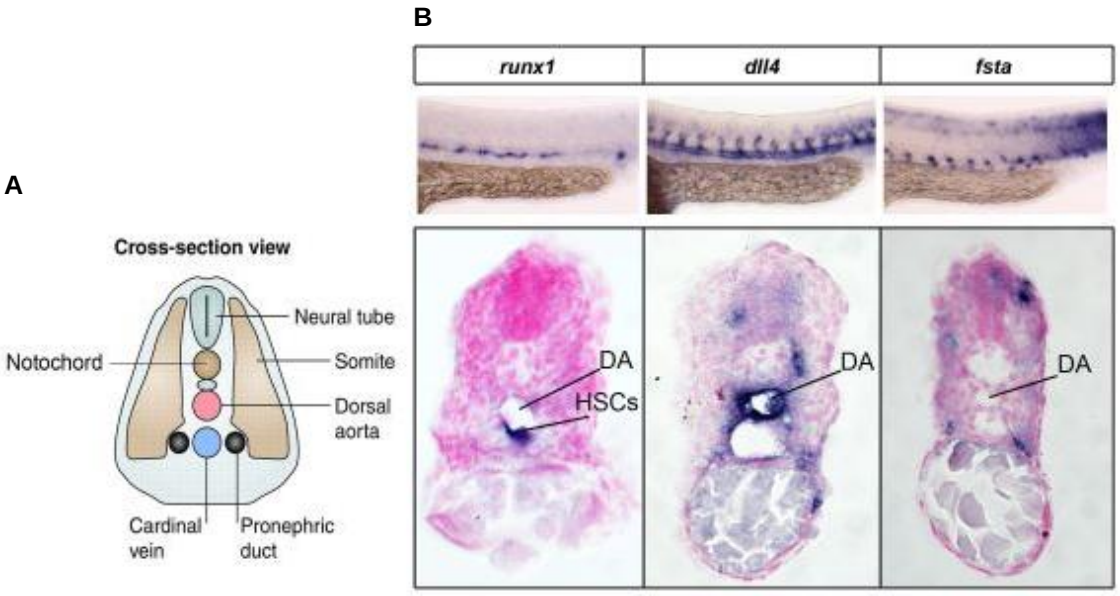

Figure 4.3 – Analysis of *runx1,dll4* and *fsta* expression patterns in transverse sections of the trunk of 26 hpf wild type embryos. (A) Scheme of a cross-section of the trunk of a zebrafish embryo. Scheme adapted from (Medvinsky et al., 2011); (B) Expression pattern of *runx1, dll4* and *fsta* in the trunk of 26 hpf Wt embryo; lateral view and transverse section of the trunk. Expression of *runx1* in the VDA; expression of *dll4* in the DA and intersomitic vessels; expression of f*sta* in the ventral region of the somites and in the neural tube.

4.3. *fsta* knockdown during zebrafish embryonic development

To clarify whether *fsta gene* is important or required for HSC development, we knockdown *fsta* expression in zebrafish embryos using a previously characterized antisense splice blocking morpholino. *fsta* MO1 spans the splice donor sequence of exon 2 (**Figure 4.4** ;(Tsukada, 2010)).

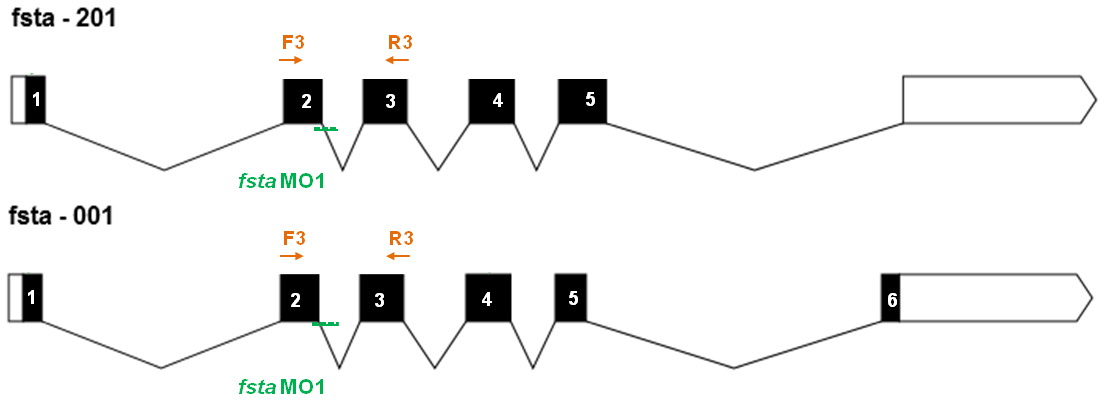

Figure 4.4 –. Schematic representation of the design of *fsta* morpholino. Genomic structures of both *fsta*-201 and *fsta*-001 transcripts, constituted by five and six exons respectively (black boxes) (http://wormweb.org/exonintron), with the binding place of *fsta* MO1 and of the primers used to test the *fsta* MO1 by RT-PCR (F3 and R3).

The morpholino used in the present study have been previously described, however we performed a titration between 5 ng/nL to 40 ng/nL. Was injected 0.5 nL of morpholino per embryo with the objective of determining the ideal working concentration. This was determined to be in the range of 5 to 10ng/nl, where the embryos do not present any apparent morphological defect and the circulation and heart beat were normal (**Figure 4.5**).

Figure 4.5 – Phenotypes of embryos injected with different concentrations of *fsta* MO1. Lateral view of live 26 hpf embryos injected with 15, 20, 30 and 40 ng of *fsta* MO1. Embryos injected with high concentrations of *fsta* MO1 [20-40 ng/nL] (injected 0.5 nL) start to display morphology defects in the tail, reduced eyes and brain necrosis.

To investigate whether the splice blocking morpholino interfere with the normal *fsta* pre-mRNA splicing and subsequent translation, RT-PCR analysis and western blot were performed using anti-Follistatin a antibody for 36 hpf and/or 4 dpf embryos injected with *fsta* MO1. These analyses revealed an abolition of Follistatin a protein expression (**Figure 4.6 C**) but formation of two aberrant forms of *fsta* splicing in the morphants compared to the Wt (**Figure 4.6 A** - red

arrows). Sequencing of these two additional products revealed an inclusion of 36 nucleotides of intron 2, due to the use of a cryptic splice site, for the larger transcript (**Figure 4.6 B)**, upper red arrow) which caused an in-frame insertion resulting in a larger protein. This likely affect normal function of the protein, as the N-terminal domain and the first two domains of the protein will not be able to rearranged correctly for binding and neutralization of its targets (Keutmann et al., 2004a) (**Figure 4.6 C**). The sequencing of the smaller transcript, in turn, has demonstrated the skipping of exon 2 and part of exon 3, leading to the expression of a completely different protein, which most likely will be degraded (**Figure 4.6 B)** - lower red arrow).

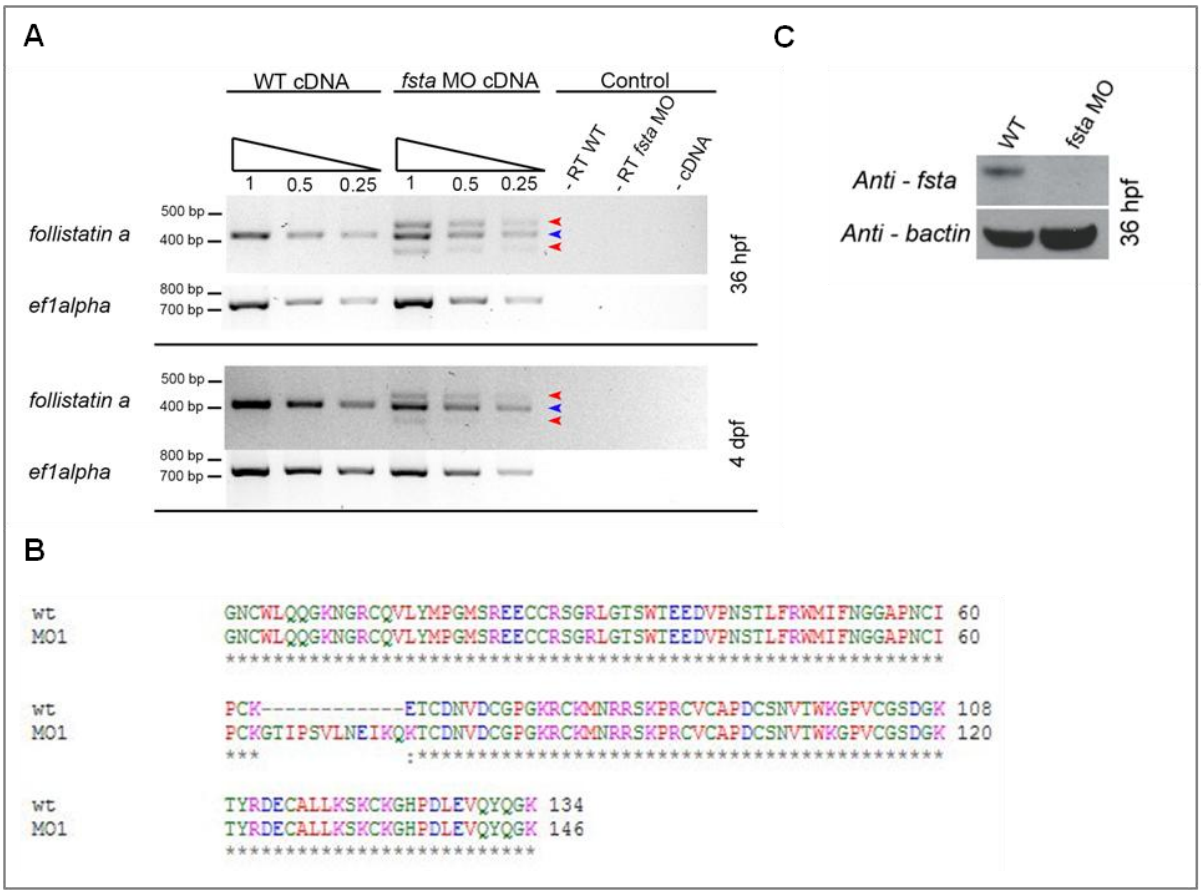

Figure 4.6 – *fsta* gene expression is knowcked down by *fsta* MO1 injection. (A) RT-PCR using primers in exons 2 and 3 on cDNA made from total RNA isolated from Wt and morphant embryos (7.5 ng *fsta* MO1) at 36 hpf and 4 dpf, revealed the formation of alternative splice products following *fsta* MO1 injection (red arrows), in addition to Wt product (blue arrow). *ef1α* (692 bp) was used as an internal loading control. Decreasing amounts of cDNA were analysed; (B) DNA sequence of the alternative splice product ((A) upper red arrow) showed a inclusion of 12 aminoacids, which caused an in-frame insertion resulting in a larger protein; (C) The expression levels of Follistatin a were measured by western blot of control (Wt) and *fsta* morphants (7.5 ng *fsta* MO1) at 36 hpf. β-actin was used as loading control. Anti-fsta – Antibody anti-Follistatin a; Anti-bactin - Antibody anti-β-actin.

4.4. Loss of *fsta* gene increases HSC numbers

In the previous chapter, we found that *fsta* expression was up-regulated in both *dll4* and *runx1* morphants, which suggests a potential role for Follistatin a in the regulation of HSCs development. In order to clarify the precise function of this glycoprotein in haematopoiesis process, we examined the formation of definitive HSCs in *fsta* morphants. Initially we analysed the expression of transcriptional regulators of HSC specification: the genes *runx1, c-myb,* and *ikaros,* which provide the earliest established markers of definitive HSCs in zebrafish (Kalev-Zylinska et al., 2002; Thompson et al., 1998; Willett et al., 2001; Zhang et al., 2011). As mention above, *runx1* morphants at 26 hpf have an increased expression of *fsta*, suggesting that *fsta* acts down-stream of *runx1* at this developmental period. Although *runx1* is required for HSC emergence, this TF also plays a pivotal role in the survival of these cells. Indeed, it seems that other factors, for example blood flow, are required by *runx1* in the early maintenance of HSCs (Lam et al., 2010; North et al., 2009). Taking this into account, we decided to also analyse *runx1* expression in *fsta* morphants. By WISH analysis, we found that, in morphants at 36 hpf, the expression levels of *c-myb* and *runx1* increased in the VDA (**Figure 4.7**). We also observed an increase of the expression of *ikaros,* a DNA-binding protein required for lymphoid development in the same region and time-point (**Figure 4.7**) (Georgopoulos et al., 1997) .The results here represented correspond to one experiment.

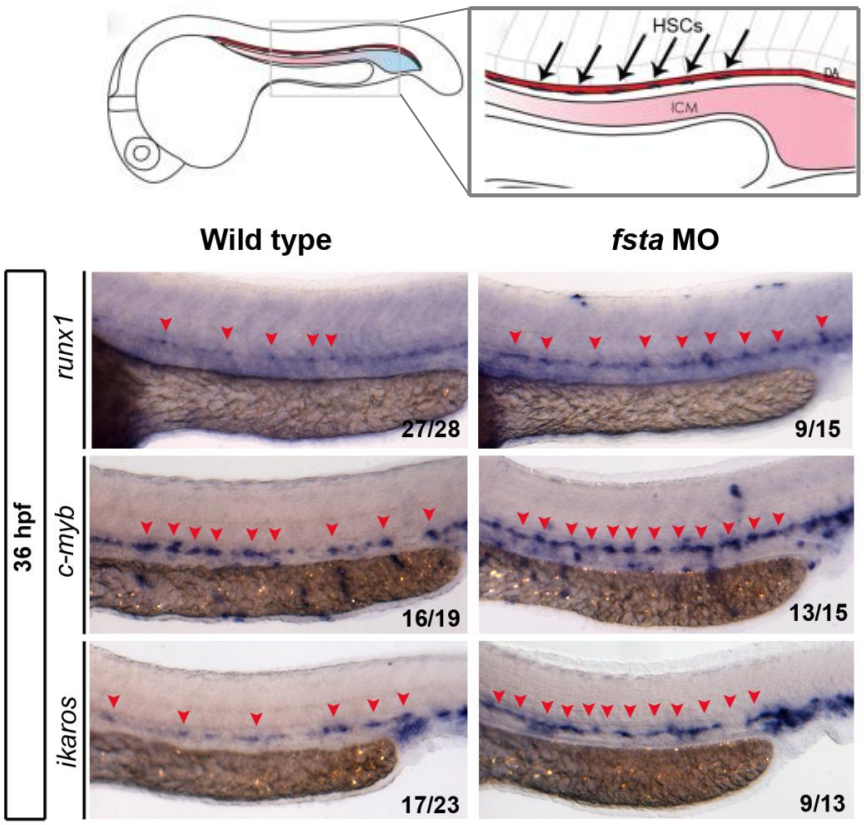

Figure 4.7 – Follistatin a is an important modulator of HSC development. WISH analysis of *runx1, c-myb*, and *ikaros* at 36 hpf in Wt and *fsta* morphant of zebrafish embryos – increased expression of all the markers in the morphants comparing with Wt ; (x/y), x - corresponds to the number of embryos with the phenotype represented in the picture and y – total number of embryos analysed. Scheme from (Monteiro, unpublished).

Consistent with our hypothesis, we demonstrated that inactivation of *fsta* gene causes an increase of definitive progenitors of HSCs. These results provide strong evidence that *fsta* is a negative regulator of HSC development.

4.5. Increased thymus seeding of HSCs in *fsta* morphants

In order to clarify whether the morpholino-induced increase of HSC progenitors in the DA truly reflected an increase of definitive HSCs, we decided to analyse the thymocytes, the first mature product of the adult blood stem cell easily identified in zebrafish embryos (Burns et al., 2005). To clarify if T cell progenitor population are differentially regulated by *fsta,* we assessed the effect of *fsta* silencing on development of T cell progeny in morphants at 4 dpf by

WISH, using probes for *rag1,* a lymphocyte-specific nuclease required for T cell antigen receptor (TCR) gene rearrangement (Langenau et al., 2004; Willett et al., 1997) and *foxn1*, a TF required for generation of thymic epithelium (Su et al., 2003). We also analysed the development of T cells labbeled to *lck*: EGFP transgene at 4 dpf. *lck,* is a tyrosine kinase required for T cell development (**Figure 4.8**) (Langenau et al., 2004).

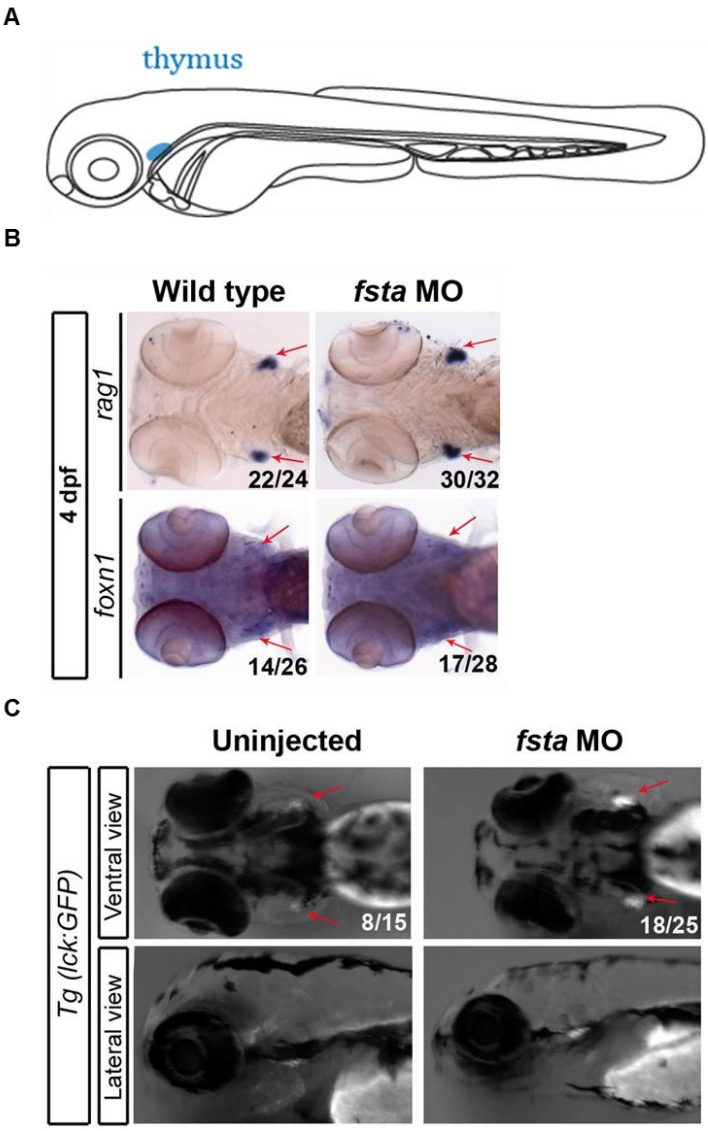

Figure 4.8 – Loss of *fsta* increases thymic seeding of HSCs. (A) Schematic representation of the thymus (blue) at 4 dpf zebrafish embryo. Scheme from (Schneider, unpublished); (B) At 4 dpf *rag1* and *foxn1* are expressed in the thymus; the expression of *rag1* and *foxn1* in the morphants are increased comparing to Wt (ventral view). (C) Knockdown of *fsta* in Tg (*lck*:EGFP) increase the GFP-marked T cell progenitors comparing to uninjected embryos at 4 dpf (ventral and dorsal view); (x/y), x - correspond to the number of embryos with the phenotype represented in the picture and y – total of embryos analysed.

WISH using a *rag1* probe, which labels T lineage progenitors, revealed that knockdown of *fsta* increases the seeding of the thymus. In fact, at 4 dpf *rag1*$^{+}$ cells were found in the thymus at higher levels compared with Wt embryos (**Figure 4.8 B**). These results have been confirmed by the observation of increased levels of GFP-marked T cell progenitors in Tg (*lck*:EGFP) zebrafish embryos injected with *fsta* MO1, when compared with uninjected embryos (**Figure 4.8 C**). Additionally, analysis of the *foxn1* expression levels in the thymic epithelium showed that this gene was still unaffected, thus suggesting that the increase of *rag1* expression might result from an increase of T-cell numbers, and not from a decrease in thymus size.

4.6. Myeloid and erythroid lineages are affected in *fsta* knockdown embryos

HSCs give rise to myeloid as well as erythroid cells in the CHT. In order to determine if the myeloid lineage was affected in the *fsta* morphant, we analysed the expression of the myeloid marker, *myeloid-specific peroxidase (mpx;* granulocytes (Bennett et al., 2001)) at 4 dpf. Notably, 4 dpf *mpx*$^{+}$ cells were found at higher levels in the *fsta* morphant CHT when compared with Wt (**Figure 4.9 B**), suggesting that definitive myeloid differentiation is increased in the absence of *fsta*.

To clarify whether the erythroid lineage was indeed impaired in these conditions, we analysed by WISH the expression of erythroid derivatives, *hbbe1.1 (Brownlie et al., 2003; Quinkertz and Campos-Ortega, 1999)*, in the CHT of 4 dpf morphants. Curiously, *hbbe1.1* $^{+}$ cells were found in the *fsta* morphant CHT at lower levels, when compared with Wt (**Figure 4.9 B**). In addition, the expression of definitive erythroid progenitors *CD41* at 4 dpf in the CHT was evaluated*,* through the use of the transgenic line Tg (*CD41*:EGFP) (Lin et al., 2005), where GFP is under the control of *CD41 (*also known as *itga2b)*. The knockdown of *fsta* in Tg (*CD41*:EGFP), allowed us to observe a higher accumulation of *CD41*$^{+}$ cells in the CHT at 4 dpf, when compared with Tg (*CD41*:EGFP) uninjected (**Figure 4.9 C**). These results are intriguing and further investigation is required to confirm this preliminary data. However these results could indicate that *fsta* plays different roles in HSC specification; being either a positive regulator of *hbbe1.1*$^{+}$cells and a negative regulator of *CD41*$^{+}$cells.

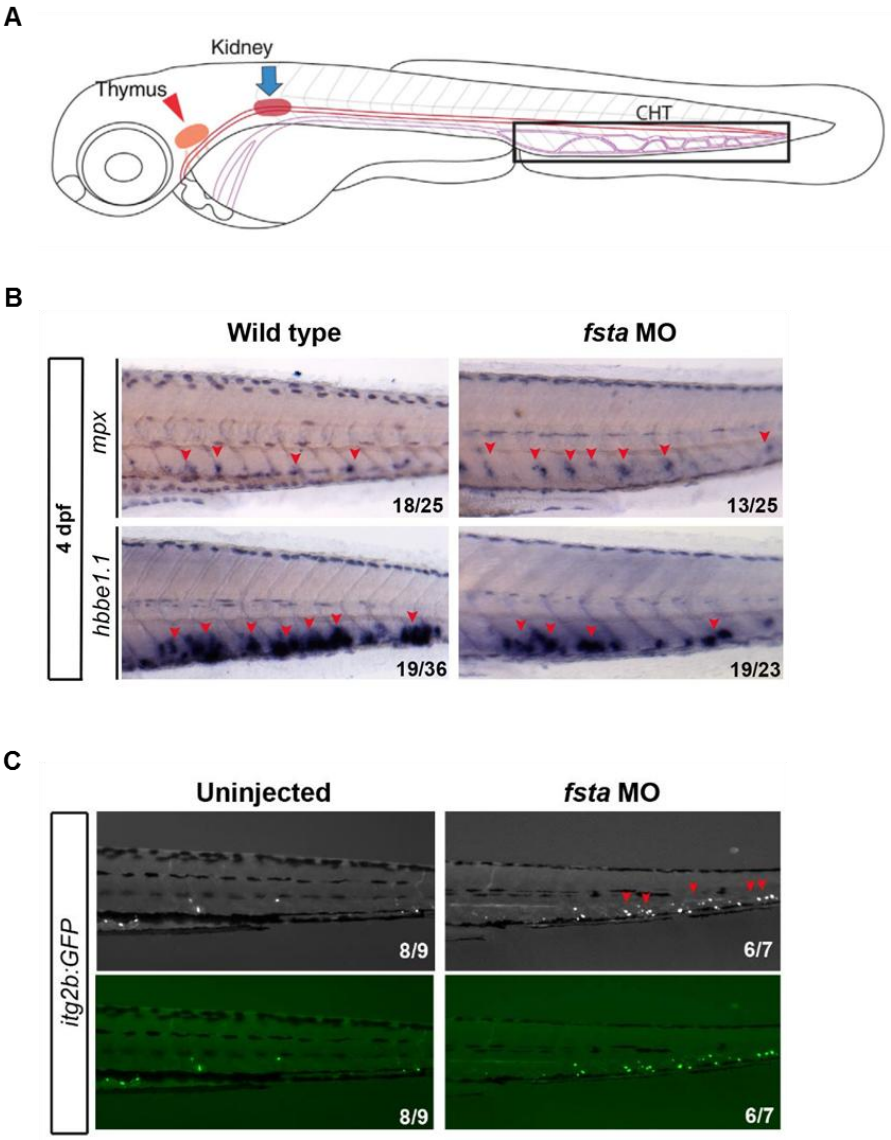

Figure 4.9 – Analysis of myeloid and erythroid markers in *fsta* knockdown embryos. (A) Schematic representation of zebrafish embryo at 4 dpf with the highlight to the CHT. Scheme adapted from (Monteiro et al., 2011); (B) Analysis by WISH of the increased expression levels of *mpx* and decreased expression levels of *hbbe1.1* in the *fsta* morphants comparing with Wt. (C) knockdown of *fsta* in Tg (*CD41*:EGFP) increase the GFP-marked *CD41* cells comparing to uninjected embryos at 4 dpf in the CHT; (x/y), x - correspond to the number of embryos with the phenotype represented in the picture and y – total of embryos analysed.

Thus, our results provided evidence that *fsta* is required for specification of the definitive HSC fate. However, further analyses of this knockdown are needed for a better understanding of *fsta* role.

As HSC emergence and endothelial specification are intimately linked, potential roles of *fsta* in vascular development was also investigated.

4.7. Follistatin a plays a role in the modulation of HSC and endothelial programming

Blood programming is strongly related with endothelial programming. Indeed, both lineages share the common progenitor cells, haemangioblasts, up to the emergence of HSC from the haemogenic endothelium (reviewed in (Dzierzak and Speck, 2008). To clarify whether the increased HSC number in *fsta* morphants was specific to the HSC rather than due to the alteration of endothelial programming, we examined endothelial programming under *fsta* knockdown. For that, the endothelial marker *kdrl* (the *Vegf* receptor II) was evaluated by WISH.

Although we observed a slight increase of *kdrl* expression in the PCV region, WISH analysis of *kdrl* at 36 hpf showed that ISVs develop apparently normally in *fsta* morphants (**Figure 4.10 (A)**). To further dissect the molecular mechanism by this happens we followed the endothelial programming in a transgenic line expressing GFP under the control of the *kdrl* promoter (Hogan et al., 2009a). We have used a double transgenic line Tg (*kdrl*:GFP/*gata1:*DsRed*)* (Jin et al., 2005; Traver et al., 2003) in which *fsta* MO1 was injected at the one cell stage. In both injected and uninjected embryos, angiogenesis from the DA appeared normal; where the sprouting from the DA is clearly visible along with the initial formation of the DLAV. The development of the CHT also involves angiogenesis, and in fact we observed an increase of the vein sprouts in the CHT at 4 dpf in embryos injected with the *fsta* MO1 (**Figure 4.10 (B)**).

Additionally, the number of *gata1*$^{+}$ cells in the injected embryos with *fsta* MO1 seems increased at 4 dpf, when compared with uninjected embryos (**Figure 4.10**). Altogether, these results suggest that *fsta* is also an important regulator of the blood and venous programming.

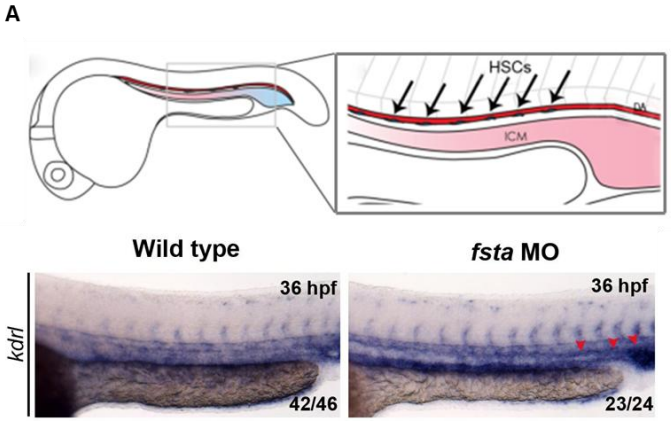

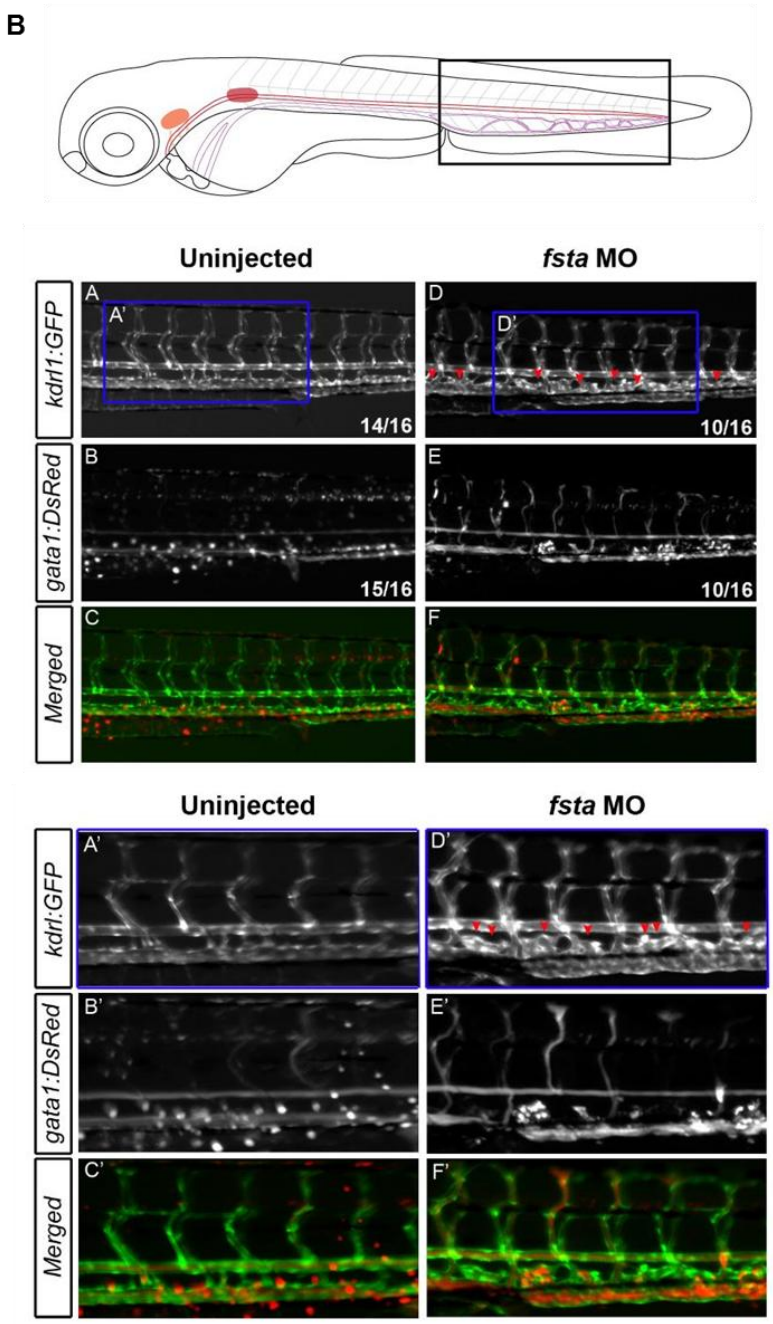

Figure 4.10 – *fsta* play a role in the modulation of the HSCs and endothelial programming. (A) Analysis of *kdrl* expression by WISH at 36 hpf. Scheme from (Monteiro, unpublished); (B) Analysis of Tg (*kdr*l:GFP/ *gata1:*DsRed*),* first panel -lower magnification and second panel – higher magnification; (x/y), x - correspond to the number of embryos with the phenotype represented in the picture and y – total of embryos analysed. Scheme adapted from (Monteiro et al., 2011).

4.8. Discussion

In the previous chapter, we identified *fsta* as a potential candidate gene required for HSCs specification. In this chapter, we investigated the role of *fsta* in HSC emergence, concluding that loss of *fsta* leads to an increase of HSC numbers. Additionally we also observed that the loss of *fsta* leads to an increase in vein sprouting. Our data provide the first evidence of a role of *fsta* in HSC and venous specification.

Specifically, the results presented here suggest that signalling by *fsta* is required to restrict HSC specification. In the angiogenesis context, *fsta* seems to forms part of an essential mechanism to keep vein angiogenesis under proper control.

Taking into account that morpholinos can lead to off-target effects, which in turn can lead to a misinterpretation of potential phenotypes, it would be important to control potential artefacts in future experiments (Eisen and Smith, 2008). For example, the use of a second morpholino would be important to phenocopy the results obtained for *fsta* MO1. Other possibility would be the rescue the phenotype in the morphants by specifically re-expressing the targeted gene. In this respect, the use of a transgenic line with a construct of *fsta* under the control of a heat-shock promoter would help to clarify whether the observed effects were due to inactivation or activation of *fsta* gene.

Moreover, since *fsta* is normally expressed early in development (**Figure 4.4**) therefore the knockdown of *fsta* should be performed just prior to HSC emergence. To confirm that observed phenotypes in HSC and venous specification were not secondary effects of an early phenotype that was not identified, it would be important to perform an experiment with a sense photo-morpholino, which can be inactivated at specific time points with UV light (365nm) exposure, thereby releasing the anti-sense morfolino; in this case just prior HSC emergence.

Finally, previous studies showed that BMP signalling is important in multiple steps of HSC programming (McReynolds et al., 2007; Wilkinson et al., 2009). In zebrafish, BMP signalling has been shown to be required in the initiation and maintenance of HSC in the VDA (Wilkinson et al., 2009); BMP4, ligand of the BMP pathway, is necessary for *runx1* expression in the DA (Wilkinson et al., 2009). BMP signalling has also been demonstrated to be important in venous programming in zebrafish (Wiley et al., 2011). It was shown that BMP signalling regulates

venous angiogenesis and that Bmp2b overexpression promotes ectopic sprouting in the PCV (Wiley et al., 2011). Wiley and colleagues demonstrated that BMP signalling mediates venous angiogenesis independently of a significant contribution of Vegf-A (Wiley et al., 2011). Besides, it is also known that Follistatin is a BMP antagonist, being often expressed in zebrafish in close proximity to expression regions of the BMP ligands, such as bmp2b and bmp4 (Bauer et al., 1998).

These findings strongly suggest that Follistatin acts via BMP in both HSC specification and vein angiogenesis processes. To address this hypothesis, it will be important to analyse the effects of morpholinos targeting the known zebrafish BMP ligands at the same time that *fsta* is knocked down.

The observations here described indicate that *fsta* provides a way to down-regulate two different biological processes intimately related, stressing the complexity of *fsta* inputs in both HSC specification and vein angiogenesis processes.

5. Conclusions and Future Perspectives

The present study provides the first evidence for a role of *fsta* in both haematopoietic and venous programming in zebrafish. In fact, we were able to identify *fsta* as a novel signalling molecule important for HSC specification. We showed that knockdown of *dll4* and *runx1* leads to an increase of *fsta* expression levels. In addition, by using a morpholino to knockdown this gene, the functional characterisation of *fsta* was also performed, demonstrating that both embryonic haematopoietic development and vein sprouting were affected by loss of *fsta*.

Importantly, the fact that *fsta* is expressed in the somites, and also plays a role in HSC specification, highlights the increasing evidence for an important regulatory role of the somites in HSC specification. Given the interesting phenotype observed in the *fsta* morphants, further functional analyses must be performed to understand the way by which this gene fits into the overall genetic regulatory network establishing and maintaining the HSCs. We speculate that both Dll4 and Runx1 are antagonizing Fsta. On the other hand, Fsta is antagonizing BMP which in turn is controlling *runx1* expression and consequently HSCs emergence and/or specification.

As future perspective, it will be interesting clarify whether fsta is an important regulator of primitive erythropoiesis, since this protein is expressed early during development and additionally because of known role of BMP in this process (Schmerer and Evans, 2003). Moreover, it will be important to identify the molecular mechanisms by which the endothelial and HSC programmes are modulated by *fsta*, as well as the specific co-modulators.

Clearly, several important regulators of HSC programming are still unknown and remain to be determined. *Follistatin* gene is also present in humans and its functions are highly conserved between vertebrates. And so, the identification of the regulatory mechanism by which *fsta* modulates HSCs and venous programming would certainly, contribute to improve our understanding on the timed signals of haematopoiesis, and possibly for the design of efficient protocols for generation of HSCs *in vitro*, crucial for a more efficient use of stem cells based-replacement therapy.

6. References

Amthor, H., Christ, B., Rashid-Doubell, F., Kemp, C., Lang, E., and Patel, K. (2002). Follistatin regulates bone morphogenetic protein-7 (BMP-7) activity to stimulate embryonic muscle growth. Developmental biology *243*, 115-127.

Aniket, V.G., Kathryn, M., Young, R.C., Weijun, P., and Brant, M.W. (2012). Vascular Development in the Zebrafish. Cold Spring Harb Perspect Med.

Bauer, H., Meier, A., Hild, M., Stachel, S., Economides, A., Hazelett, D., Harland, R., and Hammerschmidt, M. (1998). Follistatin and noggin are excluded from the zebrafish organizer. Developmental biology *204*, 488-507.

Beets, K., Huylebroeck, D., Moyon, D., Umans, L., and Zwijsen, A. (2013). Robustness in angiogenesis: Notch and BMP shaping waves. Cell Trends in Genetics *29*, 140-149.

Benedito, R., and Duarte, A. (2005). Expression of Dll4 during mouse embryogenesis suggests multiple developmental roles. Gene Expr Patterns *5(6)*, 750-755.

Bennett, C., Kanki, J., Rhodes, J., Liu, T., Paw, B., Kieran, M., Langenau, D., Delahaye-Brown, A., Zon, L., Fleming, M.*, et al.* (2001). Myelopoiesis in the zebrafish, Danio rerio. Blood *98*, 643-651.

Bertrand, J.Y., Chi, N.C., Santoso, B., Teng, S., Stainier, D.Y.R., and Traver, D. (2010). Haematopoietic stem cells derive directly from aortic endothelium during development. Nature *464*, 108-111.

Bertrand, J.Y., Kim, A.D., Teng, S., and Traver, D. (2008). $CD41^{+}$ $cmyb^{+}$ precursors colonize the zebrafish pronephros by a novel migration route to initiate adult hematopoiesis. Development *135*, 1853-1862.

Bertrand, J.Y., Kin, A.D., Violette, E.P., Stachura, D.L., Cisson, J.L., and Traver, D. (2007). Definitive hematopoiesis initiates through a committed erythromyeloid progenitor in the zebrafish embryo. Development *134*, 4147-4156.

Bigas, A., and Espinosa, L. (2012). Hematopoietic stem cells: to be or Notch to be. . blood *119*, 3226-3235.

Blum, Y., Belting, H.G., Ellertsdottir, E., Herwig, L., Luders, F., and Affolter, M. (2008). Complex cell rearrangements during intersegmental vessel sprouting and vessel fusion in the zebrafish embryo. Dev Biol *316*, 312-322.

Brownlie, A., Hersey, C., Oates, A., Paw, B., Falick, A., Witkowska, H., Flint, J., Higgs, D., Jessen, J., Bahary, N.*, et al.* (2003). Characterization of embryonic globin genes of the zebrafish. Developmental biology *255*, 48-61.

Burns, C., DeBlasio, T., Zhou, Y., Zhang, J., Zon, L., and Nimer, S. (2002). Isolation and characterization of runxa and runxb, zebrafish members of the runt family of transcriptional regulators. Experimental hematology *30*, 1381-1389.

Burns, C.E., Galloway, J.L., Smith, A.C.H., Keefe, M.D., Cashman, T.J., Paik, E.J., Mayhall, E.A., Amsterdam, A.H., and Zon, L.I. (2009). A genetic screen in zebrafish defines a hierarchical network of pathways required for hematopoietic stem cell emergence. Blood *113*, 5776-57782.

Burns, C.E., Traver, D., Mayhall, E., Shepard, J.L., and Zon, L.I. (2005). Hematopoietic stem cell fate is established by the Notch-Runx pathway. Genes Dev *19*, 2331–2342.

Cannon, J., Place, E., Eve, A., Bradshaw, C., Sesay, A., Morrell, N., and Smith, J. (2013). Global analysis of the haematopoietic and endothelial transcriptome during zebrafish development. Mechanisms of development *130*, 122-131.

Caolo, V., Molin, D.G.M., and Post, M.J. (2012). Notch Regulation of Hematopoiesis, Endothelial Precursors Cells, and Blood Formation: Orchestrating and Vasculature. Stem Cells International.

Chen, A.T., and Zon, L.I. (2009). Zebrafish Blood Stem Cells. Journal of cellular Biochemistry *108*, 35-42.

Clements, W., and Traver, D. (2013). Signalling pathways that control vertebrate haematopoietic stem cell specification. Nature reviews Immunology *13*, 336-348.

Clements, W.K., Kim, A.D., Ong, K.G., Moore, J.C., Lawson, N.D., and Traver, D. (2011). A somitic Wnt16/Notch pathway specifies haematopoietic stem cells. Nature *474*.

Dal-Pra, S., Fürthauer, M., Van-Celst, J., Thisse, B., and Thisse, C. (2006). Noggin1 and Follistatin-like2 function redundantly to Chordin to antagonize BMP activity. Developmental biology *298*, 514-526.

Dalcq, J., Pasque, V., Ghaye, A., Larbuisson, A., Motte, P., Martial, J., and Muller, M. (2012). RUNX3, EGR1 and SOX9B form a regulatory cascade required to modulate BMP-signaling during cranial cartilage development in zebrafish. PLoS ONE *7*.

de Kretser, D., O'Hehir, R., Hardy, C., and Hedger, M. (2012). The roles of activin A and its binding protein, follistatin, in inflammation and tissue repair. Molecular and cellular endocrinology *359*, 101-106.

de Winter, J., ten Dijke, P., de Vries, C., van Achterberg, T., Sugino, H., de Waele, P., Huylebroeck, D., Verschueren, K., and van den Eijnden-van Raaij, A. (1996). Follistatins neutralize activin bioactivity by inhibition of activin binding to its type II receptors. Molecular and cellular endocrinology *116*, 105-114.

Dooley, K.A., Davidson, A.J., and Zon, L. (2005). Zebrafish *scl* functions independently in hematopoietic and endothelial development. Dev Biol *277*, 522-536.

Dussault, A.A., and Pouliot, M. (2006). Rapid and simple comparison of messenger RNA levels using real-time PCR. Biol Proced Online *8*, 1-10.

Dzierzak, E., and Speck, N.A. (2008). Of lineage and legacy: the development of mammalian hematopoietic stem cells. Nat Immunol *9*, 129-136.

Eisen, J., and Smith, J. (2008). Controlling morpholino experiments: don't stop making antisense. Development (Cambridge, England) *135*, 1735-1743.

Fitch, S.R., Kinmber, G.M., Wilson, N.K., Parker, A., Mirshekar-Syahkal, B., Gottgens, B., Medvinsky, A., Dzierzak, E., and Ottersbach, K. (2012). Signaling from the Sympathetic Nervous System Regulates Hematopoietic Stem Cell Emergence during Embryogenesis. Cell Stem Cell *11*, 554-556.

Fouquet, B., Weinstein, B.M., Serluca, F.C., and Fishman, M.C.V.p.i.t.e.o.t.z.g.b.n. (1997). Vessel patterning in the embryo of the zebrafish: guidance by notochord. Dev Biol *183*, 37-48.

Gale, N.W., Dominguez, M.G., Noguera, I., Pan, L., Hughes, V., Valenzuela, D.M., Murphy, A.J., Adams, N.C., Lin, H.C., Holash, J.*, et al.* (2004). Haploinsufficiency of delta-like 4 ligand results in embryonic lethality due to major defects in arterial and vascular development. Proc Natl Acad Sci U S A *101(45)*, 15949-15954.

Gamer, L., Wolfman, N., Celeste, A., Hattersley, G., Hewick, R., and Rosen, V. (1999). A novel BMP expressed in developing mouse limb, spinal cord, and tail bud is a potent mesoderm inducer in Xenopus embryos. Developmental biology *208*, 222-232.

Georgopoulos, K., Winandy, S., and Avitahl, N. (1997). The role of the Ikaros gene in lymphocyte development and homeostasis. Annual review of immunology *15*, 155-176.

Gerety, S.S., Wang, H.U., Chen, Z.F., and Andersson, D.J. (1999). Symmetrical mutant phenotypes of the receptor EphB4 and specific transmembrane ligand *efnB2* in cardiovascular development. Mol Cell *4*, 403-414.

Gering, M., and Patient, R. (2005). Hedgehog signaling is required for adult blood stem cell formation in zebrafish embryos. Developmental cell *8*, 389-400.

Gering, M., and Patient, R. (2009). Notch signalling and haematopoietic stem cell formation during embryogenesis. Journal of cellular physiology *222*, 11-16.

Gering, M., Rodaway, A., Göttgens, B., Patient, R., and Green, A. (1998). The SCL gene specifies haemangioblast development from early mesoderm. The EMBO journal *17*, 4029-4045.

Geudens, I., Herpers, R., Hermans, K., Segura, I., Ruiz de Almodovar, C., Bussmann, J., De Smet, F., Vandevelde, W., Hogan, B.M., Siekmann, A.*, et al.* (2010). Role of delta-like-4/Notch

in the formation and wiring of the lymphatic network in zebrafish. . Arterioscler Thromb Vasc Biol *30*, 1695-1702.

Glister, C., Kemp, C., and Knight, P. (2004). Bone morphogenetic protein (BMP) ligands and receptors in bovine ovarian follicle cells: actions of BMP-4, -6 and -7 on granulosa cells and differential modulation of Smad-1 phosphorylation by follistatin. Reproduction (Cambridge, England) *127*, 239-254.

Heasman, J. (2002). Morpholino oligos: making sense of antisense? Developmental biology *243*, 209-214.

Hemmati-Brivanlou, A., Kelly, O., and Melton, D. (1994). Follistatin, an antagonist of activin, is expressed in the Spemann organizer and displays direct neuralizing activity. Cell *77*, 283-295.

Herbomel, P., Thisse, B., and Thisse, C. (1999). Ontogeny and behaviour of early macrophages in the zebrafish embryo. Development *126(17)*, 3735-3745.

Hogan, B.M., Bos, F.L., Bussmann, J., Witte, M., Chi, N.C., Duckers, H.J., and Schulte-Merker, S. (2009a). ccbe1 is required for embryonic lymphangiogenesis and venous sprouting. Nat Genet *41*, 396-398.

Hogan, B.M., Herpers, R., Witte, M., Helotera, H., Alitalo, K., Duckers, H.J., and Schulte-Merker, S. (2009b). Vegfc/Flt4 signalling is suppressed by Dll4 in developing zebrafish intersegmental arteries. Development *136*, 4001-4009.

Iemura, S., Yamamoto, T., Takagi, C., Uchiyama, H., Natsume, T., Shimasaki, S., Sugino, H., and Ueno, N. (1998). Direct binding of follistatin to a complex of bone-morphogenetic protein and its receptor inhibits ventral and epidermal cell fates in early Xenopus embryo. Proceedings of the National Academy of Sciences of the United States of America *95*, 9337-9342.

Isogai, S., Lawson, N.D., Torrealday, S., Horiguchi, M., and Weinstein, B.M. (2003). Angiogenic network formation in the developing vertebrate trunk. Development *130(21)*, 5281-5290.

Ito, Y., and Miyazono, K. (2003). Runx transcription factors as key targets of TGF-B superfamily signaling. Current Opinion in Genetics & Development *13*, 43-47.

Jagannathan-Bogdan, M., and Zon, L.I. (2013). Hematopoiesis. Development *140*, 2463-2467.

Jakobsson, L., Bentley, K., and Gerhardt, H. (2009). VEGFRs and Notch: a dynamic collaboration in vascular patterning. Biochem Soc Trans *37*, 1233-1236.

Jin, H., Sood, R., Xu, J., Zhen, F., English, M.A., Liu, P.P., and Wen, Z. (2009). Definitive hematopoietic stem/progenitor cells manifest distinct differentiation outpout in the zebrafish VDA and PBI. Development *136*, 647-654.

Jin, H., and Wen, Z. (2007). Migratory path of definitive hematopoietic stem/progenitor cells during zebrafish development. Blood *109*, 5208-5214.

Jin, S.W., Beis, D., Mitchell, T., Chen, J.N., and Stainier, D.Y. (2005). Cellular and molecular analyses of vascular tube and lumen formation in zebrafish. Development *132 (23)*, 5199-5209.

Kalev-Zylinska, M., Horsfield, J., Flores, M., Postlethwait, J., Vitas, M., Baas, A., Crosier, P., and Crosier, K. (2002). Runx1 is required for zebrafish blood and vessel development and expression of a human RUNX1-CBF2T1 transgene advances a model for studies of leukemogenesis. Development (Cambridge, England) *129*, 2015-2030.

Kennedy, M., Firpo, M., Choi, K., Wall, C., Robertson, S., Kabrun, N., and Keller, G. (1997). A common precursor for primitive erythropoiesis and definitive haematopoiesis. Nature *386(6624)*, 488-493.

Keutmann, H., Schneyer, A., and Sidis, Y. (2004a). The role of follistatin domains in follistatin biological action. Molecular endocrinology (Baltimore, Md) *18*, 228-240.

Kimmel, C.B., Ballard, W.W., Kimmel, S.R., Ullmann, B., and Schilling, T.F. (1995). Stages of embryonic development of the zebrafish. Dev Dyn *203*, 253-310.

Kissa, K., and Herbomel, P. (2010). Blood stem cells emerge from aortic endothelium by a novel type of cell transition. Nature *464*, 112-115.

Kissa, K., Murayama, E., Zapata, A., Cortés, A., Perret, E., Machu, C., and Herbomel, P. (2008). Live imaging of emerging hematopoietic stem cells and early thymus colonization. Blood *111(3)*, 1147-1156.

Kobayashi, A., Senzaki, K., Ozaki, S., Yoshikawa, M., and Shiga, T. (2012). Runx1 promotes neuronal differentiation in dorsal root ganglion. Molecular and Cellular Neuroscience *49*, 23-31.

Krebs, L.T., Shutter, J.R., Tanigaki, K., Honjo, T., Stark, K.L., and Gridley, T. (2004). Haploinsufficient lethality and formation of arteriovenous malformations in Notch pathway mutants. Genes Dev *18*, 2469-2473.

Kumano, K., Chiba, S., Kunisato, A., Sata, M., Saito, T., Nakagami-Yamaguchi, E., Yamaguchi, T., Masuda, S., Shimizu, K., Takahashi, T.*, et al.* (2003). Notch1 but not Notch2 is essential for generating hematopoietic stem cells from endothelial cells. . Immunity *18*, 699–711.

Kwon, H.-J., and Riley, B. (2009). Mesendodermal signals required for otic induction: Bmp-antagonists cooperate with Fgf and can facilitate formation of ectopic otic tissue. Developmental dynamics : an official publication of the American Association of Anatomists *238*, 1582-1594.

Lam, E.Y., Hall, C.J., Crosier, P.S., Crosier, K.E., and Flores, M.V. (2010). Live imaging of Runx1 expression in the dorsal aorta tracks the emergence of blood progenitors from endothelial cells. . Blood *116*, 909-914.

Langenau, D.M., Ferrando, A.A., Traver, D., Kutok, J.L., Hezel, J.P., Kanki, J.P., Zon, L.I., Look, A.T., and Trede, N.S. (2004). In vivo tracking of T cell development, ablation, and engraftment in transgenic zebrafish. PNAS *101(19)*, 7369-7374.

Lawson, N.D., Scheer, N., Pham, V.N., Kim, C.-H., Chitnis, A.B., Campos-Ortega, J.A., and Weinstein, B.M. (2001). Notch signaling is required for arterial-venous differentiation during embryonic vascular development. Development *128*, 3675-3683.

Lawson, N.D., Vogel, A.M., and Weinstein, B.M. (2002). Sonic hedgehog and vascular endothelial growth factor act upstream of the Notch pathway during arterial endothelial differentiation. Dev Cell *3(1)*, 127-136.

Lawson, N.D., and Weinstein, B.M. (2002). Arteries and Veins: Making a Difference With Zebrafish. Nature Reviews - Genetics *3*, 674-682.

Lawson, N.D., and Weinstein, B.M. (2002). In vivo imaging of embryonic vascular development using transgenic zebrafish. . Dev Biol *248*, 307-318.

Leslie, J., Ariza-McNaughton, L., Bermange, A., McAdow, R., Johnson, S., and Lewis, J. (2007). Endothelial signalling by the Notch ligand Delta-like 4 restricts angiogenesis. Development (Cambridge, England) *134*, 839-844.

Li, X., Nie, F., Yin, Z., and He, J. (2011). Enhanced hyperplasia in muscles of transgenic zebrafish expressing Follistatin1. Science China Life sciences *54*, 159-165.

Lieschke, G.J., Oates, A.C., Paw, B.H., Thompson, M.A., Hall, N.E., Ward, A.C., Ho, R.K., Zon, L.I., and Layton, J.E. (2002). Zebrafish SPI-1 (PU.1) marks a site of myeloid development independent of primitive erythropoiesis: implications for axial patterning. Dev Biol *246(2)*, 274-295.

Lin, H.F., Traver, D., Zhu, H., Dooley, K., Paw, B.H., Zon, L.I., and Handin, R.I. (2005). Analysis of thrombocyte development in CD41-GFP transgenic zebrafish. Blood *106(12)*, 3803-3810.

Loeffler, D., Kokkaliaris, K.D., and Schroeder, T. (2011). Wnt to Notch Relay Signaling Induces Definitive Hematopoiesis. Cell Stem Cell *9*, 2-4.

Macqueen, D., and Johnston, I. (2008). Evolution of follistatin in teleosts revealed through phylogenetic, genomic and expression analyses. Development genes and evolution *218*, 1-14.

Marcks-Bluth, J., and Pimanda, J.E. (2012). Cell signalling pathways that mediate haematopoietic stem cell specification. The International Journal of Biochemistry & Cell Biology.

Matzuk, M.M., Lu, N., Vogel, H., Sellheyer, K., Roop, D.R., and Bradley, A. (1995). Multiple defects and perinatal death in mice deficient in follistatin. . Nature *374*, 360-363.

McCurley, A.T., and Callard, G.V. (2008). Characterization of housekeeping genes in zebrafish: male-female differences and effects of tissue type, developmental stage and chemical treatment. BMC Mol Biol *9:102*.

McGrath, K.E., Frame, J.M., Fromm, G.J., Koniski, A.D., Kingsley, P.D., Little, J., Bulger, M., and Palis, J. (2011). A transient definitive erythroid lineage with unique regulation of the B-globin locus in the mammalian embryo. Blood *117*, 4600-4608.

McReynolds, L., Gupta, S., Figueroa, M., Mullins, M., and Evans, T. (2007). Smad1 and Smad5 differentially regulate embryonic hematopoiesis. Blood *110*, 3881-3890.

Medvinsky, A., Rybtson, S., and Taoudi, S. (2011). Embryonic origin of the adult hematopoietic system: advances and questions. Development *138*, 1017-1031.

Monteiro, R., Pouget, C., and Patient, R. (2011). The gata1/pu. 1 lineage fate paradigm varies between blood populations and is modulated by tif1γ. The EMBO journal.

Morrison, R., Schleicher, S.M., Sun, Y., Niermann, K.J., Kim, S., Spratt, D.E., Chung, C.H., and Lu, B. (2011). Targeting the mechanisms of resistance to chemotherapy and radiotherapy with the cancer stem cell hypothesis. J Oncol.

Motoike, T., Markham, D.W., Rossant, J., and Sato, T.N. (2003). Evidence for novel fate of Flk1+ progenitor: contribution to muscle lineage. Genesis *35*, 153–159.

Murayama, E., Kissa, K., Zapata, A., Mordelet, E., Briolat, V., Lin, H.F., Handin, R.I., and Herbomel, P. (2006). Tracing hematopoietic precursor migration to successive hematopoietic organs during zebrafish development. Immunity *25(6)*, 963-975.

Nakamura, T., Takio, K., Eto, Y., Shibai, H., Titani, K., and Sugino, H. (1990). Activin-binding protein from rat ovary is follistatin. Science (New York, NY) *247*, 836-838.

North, T., Gu, T., Stacy, T., Wang, Q., Howard, L., Binder, M., Marín-Padilla, M., and Speck, N. (1999). Cbfa2 is required for the formation of intra-aortic hematopoietic clusters. Development (Cambridge, England) *126*, 2563-2575.

North, T.E., Goessling, W., Peeters, M., Li, P., Ceol, C., Lord, A.M., Weber, G.J., Harris, J., Cutting, C.C., Huang, P.*, et al.* (2009). Hematopoietic Stem Cell Development Is Dependent on Blood Flow. Cell *137*, 736–748.

Nottingham, W.T., Jarratt, A., Burgess, M., Speck, C.L., Cheng, J.F., Prabhakar, S., Rubin, E.M., Li, P.S., Sloane-Stanley, J., Kong, A.S.J.*, et al.* (2007). Runx1-mediated hematopoietic stem-cell emergence is controlled by Gata/Ets/SCL-regulated enhancer. Blood *110*, 4188-4197.

Orkin, S., and Zon, L. (2008). Hematopoiesis: an evolving paradigm for stem cell biology. Cell *132*, 631-644.

Otsuka, F., Moore, R., Iemura, S., Ueno, N., and Shimasaki, S. (2001). Follistatin inhibits the function of the oocyte-derived factor BMP-15. Biochemical and biophysical research communications *289*, 961-966.

Paik, E.J., and Zon, L.I. (2010). Hematopoietic development in the zebrafish. Int J Dev Biol *54*, 1127-1137.

Pajcini, K.V., Speck, N.A., and Pear, W.S. (2011). Notch signaling in mammalian hematopoietic stem cells. Leukemia *25*, 1525-1532.

Palis, J., and Yoder, M.C. (2001). Yolk-sac hematopoiesis: the first blood cells of mouse and man. Experimental hematology *29*, 927-236.

Patterson, L.J., Gering, M., and Patient, R. (2005). Scl is required for dorsal aorta as well as blood formation in zebrafish embryos. Blood *105*, 3502-3511.

Phillips, D., and de Kretser, D. (1998). Follistatin: a multifunctional regulatory protein. Frontiers in neuroendocrinology *19*, 287-322.

Quinkertz, A., and Campos-Ortega, J.A. (1999). A new beta-globin gene from the zebrafish, betaE1, and its pattern of transcription during embryogenesis. Dev Genes Evol *209(2)*, 126-131.

Ragland, J., and Raible, D. (2004). Signals derived from the underlying mesoderm are dispensable for zebrafish neural crest induction. Developmental biology *276*, 16-30.

Ransom, D.G., Haffter, P., Odenthal, J., Brownlie, A., Vogelsang, E., Kelsh, R.N., Brand, M., vanEeden, F.J.M., FurutaniSeiki, M., Granato, M.*, et al.* (1996). Characterization of zebrafish mutants with defects in embryonic hematopoiesis. Development *123*, 311-319.

Robert-Moreno, A., Espinosa, L., de la Pompa, J.L., and Bigas, A. (2005). RBPjkappa-dependent Notch function regulates Gata2 and is essencial for the formation of intra-embryonic hematopoietic cells. Development *132*, 1117-1126.

Roca, C., and Adams, R.H. (2007). Regulation of vascular morphogenesis by Notch signalling. Genes Dev *21*, 2511-2524.

Ryu, S., Holzschuh, J., Erhardt, S., Ettl, A., and Driever, W. (2005). Depletion of minichromosome maintenance protein 5 in the zebrafish retina causes cell-cycle defect and apoptosis. PNAS *102*, 18467-18472.

Schmerer, M., and Evans, T. (2003). Primitive erythropoiesis is regulated by Smad-dependent signaling in postgastrulation mesoderm. Blood 3196-3205.

Siekmann, A.F., and Lawson, N.D. (2007). Notch signalling limits angiogenic cell behaviour in developing zebrafish arteries. Nature *445*, 781-784.

Speck, N.A., and Gilliland, D.G. (2002). Core-binding factors in hematopoiesis and leukemia. Nat Rev Cancer *2*, 502-513.

Stainier, D.Y.R., Weinstein, B.M., Detrich, H.W., Zon, L.I., and Fishman, M.C. (1995). Cloche, an Early Acting Zebrafish Gene, Is Required by Both the Endothelial and Hematopoietic Lineages. Development *121*, 3141-3150.

Su, D.-m., Navarre, S., Oh, W.-j., Condie, B., and Manley, N. (2003). A domain of Foxn1 required for crosstalk-dependent thymic epithelial cell differentiation. Nature Immunology *4*, 1128-1135.

Swift, M.R., and Weinstein, B.M. (2009). Arterial-venous specification during development. Circ Res *104(5)*, 576-588.

Tanaka, Y., Joshi, A., Wilson, N., Kinston, S., Nishikawa, S., and Göttgens, B. (2012). The transcriptional programme controlled by Runx1 during early embryonic blood development. Developmental biology *366*, 404-419.

Tang, R., Dodd, A., Lai, D., Mcnabb, W.C., and Love, D.R. (2007). Validation of Zebrafish (Danio rerio) Reference Genes for Quantitative Real-time RT-PCR Normalization. Acta Biochimica et Biophysica Sinica *39(5)*, 384-390.

Theriault, F.M., Nuthall, H.N., Dong, Z., Lo, R., Barnabe-Heider, F., Miller, F.D., and Stifani, S. (2005). Role for Runx1 in the Proliferation and Neuronal Differentiation of Selected Progenitor Cells in the Mammalian Nervous System. The Journal of Neuroscience *25 (8)*, 2050-2061.

Thisse, B., Pflumio, S., Fürthauer, M., Loppin, B., Heyer, V., Degrave, A., Woehl, R., Lux, A., Steffan, T., Charbonnier, X.Q.*, et al.* (2001). Expression of the zebrafish genome during embryogenesis. ZFIN Direct Data Submission *(NIH R01 RR15402)*.

Thompson, M.A., Ransom, D.G., Pratt, S.J., MacLennan, H., Kieran, M.W., Detrich, H.W., Vail, B., Huber, T.L., Paw, B., Brownlie, A.J.*, et al.* (1998). The cloche and spadetail genes differentially affect hematopoiesis and vasculogenesis. DEv Biol *197 (2)*, 248-269.

Thompson, T., Lerch, T., Cook, R., Woodruff, T., and Jardetzky, T. (2005). The structure of the follistatin:activin complex reveals antagonism of both type I and type II receptor binding. Developmental cell *9*, 535-543.

Traver, D., Paw, B.H., Poss, K.D., Penberthy, W.T., Lin, S., and Zon, L.I. (2003). Transplantation and in vivo imaging of multilineage engraftment in zebrafish bloodless mutants. Nat Immunol *4(12)*, 1238-1246.

Tsukada, Y., Ishitani, T., and Nakayama, K.I. (2010). KDM7 is a dual demethylase for histone H3 Lys 9 and Lys 27 and functions in brain development. Genes Dev *24(5)*, 432-437.

Vogeli, K.M., Jin, S.W., Martin, G.R., and Stainier, D.Y.R. (2006). A common progenitor for haematopoietic and endothelial lineages in the zebrafish gastrula. Nature *443*, 337-339.

von Heijne, G. (1986). A new m ethod for predicting signal sequence cleavage sites. Nucleic Acids Res *14*, 4883- 4890.

Wang, H.U., Chen, Z.F., and Andersson, D.J. (1998). Molecular distinction and angiogenic interaction between embryonic arteries and veins revealed by *efnB2* and its receptor Eph-B4. Cell *93*, 741-753.

Weinstein, B.M., Schier, A.F., Abdelilah, S., Malicki, J., SolnicaKrezel, L., Stemple, D.L., Stainier, D.Y.R., Zwartkruis, F., Driever, W., and Fishman, M.C. (1996). Hematopoietic mutations in the zebrafish. Development *123*, 303-309.

Wiley, D., Kim, J.-D., Hao, J., Hong, C., Bautch, V., and Jin, S.-W. (2011). Distinct signalling pathways regulate sprouting angiogenesis from the dorsal aorta and the axial vein. Nature cell biology *13*, 686-692.

Wilkinson, A.C., and Göttgens, B. (2013). Transcriptional regulation of haematopoietic stem cells. Adv Exp Med Biol *786*, 187-212.

Wilkinson, R., Pouget, C., Gering, M., Russell, A., Davies, S., Kimelman, D., and Patient, R. (2009). Hedgehog and Bmp polarize hematopoietic stem cell emergence in the zebrafish dorsal aorta. Developmental cell *16*, 909-916.

Willett, C.E., Cherry, J.J., and Steiner, L.A. (1997). Characterization and expression of the recombination activating genes (rag1 and rag2) of zebrafish. Immunogenetics *45 (6)*, 394-404.

Willett, C.E., Kawasaki, H., Amemiya, C.T., Lin, S., and Steiner, L.A. (2001). Ikaros expression as a marker for lymphoid progenitors during zebrafish development. Dev Dyn *222 (4)*, 694-698.

Wolpert, L., Beddington, R., Jessell, T., Lawrence, P., Meyerowitz, E., and Smith, J. (2001). Principles of Development, 2 edn (Oxford, Oxford University Press).

Yaniv, K., Isogai, S., Castranova, D., Dye, L., Hitomi, J., and Weinstein, B.M. (2006). Live imaging of lymphatic development in the zebrafish. Nat Med *12(6)*, 711-716.

Zagami, C.J., and Stifani, S. (2010). Molecular Characterization of the Mouse Superior Lateral Parabrachial Nucleus through Expression of the Transcription Factor Runx1. PLoS ONE *5*.

Zhang, C., Patient, R., and Liu, F. (2013). Hematopoietic stem cell development and regulatory signaling in zebrafish. Bichimica et Biophysica Acta *1830*, 2370-2374.

Zhang, X.T., and Rodaway, R.F. (2007). *SCL*-GFP transgenic zebrafish: In vivo imaging of blood and endothelial development and identification of the initial site of definitive hematopoiesis. DEv Biol *307*, 179-194.

Zhang, Y., Jin, H., Li, L., Qin, F., and Wen, Z. (2011). cMyb regulates hematopoietic stem/progenitor cell mobilization during zebrafish hematopoiesis. Blood *118*, 4093-4101.

Zong, S., Jiang, X., Sun, C., and Zou, S. (2013). Identification of a second *follistatin* gene in grass carp (*Ctenopharyngodon idellus*) and its regulatory function in myogenesis during embryogenisis. General and Comparative Endocrinology *185*, 19-27.

- http://www.cores.utah.edu/wp-content/uploads/2013/07/stage2.jpg – November 11, 2013.